Electrostatic separation for functional food ingredient production

Jue Wang

Thesis committee

Promotor

Prof. Dr R.M. Boom
Professor of Food Process Engineering
Wageningen University

Co-promotor

Dr M.A.I. Schutyser
Associate professor, Laboratory of Food Process Engineering
Wageningen University

Other members

Prof. Dr V. Fogliano, Wageningen University
Dr V. Lullien-Pellerin, INRA, Montpellier, France
Prof. Dr R.F. Mudde, Delft University of Technology
Dr H.C. Langelaan, Food & Biobased Research - Wageningen UR

This research was conducted under the auspices of the Graduate School VLAG (Advanced studies in Food Technology, Agrobiotechnology, Nutrition and Health Sciences).

Electrostatic separation for functional food ingredient production

Jue Wang

Thesis

submitted in fulfilment of the requirements for the degree of doctor

at Wageningen University

by the authority of the Rector Magnificus

Prof. Dr A.P.J. Mol

in the presence of the

Thesis Committee appointed by the Academic Board

to be defended in public

on Wednesday 16 March 2016

at 4 p.m. in the Aula.

Jue Wang
Electrostatic separation for functional food ingredient production
178 pages

PhD thesis, Wageningen University, Wageningen, NL (2016)
With references, with summary in English

ISBN 978-94-6257-651-3

Table of contents

General introduction

Introduction

From purity to functionality and sustainability – opportunity for dry fractionation

State of the art food manufacturing often uses dry and highly refined ingredients, continuously driving ingredient producers to develop processes to increase purity of their food ingredients (van der Goot et al., 2016). However, achieving such high purities requires processes that consume significant amounts of water and solvents, and involve harsh conditions such as high temperature or extreme pH. This not only leads to large energy consumption for drying, but also to loss of native functionality of the ingredients (Schutyser and van der Goot, 2011). Taking pea protein isolation as an example, 50 kg water is needed to produce 1 kg pea protein by wet fractionation. Subsequent removing of the added water by spray drying is the main contribution to the high energy consumption (54 MJ/kg recovered protein) of the whole process (Figure 1).

Nevertheless, almost all foods are prepared from more than one ingredient, making it not always necessary to completely fractionate agro-material into its pure constituents. Moreover, food products may even benefit from the complex composition and native functional properties of raw materials. For example, in the extrusion for meat analogue production, soy protein concentrate provides better fibrous material than soy protein isolate (Cheftel et al., 1992). Therefore, less purified ingredient fractions that retain their native functional properties can be very interesting for food production. Thus, there is potential for more sustainable and mild fractionation processes that can deliver functional rather than pure ingredients. Dry fractionation perfectly matches with such requirements.

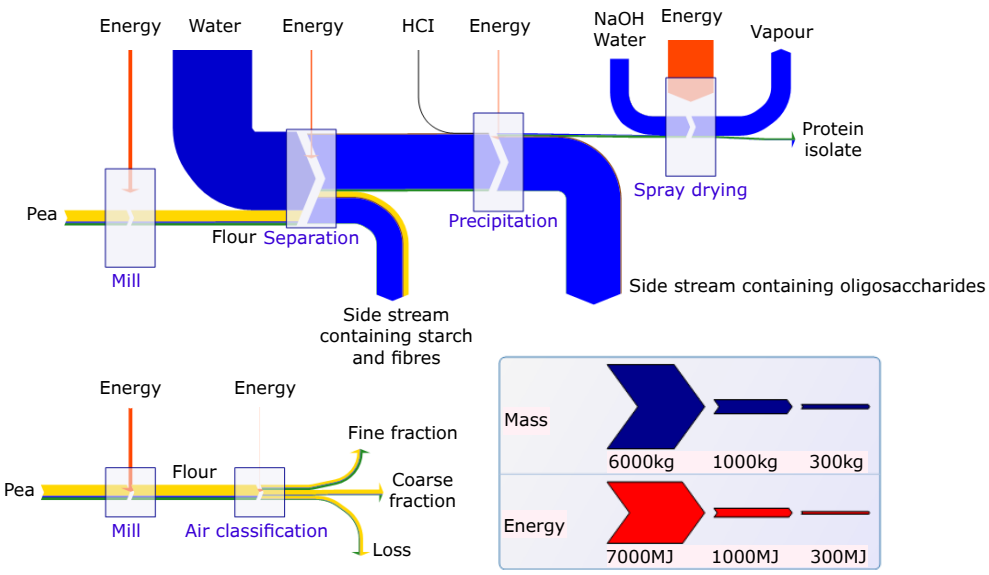

Figure 1. Sankey diagrams of wet fractionation of peas into pea protein isolate (upper) and dry fractionation of peas using air classification into a pea protein fraction (lower) (Adapted from Schutyser et al. (2015)).

Dry fractionation combines milling and dry separation techniques, such as air classification and sieving, and can fractionate cereal and legumes into protein-enriched and protein-depleted fractions (Pelgrom et al., 2014; Pelgrom et al., 2013a; Stevens et al., 1963; Wu and Stringfellow, 1995). As indicated in Figure 1, it uses hardly any water, consumes very little energy, and retains the native structure and functionality by avoiding harsh conditions (high temperatures, or extreme pH). For example the dry fractionation for pea protein production consumes no water and the energy consumption is 3.6 MJ/ kg recovered protein, which is a factor 15 lower than the energy consumption of wet fractionation (Schutyser et al., 2015). The fractions produced by dry fractionation have lower purity, but may retain different functional properties. For example, lupine protein concentrate produced by milling and air classification could provide more stable foam compared to wet isolated protein (Pelgrom et al., 2014). Moreover, a lower viscosity of suspensions with dry enriched lupine protein was attributed to its higher solubility, suggesting future application of such fractions in high protein beverages (Pelgrom et al., 2014).

Electrostatic separation – a novel dry separation process for food ingredients

Conventional dry separation processes, such as air classification and sieving, use differences in particle size and/or density as driving force. However, particles with different compositions may be milled to similar sizes, which limits the maximum purity that can be reached. Considering lupine as an example, we can obtain a fine fraction rich in protein after fine milling and air classification. This fine fraction consists mainly of individual protein bodies, but also of milled hull fragments of similar size. If we could separate these fibre fragments from the protein bodies this could further increase the protein content of the fine fraction (Pelgrom et al., 2014). However, because of the similar particle size, a separation relying on a different driving force is needed. An interesting option here is electrostatic separation, which separates particles based on their different triboelectric charging behaviour.

Electrostatic separation of particles is achieved by first charging the particles and then separating them in an external electric field (Haga, 1995). The electrostatic force (F_e) is the driving force for separation and is equal to the product of the charge on the particle (q_p) and the electric field strength (E) (Eq. 1) (Kelly and Spottiswood, 1989a).

$$F_e = q_p E \qquad \text{(Eq. 1)}$$

Three different methods exist for electrostatic charging: corona charging, induction charging, and triboelectric charging (Mazumder et al., 2006). While both corona charging and induction charging require large differences in conductivity between the materials to be separated, triboelectric charging is found effective to differentially charge particles with small differences in conductivity (Higashiyama and Asano, 1998; Kelly and Spottiswood, 1989b).

Triboelectric charging occurs when different materials are brought into close frictional contact. During contact between the two surfaces, e.g. surfaces of a particle and a plate, depending on the surface states, electrons are transferred from one surface to the other. Upon separation, at least part of the transferred

charge will remain on each surface, with the same amount but with opposite polarities (Figure 2) (Bailey, 1984; Kelly and Spottiswood, 1989b; Matsusaka et al., 2010).

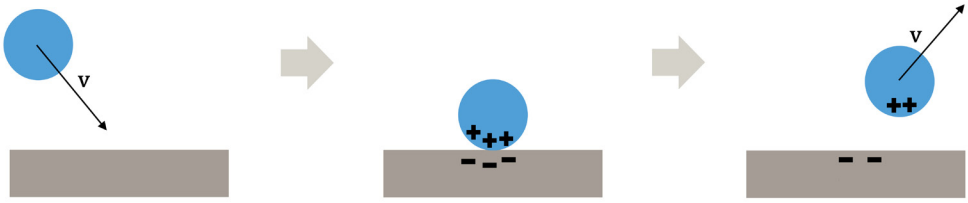

Figure 2. Schematic drawing of triboelectric charging of a particle after collision with a plate

While the fundamental mechanism of triboelectric charging is still subject of speculation, an empirical ranking of materials has been established, the so-called triboelectric series, that shows the tendency of materials to gain charge polarity when brought into contact with another material (Kwetkus, 1998). The reported triboelectric series are not very consistent amongst different studies (Table 1). This can be attributed to different factors that influence the triboelectric charging, such as the chemical, physical and electrical properties of the materials and their surfaces, number of impacts, and the velocity and angle of the impact (Bailey and Smedley, 1991; Carter et al., 1998; Eilbeck et al., 1999; Gajewski, 1989; Matsusaka et al., 2000; Matsuyama and Yamamoto, 1994, 1995; Rowley, 2001; Yamamoto and Scarlett, 1986). Moreover, environmental conditions such as temperature and relative humidity affect the charging as well (Nguyen and Nieh, 1989; Nomura et al., 2003; Rowley and Mackin, 2003).

A schematic drawing of a simple electrostatic separation process that employs triboelectric charging is shown in Figure 3. Particles are entrained by a carrier gas, e.g. nitrogen gas, through a charging tube, in which particles become charged during collisions with walls and other particles. Subsequently, the particles are separated in an electric field created by two parallel metal plate-electrodes supplied with high voltage (HV). Particles with opposite polarities move towards the different electrodes and are thus separated.
Triboelectric charging based electrostatic separation has been applied for many years in mining industries for the beneficiation of minerals and coal (Bada et

Tabel 1 Comparison of triboelectric series from four studies

	Wilcke (1759)*	Faraday (1840)*	Shaw (1917)	Adams (1987)
Positive	Glass	Cat's fur	Asbestos	Hand
	Wool	Wool	Hair	Asbestos
	Quills	Quills	Glass	Rabbit fur
	Wood	Flint glass	Mica	Glass
	Paper	Cotton	Wool	Mica
	Ground glass	Linen	Cat's fur	Hair
	Pb	Silk	Ca, Mg, Pb	Nylon
	Sulphur	Hand	Silk	Wool
	Metals	Wood	Paper	Pb
		Fe, Cu, Ag, Pb	Cotton	Silk
		Sulphur	Wood, Fe	Aluminium
			Ground glass	Paper
			Resin	Cotton
			Cu, Ag	Steel
			Sulphur	Wood
				Hard rubber
				Cu
				Ag
				Sulphur
				Polyester
				Styrene
				Polyethylene
				Polypropylene
				PVC
Negative				Silicon

*Adapted from Shaw (1917) and Vieweg (1925)

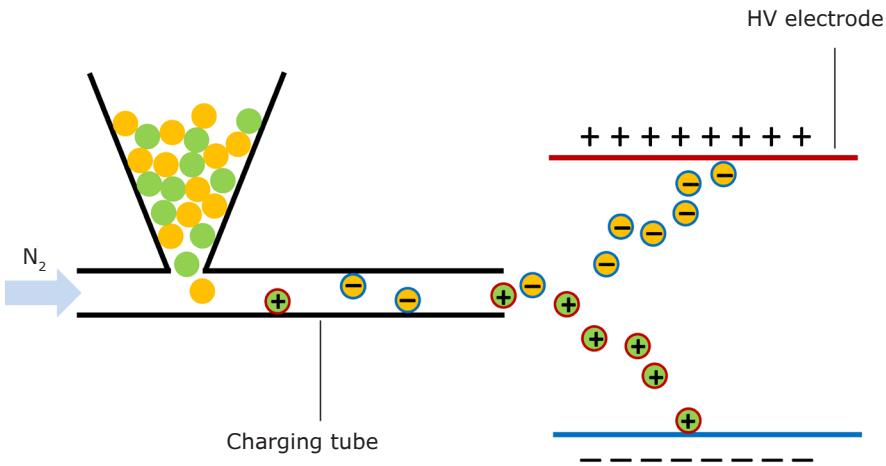

Figure 3. Schematic drawing of the electrostatic separation based on triboelectric charging

al., 2010; Ban et al., 1997; Cangialosi et al., 2008; Dwari et al., 2015; Trigwell et al., 2003), and for fractionation of plastic waste materials (Bendimerad et al., 2009; Wu et al., 2013; Younes et al., 2015), but only recently has it been proposed for dry separation of food materials. Several studies demonstrated the potential of using electrostatic separation to fractionate agro-materials, e.g. for the production of aleurone-rich fractions and fibre-rich fractions, respectively, from wheat bran and oat bran (Chen et al., 2014b; Hemery et al., 2011; Sibakov et al., 2014; Wang et al., 2015b), and for the enrichment of proteins from legumes (Pelgrom et al., 2015a). However the effectiveness in terms of purity and yield and the influence of process parameters such as particle concentration, gas flow and electric field on charging and separation of food ingredients has not been systematically studied.

Objective and outline of the thesis

The objective of the study reported in this thesis was to gain better understanding of the charging behaviour of model and agro-materials, and to evaluate how these components can be separated using an electrostatic driving force. This should give insight in the critical factors for successful electrostatic separation and facilitate exploration of the potential of this separation method for different agro-materials. The study focused on obtaining experimental understanding, rather than mechanistic insight into the specific phenomenon of triboelectric charging, as this was part of a parallel study (Korevaar et al., 2015; Korevaar et al., 2014).

Chapter 2 presents characterization of the charging behaviour of single-component model particles in nitrogen gas flowing through aluminium tubes, using a lab-scale electrostatic separator. Polystyrene particles and wheat gluten were used as model particles. The influences of particle size, charging tube length, gas velocity and relative humidity were studied.

Chapter 3 demonstrates the potential of using electrostatic separation to enrich arabinoxylans from wheat bran with the same lab-scale electrostatic separator. Different parameters such as particle size, gas velocity and charging tube length were investigated for their influence on electrostatic separation. Finally, electrostatic separation is compared to conventional sieving and the combination of electrostatic separation and sieving is explored to obtain further improved enrichment.

Chapter 4 presents a custom-built bench-scale electrostatic separator, with which well-defined charging and separation experiments of model mixtures prepared from wheat gluten and starch were carried out. The influences of particle concentration, gas flow rate, electric field strength on the charging and

separation were systematically investigated. The agglomeration of particles is hypothesized to have an important influence on separation efficiency.

Chapter 5 reports on dry fractionation by combining milling and electrostatic separation, providing an alternative to wet extraction of protein from lupine seeds. Different degrees of milling were analysed in combination with electrostatic separation. Successive electrostatic separation steps were explored to increase the purity of the obtained protein concentrate. Finally, a method was presented and investigated to improve the yield without compromising the purity.

Chapter 6 explores the possibility of enriching dietary fibre from defatted rice bran by dry fractionation. Three separation routes were studied: two-step electrostatic separation, sieving and a combination of electrostatic separation, and sieving. Fibre-enriched fractions obtained were analysed for their hydration properties and oil binding capacity and compared to wet-extracted total dietary fibre. The latter assisted in evaluating dry fractionation as a process to obtain dietary fibre fractions with similar technological properties and physiological effects compared to the wet extraction process.

Chapter 7 concludes the thesis with a general discussion on the main findings, based on which two schemes for protein enrichment and fibre enrichment were proposed. Subsequently the challenges to achieve a successful electrostatic separation for agro-material and up-scaling are discussed. Finally the chapter ends with an outlook for future research.

Analysis of electrostatic powder charging for fractionation of foods

This chapter has been published as:

Wang, J., de Wit, M., Schutyser, M.A.I., Boom, R.M., (2014). Analysis of electrostatic powder charging for fractionation of foods. Innovative Food Science & Emerging Technologies 26(0), 360-365.

Abstract

Electrostatic separation based on different triboelectric charging behaviours of components has emerged as a novel, sustainable dry fractionation process. This study aims to characterize charging behaviour of single-component particles in nitrogen gas flowing through aluminium tubes. Polystyrene (PS) particles and wheat gluten were used as model particles. Specific charge increased linearly with gas velocity up to 28 m/s for both materials. Surface charge densities of different-sized PS particles overlapped for laminar gas flow. For stronger gas flow, surface charge density of the smallest particles deviated from that of larger particles. Specific charge of PS particles increased linearly with increasing tube length from 125 to 225 mm. Charging of PS particles was unaffected by relative humidity (RH) of gas. Specific charge of wheat gluten decreased for RH > 80%. The results provide insight in critical parameters affecting charging behaviour, which provides input for developing electrostatic separation processes to fractionate food ingredients.

Introduction

Conventional wet fractionation of agro-materials into food ingredients uses copious amounts of water and energy. Moreover, the harsh conditions during wet fractionation, such as high temperature and pH, are detrimental to the native functionality of individual components. In contrast, dry fractionation is a more sustainable alternative and retains the functionality of the produced fractions significantly better (Schutyser and van der Goot, 2011). Dry fractionation conventionally, e.g. for pea fractionation, combines milling and air classification or sieving to obtain protein and starch enriched fractions (Pelgrom et al., 2013a; Pelgrom et al., 2013b). Milling is applied to achieve the physical disentanglement of individual components while air classification or sieving fractionates the millings on the basis of particle density and/or particle size into enriched fractions. However, especially when particles differ little in density and/or particle size, the final purity that can be achieved towards a specific component is limited.

More recently, electrostatic separation has emerged as a novel process for dry food ingredient fractionation, although the principle has been applied for decades for mineral enrichment (Fraas and Balston, 1940; Gaudin and Mora, 1958; Kwetkus, 1998; Trigwell et al., 2003). The separation is based on differences in triboelectric charging behaviour of materials (Higashiyama and Asano, 1998; Kelly and Spottiswood, 1989b). It is achieved by charging particles with a gas-assisted flow in a charging device. The subsequent particle separation takes place under the influence of an external electrostatic field (Fraas and Balston, 1940; Kelly and Spottiswood, 1989c).

The charging step is critical to the effectiveness of the separation and is based on the phenomenon that two different materials become charged when they rub against each other. When two surfaces contact with each other, depending on the surface states, electrons will transfer from one surface to the other. Upon separation, the two surfaces become charged in the same amount but

with opposite polarities (Bailey, 1984, 1993; Kelly and Spottiswood, 1989a; Matsusaka et al., 2010). Triboelectric charging is influenced by many factors, such as the chemical, physical and electrical properties of particle and contact surface (Bailey and Smedley, 1991; Carter et al., 1998; Eilbeck et al., 1999; Gajewski, 1989; Rowley, 2001), number of impacts (Matsusaka et al., 2000; Matsuyama and Yamamoto, 1995), and velocity and angle of the impact (Matsuyama and Yamamoto, 1994; Yamamoto and Scarlett, 1986). Moreover, environmental conditions such as temperature and relative humidity also affect the charging (Bailey and Smedley, 1991; Gajewski, 1989; Nguyen and Nieh, 1989; Nomura et al., 2003; Rowley and Mackin, 2003). While several studies have demonstrated the possibility of using electrostatic separation to fractionate agro-materials, e.g. for the production of aleurone-rich fractions from (fine) milled wheat bran (Bohm et al., 2003; Hemery et al., 2011; Hemery et al., 2009b), the triboelectric charging behaviour of agro-materials has not yet been systematically studied.

The aim of the study reported here is to characterize triboelectric charging behaviour of single-component particles under different conditions. Purified wheat gluten was used as an agro-material. Moreover, well-defined spherical particles made from polystyrene were used as a model system to avoid the complexity caused by the natural composition and irregular shape of agro-materials. Three aluminium tubes with different lengths were used to charge particles. The experiments were designed to evaluate the influence of several factors: the carrier gas velocity, the particle size, the charging tube length, the carrier gas relative humidity and the material water activity.

Materials and methods

Materials

Three differently sized Spherical Polystyrene® (PS) particles were purchased from Maxi-Blast, Inc. (US). The particle size distributions were measured by Mastersizer 2000 with the Scirocco 2000 dry dispersion unit (Malvern Instruments, Worcestershire, UK). The volumetric mean diameters, D[4,3], were 218 μm, 304 μm and 450 μm, respectively. A scanning electron microscope (SEM) image of PS particles was made by Phenom G2 pure Scanning Electron Microscope (Phenom-World BV, The Netherlands). Figure 4-A shows that the PS particles were perfectly spherical and had a smooth surface.

Vital wheat gluten was obtained from Roquette (France) with the following specifications: moisture 6% (w/w), protein 75~80% (w/w), starch 9% (w/w), cellulose <1% (w/w), fat 7% (w/w) and ash 1% (w/w). A SEM image is shown in Figure 4-B and it can be observed that the particles have an irregular shape and a rough surface with pores smaller than several microns.

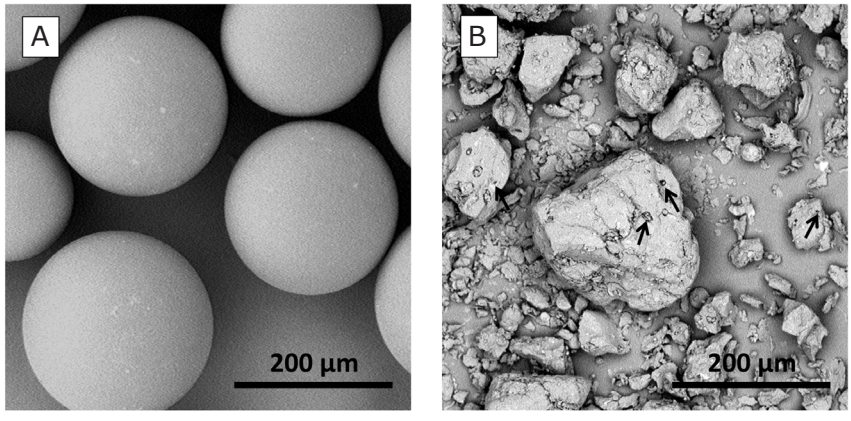

Figure 4. Scanning electron microscope (SEM) images of A) PS particles (D[4,3] = 218 μm) and B) wheat gluten (D[4,3] = 68.6 μm), arrows indicate the pores on the surface of wheat gluten

Charging experiments

A lab-scale electrostatic charging device consisting of a funnel and a squared charging tube, both made from aluminium, was used for charging experiments (Figure 5). The inner dimension of the tube was 1.8 mm × 1.8 mm. To avoid any external electrical interference, the charging tube was shielded by wrapping the tube with an insulating plastic foil and then an aluminium foil layer which was grounded. The funnel was also grounded via direct contact with the aluminium foil layer. An electrometer (Keithley Model 6215) was connected to the charging tube to measure the impact charge obtained by the tube. Since the particles and the tube are charged in the same amount but opposite polarities, the read charge Q_{read} needs to be converted into the charge of particles Q_p by Eq. 2.

$$Q_p = - Q_{read} \qquad \text{(Eq. 2)}$$

Two terms were used to express the charge obtained by the particles: the specific charge which is defined as the charge-to-mass ratio (in μC/g) and the surface charge density, which is defined as the charge-to-surface ratio (in μC/m^2).

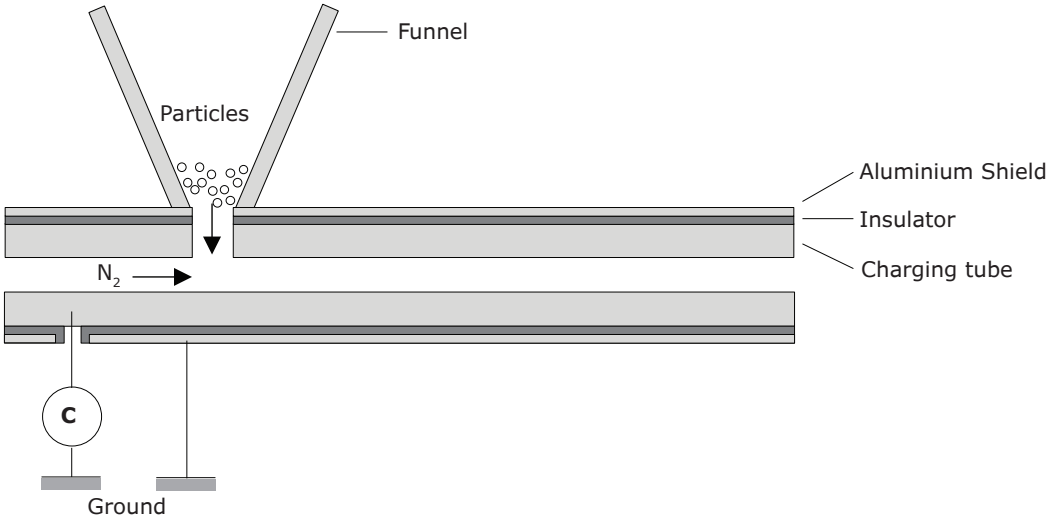

Figure 5. Schematic drawing of the charging device

Before each charging experiment, the entire system was flushed with nitrogen. Then the electrometer was corrected for zero reading and 3 grams of sample were poured into the funnel. According to Bernoulli's law, a pressure drop exists between the funnel and the nitrogen gas flowing through the tube at the outlet of the funnel. This phenomenon is also known as the Venturi effect. The pressure difference (Δp) is proportional to the kinetic energy of the flowing gas in the tube as expressed with Eq. 3.

$$\Delta p = \frac{1}{2}\rho_g v_g^2 \qquad \text{(Eq. 3)}$$

where ρ_g is the density of the nitrogen, and v_g is the velocity of the nitrogen gas. Due to this pressure difference, particles are drawn into the charging tube. Subsequently, particles are accelerated by the nitrogen flow in the tube, and impact and exchange charge with the tube wall. The cumulative charge on the tube was measured by the electrometer. After the complete sample was dispersed in the tube, the final reading of the electrometer was recorded. Thereafter, the funnel and charging tube were cleaned with a vacuum cleaner and compressed air for the next measurement. All measurements were carried out in duplicate.

Three process parameters were varied: Gas velocity (13 ~ 36 m/s); Charging tube length (125 mm ~ 425 mm) and RH of nitrogen (0 ~ 100%). To investigate the influence of the individual parameters, only one parameter was varied at a time while the others were kept constant.

Conditioning of wheat gluten

To investigate the influence of water activity (a_w) of wheat gluten on the charging behaviour, conditioned wheat gluten with varying a_w between 0 and 0.85 was used. The conditioned sample was obtained by equilibrating 3 grams of wheat gluten in a climate chamber (Memmert Model CTC256, Germany) at 25 °C flushing with humidified air at certain RH. After 24 hours, the sample was taken out from the climate chamber, weighed and directly used for charging experiment.

Results and Discussions

Particle charging as a function of gas velocity

The experiments to investigate the influence of gas velocity on charging behaviour of all three PS particles were carried out with the 225 mm charging tube (Figure 6-A). The specific charge increased linearly with the gas velocity up to 28 m/s. After 28 m/s, the increase in the specific charge became less than proportional. A similar behaviour was observed with wheat gluten. Yamamoto and Scarlett (1986) observed that charging of particles is primarily dependent on the normal component of the impact velocity, which determines the contact area during the collision. In our case, according to Eq. 3, when the gas velocity is increased, a larger pressure difference is created between the position in the funnel and the outlet of the funnel. As a consequence, particles are subjected to a larger force in the vertical direction which leads to a higher normal component of impact velocity. In addition, a higher tangential component of the impact velocity may lead to more sliding during contact which also contributes to the charging (Tatsushi and Hideo, 1997).

Particle charging as a function of particle size

Figure 6-A also shows the effect of the particle size on the charging of the PS particles with a 225 mm charging tube. The specific charge is inversely related to particle size within the whole range of the tested gas velocities. This can be explained by the larger surface to volume ratio of smaller particles (Gajewski, 1989). Because triboelectric charging is a surface phenomenon, smaller particles will have more particle-wall contacts and consequently take more charge. To further confirm this explanation, the specific charge was recalculated into surface charge density to eliminate the influence of the surface area. Instead of the gas velocity, the surface charge density is plotted against the Reynolds number (Figure 6-B).

The three curves in Figure 6-B overlap only partially, which indicates that the difference in the surface to volume ratio is not the only reason for the different charging behaviour of particle with different sizes. When Re increases above 2250, the curve of the smallest particle starts to deviate from the other two. With further increasing Re (Re > 3215), the curve of the middle-sized particles also started to deviate from the largest one. This may be explained by the characteristics of the gas flow pattern in the tube, since the gas flow in the tube changes from laminar to turbulent when Re > 2300. Furthermore, it is likely that smaller particles are more affected by the gas flow pattern, resulting in more collisions between the tube wall and smaller particles.

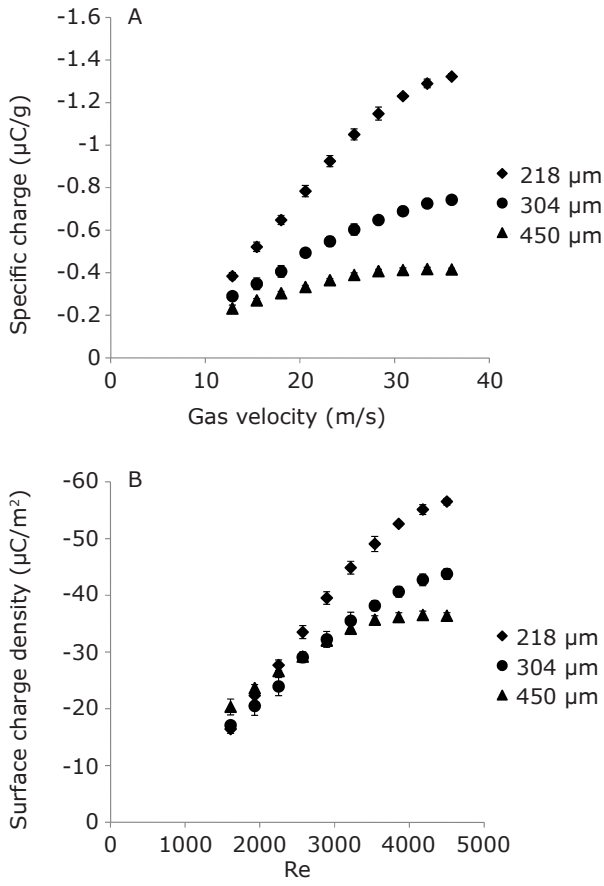

Figure 6. A) Specific charge of PS particles as a function of gas velocity and B) Surface charge density of PS particles as a function of Reynolds number. The error bars indicate the absolute deviation.

Particle charging as a function of charging tube length

Five tube lengths were evaluated for all three PS particles at a gas velocity of 21 m/s. Figure 7 shows that the specific charge of particles increased with increasing tube length from 125 mm to 225 mm. This can be explained by the increase in number of particle-wall contacts along the tube length. Beyond a tube length of 225 mm the charge of the particles did not increase further. Careful analysis showed that the dispersion of particles in the 325 mm and 425 mm tubes was affected by the high gas flow resistance in the tube. As a result the pressure below the funnel outlet became too high, which caused a back flow of nitrogen into the funnel. This will have affected the charging behaviour of the particles along the length of the 325 mm and 425 mm tubes.

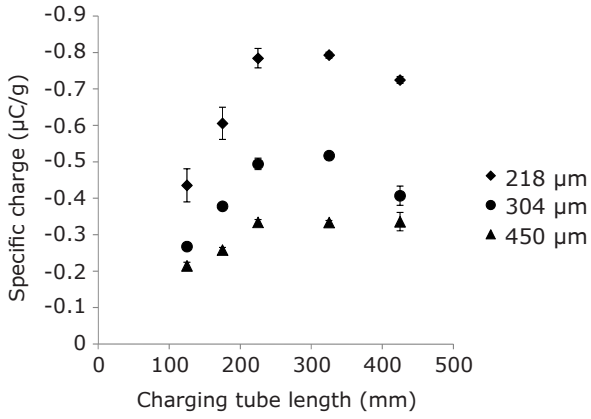

Figure 7. Specific charge of PS particles shown as a function of the charging tube length. The error bars indicate the absolute deviation.

Because no back flow was observed for the 125 mm, 175 mm and 225 mm charging tubes, they were evaluated using gas velocities between 13 and 36 m/s for the 218 µm PS particles (Figure 8-A) and for the wheat gluten powder (Figure 8-B).

In Figure 8-A, two predicted lines were plotted based on the assumption that the charging is linearly related to the length of the tube (Q_p /L="constant"). The graph shows that while this is valid at lower gas flow rates, the increase of specific charge was no longer linear with the tube length above 28 m/s. We hypothesize that after successive particle-wall impacts, the particles tend to pick a reduced extra charge (Matsusaka et al., 2000).

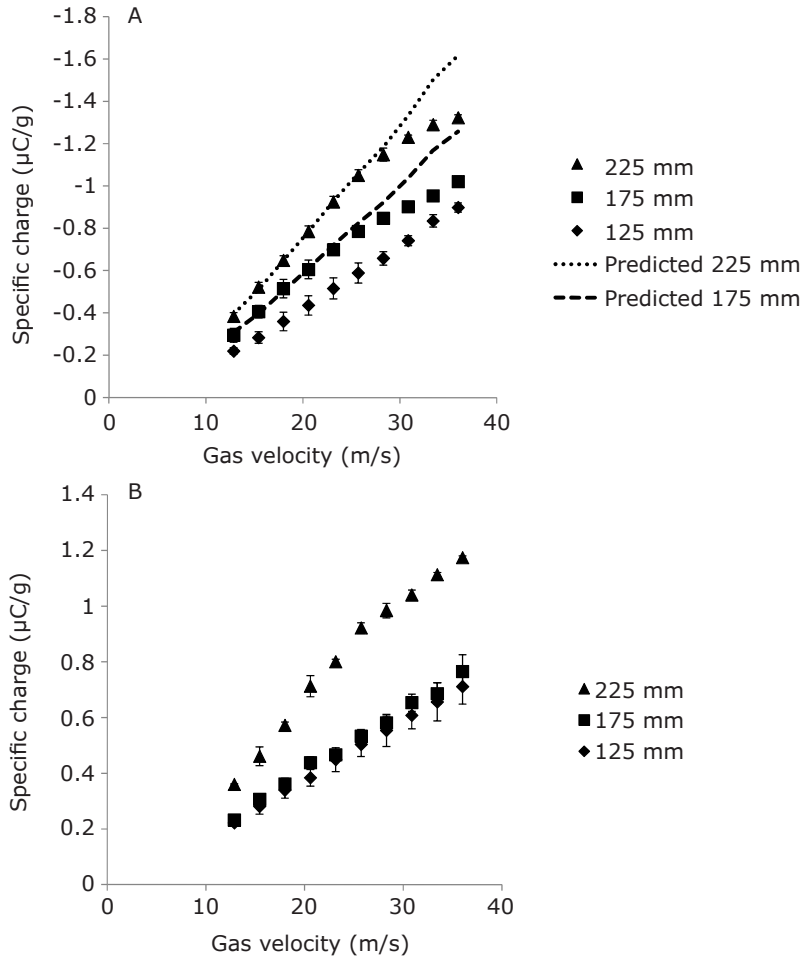

Figure 8. A) Specific charge of PS particles (D[4,3] = 218 µm) as a function of gas velocity and B) Specific charge of wheat gluten as a function of gas velocity. The error bars indicate the absolute deviation.

The dependence of the charging behaviour of the wheat gluten on the length of the charging tube is different from that of the PS particles. Figure 8-B shows that wheat gluten was charged by the 175 mm tube in the same way as by 125 mm tube, whereas the 225 mm tube resulted in a higher charge. This effect was reproducible. It might be that for wheat gluten, the 175 mm tube was not long enough to allow more discrete particle-wall contacts than the 125 mm tube. To check this hypothesis, numerical modelling of the trajectories and charging of the particles in the tube, e.g. using a discrete particle modelling approach is proposed. However, it is beyond the scope of the current paper and thus

suggested for further research. Realistic prediction of the particle dynamics and corresponding charging behaviour in the tube requires modelling of the charging process and multiple force interactions, e.g. the force imposed by the Venturi effect, the gravitational force, the drag force, the inertial lift force and the electrostatic forces. The electrostatic forces should include charge interactions with neighbouring particles and the image charge effect caused by the induced charge on the conductive tube wall (Korevaar et al., 2014; Matsuyama et al., 2009; Tanoue et al., 2001).

Particle charging as a function of relative humidity of nitrogen and material water activity

Polystyrene has extremely low affinity with water (Greenley et al., 1989), which results in a very small equilibrium moisture content of the particles (EMC), from 0 to 0.01% w/dw (measured with Dynamic Vapour Sorption), within the relative humidity (RH) range of 0 – 60%. In contrast, wheat gluten is much more hygroscopic with an EMC increasing from 3% to 15% w/dw in the water activity (a_w) range of 0.1 – 0.7 (Viollaz and Rovedo, 1999). Because of the difference in moisture sorption behaviour, the charging behaviour of the two materials with varying RH of nitrogen were expected to be different (Rowley and Mackin, 2003).

We tested the influence of the RH on the PS particles (D[4,3] = 450 µm) and wheat gluten with an a_w of 0.45, with the 225 mm tube at a gas velocity of 36 m/s. The results are shown in Figure 9. Contrary to our expectations, we found similar behaviour for both materials: within the RH range 0 – 60%, the change in the specific charge was negligible. When the RH was higher than 60% the specific charge started to decrease. At an RH of 100%, a charge reduction of approximately 0.2 µC/g was observed for both materials. The small influence of the gas RH on PS particles was expected because the particle absorbed no water onto its surface and no change of electrical or mechanical property of the surface occurred. The unexpected similar behaviour of wheat gluten might be due to the very small residence time (10 – 20 ms) of particles in the tube, which is too short for absorbing a significant amount of moisture.

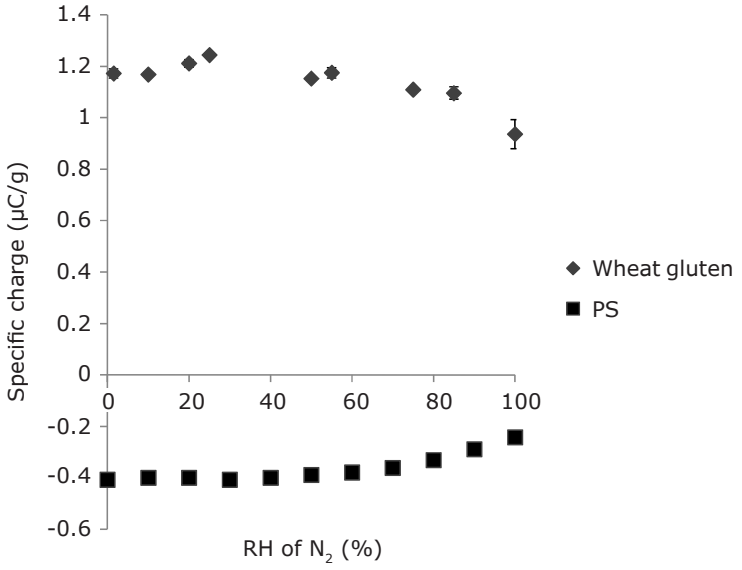

Figure 9. Specific charge of PS particles (D[4,3] = 450 µm) and wheat gluten as a function of RH of nitrogen. The error bars indicate the absolute deviation.

The moisture content, and in particular the surface moisture content, may well influence the electrostatic charging of a particle by either changing the mechanical properties of the surface or affecting the charge dissipation (Dascalescu et al., 2005). Therefore we used conditioned wheat gluten to test the influence of a_w on charging behaviour. Additionally, during the charging experiments nitrogen gas was applied with RH = 0% or RH corresponding to the set aw of the wheat gluten.

When the wheat gluten a_w is increased beyond 0.75, a sharp decrease in the specific charge is observed, which may be explained by a transition of the material from glassy to rubbery state, and subsequent bridge formation between particles. At 25 °C, wheat gluten with a_w = 0.75 and a_w = 0.85 has a water content of 16% w/dw and 20% w/dw, respectively (Viollaz and Rovedo, 1999). The corresponding glass transition temperatures (T_g) are 30 °C and 10 °C, respectively (Kalichevsky et al., 1992), which implies that the wheat gluten becomes rubbery when the aw increases from 0.75 to 0.85. Besides the glass transition, also condensation of liquid water at the surface of the particles might occur resulting in liquid bridge formation (Aguilera et al., 1993). Both phenomena also influence the dispersibility of the wheat gluten in the nitrogen gas: it was

visually observed that the wheat gluten particles aggregate at RH 85% into larger particles. This was confirmed by measuring the mean particle size, which had increased from 68.6 µm to 90 µm (a factor 2.3 increase in volume). This increase also implies a smaller surface to volume ratio, and therefore could additionally explain the lower specific charge.

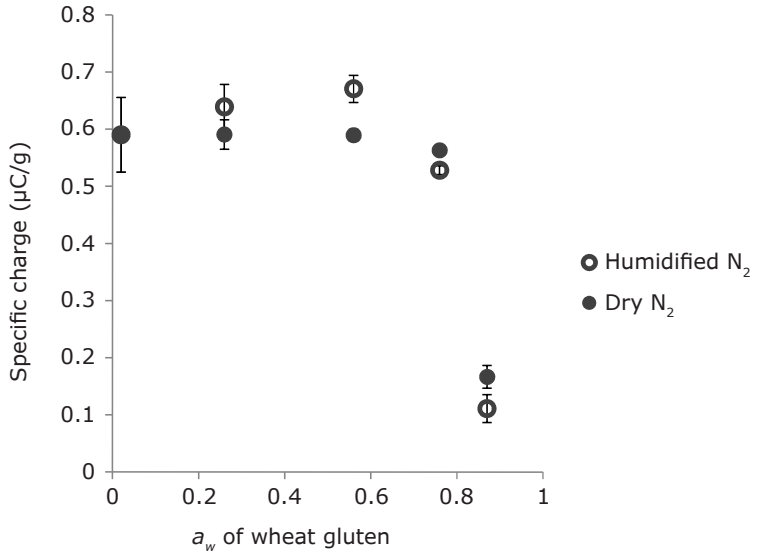

Figure 10. Specific charge of wheat gluten as a function of a_w of the material. The error bars indicate the absolute deviation.

Conclusions

The triboelectric charging behaviour of single-component particles under different conditions was analysed by using purified wheat gluten and spherical polystyrene model particles combined with aluminium charging tubes.

Higher gas velocities lead to a higher specific charge for both tested materials by increasing the normal component of impact velocity. Smaller particles gain more specific charge than larger ones because of their higher surface to volume ratio and their sensitivity towards gas flow pattern changes. Smaller particles possibly experience more frequent particle-wall contacts when flow transits from laminar to turbulent.

Provided that the powder is well dispersed in the tube, the specific charge of PS particles increases linearly with increasing tube length. Different results were obtained for wheat gluten: tubes of 125 and 175 mm length gave the same charging, while a tube of 225 mm gave stronger charging. To check the hypothesis of discrete effects influencing the charging of particles, e.g. for wheat gluten, it is proposed to develop a more detailed discrete particle modelling approach.

The charging of wheat gluten and PS particles is unaffected by the water activity and relative humidity of the nitrogen gas flow. Only for water activities above 0.75 a sudden decline of specific charge was observed for wheat gluten. This was explained by glass transition of the material, which again affected dispersibility behaviour of the individual wheat gluten particles in the gas flow.

The results presented in this paper provide insight in several critical parameters that affect charging behaviour, which provides amongst others input for development of electrostatic separation processes, e.g. for fractionation of food ingredients.

Acknowledgements

This research is supported by the Dutch Technology Foundation STW and the Institute for Sustainable Process Technology, ISPT through the DRYFRAC project (grant number 11399). The authors would like to thank their co-workers within the DRYFRAC project in Eindhoven, Korevaar and Padding, and the user committee for stimulating discussions on dry separation.

Arabinoxylans concentrates from wheat bran by electrostatic separation

This chapter has been published as:

Wang, J., Smits, E., Boom, R.M., Schutyser, M.A.I., (2015). Arabinoxylans concentrates from wheat bran by electrostatic separation. Journal of Food Engineering 155(0), 29-36.

Abstract

Electrostatic separation has been recently proposed as a novel method to fractionate wheat bran into valuable ingredient fractions. However, systematic study into the influence of parameters on electrostatic separation was lacking. Therefore, we here evaluate electrostatic separation for enriching arabinoxylans (AX) from wheat bran in more details. The influence of wheat bran particle size, carrier gas velocity and charging tube length were investigated with a lab-scale electrostatic separator. A combination of larger particle size (D[4,3] of 210 μm compared to 110 μm), higher gas velocity (> 28 m/s) and shorter charging tube (125 mm compared to 225 mm) can sufficiently charge the particles, and at the mean time avoid agglomeration by oppositely charged particles. With the optimal settings, single step electrostatic separation of wheat bran could increase the AX content from 23% to 30% dry matter basis, which is similar as can be obtained by sieving. However, in comparison to sieving, the yield of the enriched fraction from electrostatic separation is lower due to the horizontal design of the setup. Improvement of the yield is expected when adjusting the system design from horizontal to vertical. A sieving step added after the electrostatic separation could effectively remove starch and protein and resulted in a fraction with an AX content of 43% dry matter basis, which is around the theoretical maximum value that can be reached by dry fractionation.

Introduction

Wheat bran, as a by-product of wheat flour production, is an undervalued constituent that could act as a food ingredient rather than being discarded or used as animal feed (Hemery et al., 2007). It is a rich source of dietary fibre (36.5–52.4 w/w %) (Bilgiçli et al., 2007; Esposito et al., 2005; Kahlon and Chow, 2000; Nandini and Salimath, 2001; Vitaglione et al., 2008), amongst which arabinoxylans (AX) have been drawing attention due to their proved healthy benefits, e.g. lowering cholesterol uptake, attenuating type II diabetes, reducing the risk for cardiovascular diseases and cancers, enhancing the absorption of certain minerals and increasing faecal bulk (Cao et al., 2011; Garcia et al., 2006; Mendis and Simsek, 2014). Therefore, more value would be added to wheat bran by extracting an AX-enriched fraction from it.

The carbohydrates AX consist of a backbone of (1-->4)-β-linked D-xylopyranosyl units (Xyl*p*). Some Xyl*p* units are mono-substituted by α-L-arabinofuranosyl (Ara*f*) at the C-(O)-2 or C-(O)-3 positions or di-substituted at both. Some arabinofuranosyl residues can carry phenolic acids, such as ferulic and p-coumaric acids (Schooneveld-Bergmans et al., 1999; Shiiba et al., 1993; Stone and Morell, 2009). More than 60% dry weight of cell walls from wheat bran is composed of AX (Stone and Morell, 2009) and these are present in all layers: 35~47% dry matter basis in the outer pericarp, 36~40% dry matter basis in the intermediate layer (inner pericarp, seed coat and nucellar epidermis), and 18~28% dry matter basis in the aleurone layer (Barron et al., 2007; Benamrouche et al., 2002; Brillouet and Joseleau, 1987; Swennen et al., 2006). In general, the AX in the pericarp (including outer and inner pericarp) are highly substituted with arabinose (Ara/Xyl > 1), whereas those in the aleurone layer are sparsely substituted (Ara/Xyl < 0.5) (Barron et al., 2007; Parker et al., 2005; Stone and Morell, 2009). The majority of wheat bran AX are water-unextractable (Maes and Delcour, 2002).

Currently, wet alkaline extraction is mostly used to extract AX from wheat bran because of the physical and chemical association between AX and other cell wall components, such as lignin and cellulose (Maes and Delcour, 2002). This process generally consists of two steps. The first step involves destarching and deproteinization by using α-amylase and protease, for which large amounts of water are needed. The second step involves the extraction of the AX using aqueous alkaline media or other combinations such as alkali and hydrogen peroxide, alkali and chlorite solutions or dimethyl sulfoxide (Benamrouche et al., 2002; Bergmans et al., 1996; Maes and Delcour, 2001). The removal of all added water by evaporation afterwards consumes copious amounts of energy. Furthermore, the alkaline conditions may cause loss of functional properties of AX by breaking down some of the functional groups of AX, such as ferulic acid (Zhou et al., 2010).

Alternatively, a dry fractionation process by combining dry milling and subsequent electrostatic separation can be used to obtain a fraction that is enriched in AX (Hemery et al., 2011), which consumes much less energy and retains the native functional properties of the original raw material compared to wet extraction (Schutyser and van der Goot, 2011). Electrostatic separation is a process relying on electrostatic forces as a driving force for separating particulate materials (Haga, 1995). To achieve the separation, the materials are first charged and then separated in an electric field. The method used to charge the materials is usually one of the three following: corona charging, induction charging, and triboelectric charging (Mazumder et al., 2006). Because of the distinct properties and compositions of the different bran layers, which results in different triboelectric charging behaviours, triboelectric charging is used in the electrostatic separation of wheat bran (Dascalescu et al., 2010; Hemery et al., 2009b). Triboelectric charging occurs when different materials are charged oppositely upon frictional contact (Higashiyama and Asano, 1998; Kelly and Spottiswood, 1989b). This is achieved by passing the milled material through a tube by entrainment in a gas, during which the particles are charged by collisions with the wall of the tube and/or interparticle contact. Subsequent particle separation takes place under the influence of an external electrostatic field. Several studies showed that it is possible to obtain fractions with different structure and compositions using electrostatic separation on finely milled wheat bran (Brouns et al., 2012;

Chen et al., 2014b; Hemery et al., 2011; Stone and Minifie, 1988). Hemery et al. (2011) obtained a fraction with an AX content of 49% dry matter basis with three successive electrostatic separation steps. However, in all existing studies, the process parameters such as the particle size, carrier gas velocity and the dimension of charging device were not varied and the influence of these parameters on the separation were not investigated. Since these parameters were found to influence the triboelectric charging process (Wang et al., 2014), they will probably also influence the effectiveness of the separation. Besides, no study was reported on combining electrostatic separation with other dry separation processes to enhance the enrichment of certain components from wheat bran.

The aim of this study is therefore to analyse and optimize a single-step electrostatic separation for enriching AX from wheat bran and to demonstrate the possibility of enhancing the separation by combining different dry separation techniques. We first developed a dry fractionation route relying on the electrostatic separation of wheat bran by applying knowledge from our previous study on triboelectric charging behaviour of agro-material (Wang et al., 2014). Then instead of applying a multi-step electrostatic separation, we combined a first step of electrostatic separation with an additional sieving to enrich AX further.

Materials and methods

Materials

Wheat bran was obtained from Koopmans Meel BV (the Netherlands), with the following specifications: moisture 15% (w/w), protein 15% (w/w), starch 13% (w/w), dietary fibre 44% (w/w), fat 6% (w/w) and ash 7% (w/w). All chemicals and reagents were of analytical grade and supplied by Sigma-Aldrich (Germany) unless specified otherwise.

Preparation of whole bran flour

The wheat bran was milled using a pin mill (Hosokawa Alpine, type 100 UPZ, Augsburg, Germany) at ambient temperature at a speed of 22000 rpm, air flow of 75 m^3/h. Four consecutive milling steps were carried out to obtain the whole bran flour (AmbientWBF), which was the starting material for all further experiments.

Cryogenic milling

Cryogenic milling was carried out to further break whole bran flour down to smaller size. A rotor mill (Pulverisette 14, Fritsch, Germany) was used with an 80 µm mesh. Whole bran flour was immersed in liquid nitrogen, after which the frozen flour was put in the centre of the milling chamber. After closing the mill, liquid nitrogen was poured in from the top before and during milling, to ensure that the flour was properly cooled and kept in a glassy state. The flour obtained by Cryogenic milling is here labelled as CryoWBF.

Electrostatic separation

A horizontal lab-scale electrostatic separator consisting of a funnel (aluminium), a squared charging tube (aluminium, side length of 0.18 cm), and a separation chamber with one grounded electrode and one positive-high-voltage electrode, was used for separation experiments (Figure 11). The distance between the electrodes was 10 cm and the voltage on positive electrode was set to 20 kV.

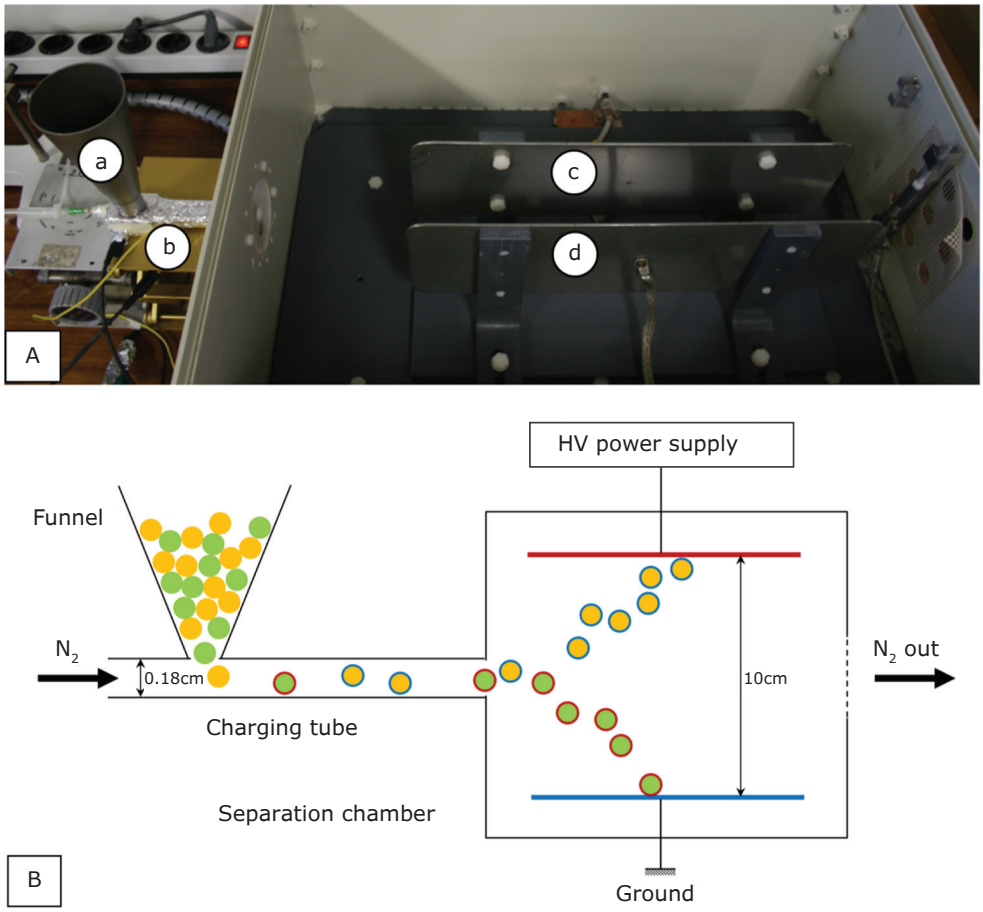

Figure 11. A) Top view of the lab-scale electrostatic separator; a: funnel; b: charging tube; c: positive-high-voltage electrode; d: grounded electrode; B) Schematic drawing of the electrostatic separation process in the lab-scale electrostatic separator (not to scale) with a top view of the separation chamber

The nitrogen flow entrained the particles at the bottom of the funnel into the charging tube, where particles were charged by triboelectric charging. The particles were then exposed to the transverse electrostatic field. The positively charged particles were attracted to the grounded electrode, while the negatively charged particles were attracted to the positive electrode.

For each electrostatic separation experiment, 5 g of starting material was used. The positively charged (P) and negatively charged (N) fractions were collected from the grounded and positive electrodes, respectively. Because of the horizontal design, the gravitational force worked against the separation by dragging the particles to the bottom of the separation chamber before the particles were attracted to the electrodes, which resulted in a large loss.

Different settings of process parameters were applied as shown in Figure 12. During electrostatic separation, charge of particles was measured indirectly from the charging tube as described in previous study (Wang et al., 2014) and expressed as specific charge (in μC/g).

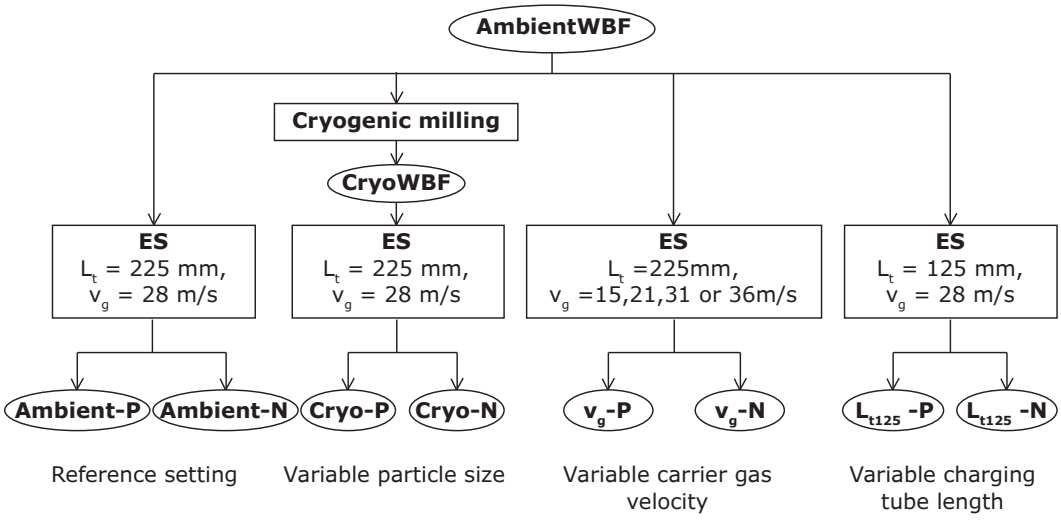

Figure 12. Different settings for electrostatic separation. AmbientWBF: whole bran flour milled at ambient temperature. CryoWBF: whole bran flour obtained by cryogenic milling the AmbientWBF. ES: electrostatic separation. L_t: charging tube length. v_g: carrier gas velocity. -P: positively charged fraction. -N: negatively charged fraction.

Air jet sieving

Various size fractions of the wheat bran flours were prepared by air jet sieving (Alpine200 LS-N, Hosokawa-Alpine, Augsburg, Germany) with a 50 µm sieve at 4000 Pa for 2 min.

Particle size distribution

The particle size distributions of the different powder fractions were determined by laser diffraction using a Mastersizer 2000 in combination with the Scirocco 2000 dry dispersion unit (Malvern Instruments Worcestershire, UK). Each measurement was performed in duplicate.

Biochemical analysis

The dry matter content was determined by drying 2 g of sample in an oven at 105 °C overnight. The total starch and β-glucans content of fractions were measured according to the approved AACC method 76-13 and AACC Method 32-23 (AACC, 2000), respectively, using Megazyme kits (Megazyme International Ireland Ltd., Ireland). The protein content was analysed using Dumas analysis (Nitrogen analyser, FlashEA 1112 series, Thermo Scientific, Interscience). A conversion factor of N × 6.31 for wheat bran protein was used (Livsmedelsverk, 1987).

The arabinoxylans content was analysed by a modified phloroglucinol method that measures pentosans content (Douglas, 1981; Finnie et al., 2006). Besides arabinoxylans, pentosans also include arabinogalactans. However, the occurrence of arabinogalactans in wheat grain is very low (0.27 to 0.38% dry matter basis) and will not interfere the determination of arabinoxylans, therefore this method is widely used to determine arabinoxylans content in wheat (Bettge and Morris, 2007; Ramseyer et al., 2011; Stone and Morell, 2009). A suspension of ca. 8 – 10 mg of wheat bran flour in 4 mL of water was prepared in a stoppered glass tube. Immediately after mixing on a vortex mixer, two times of 0.2 mL of the suspension was quickly pipetted into two stoppered glass tubes, respectively. To each tube, 1.8 mL of water was added to make the sample suspension (2

mL of total volume). Then 10 mL of freshly prepared extraction solution (110 mL of glacial acetic acid, 2 mL of concentrated hydrochloric acid, 5 mL of 20% w/v phloroglucinol in absolute ethanol and 1 mL of 1.75% w/v glucose in water) was added to each tube and the samples were incubated in a boiling water bath for 25 min, after which the samples were cooled in an ice bath. Absorbance of the samples was read at 552 and 510 nm as soon as practical after cooling, but within one hour. The absorbance reading at 510 nm was subtracted from 552 nm to eliminate the influence of hexose sugars. Arabinoxylans content was calculated by using a xylose standard concentration series (xylose standards run in triplicate of 0, 0.025, 0.05, 0.075 and 0.1 mg / mL). Two xylose standard samples were included in each batch of wheat bran flour samples as controls.

All measurements were done in duplicate. All contents reported are based on dry weight.

Results and discussion

Single-step electrostatic separation

As indicated in our previous study, a longer charging tube and a higher gas velocity facilitate the triboelectric charging of particles (Wang et al., 2014). Therefore, as a first configuration, a 225 cm tube combined with a gas velocity of 28 m/s was used. This was used as the reference condition for later optimizing the single-step electrostatic separation of wheat bran. Besides AX, the fractions were also analysed on β-glucans, starch and protein contents were also analysed to demonstrate the separation of AX from other components. The results are shown in Table 2.

For all samples, the yields of positively charged ('-P') and negatively charged ('-N') fractions did not sum up to hundred percent. This was due to the intrinsic drawback of the horizontal design of the lab-scale electrostatic separator, but is not inherent to the separation method. In the horizontal separator, the gravitational force drags part of the particles to the bottom of the separation chamber before the particles are attracted to the electrodes. The yield of Ambient-P was higher than the yield of Ambient-N, indicating that more material from the whole bran flour was charged positively. This was confirmed by the specific average charge of the total AmbientWBF, which was 0.57±0.03 μC/g. β-Glucans, starch and proteins were enriched in the positive fraction, with separation efficiencies (the percentage in the starting material that was recovered in the particular fraction) of 81%, 81% and 55%, respectively. AX was the only component that was enriched in the negative fraction (AX content of 26% dry matter basis in Ambient-N compared to 23% dry matter basis in AmbientWBF). However, due to the low yield of Ambient-N, the separation efficiency of AX was only 16%. Once more, this low yield was due to the design of the experimental system, and is not intrinsic in the method.

Table 2. Yield (% of starting material) and content of AX, β-glucans, starch and protein (% dry matter basis) in whole bran flour and fractions obtained from electrostatic separation with different particle size, charging tube length and carrier gas velocity.

	Yield	AX	β-glucans	Starch	Protein
AmbientWBF	-	23 ± 0.0	3 ± 0.1	13 ± 0.6	17 ± 0.0
Ambient-P	52 ± 1.5	18 ± 1.1	4 ± 0.0	20 ± 0.4	18 ± 0.0
Ambient-N	14 ± 0.1	26 ± 1.1	0 ± 0.0	2 ± 0.0	10 ± 0.1
CryoWBF	-	31 ± 0.5	3 ± 0.1	10 ± 0.4	15 ± 0.1
Cryo-P	65 ± 2.1	29 ± 0.3	4 ± 0.0	12 ± 0.0	15 ± 0.1
Cryo-N	9 ± 0.4	33 ± 2.6	1 ± 0.0	1 ± 0.0	10 ± 0.1
Lt125-P	49 ± 0.8	16 ± 0.5	4 ± 0.0	18 ± 0.4	20 ± 0.2
Lt125-N	16 ± 1.5	31± 2.9	0 ± 0.0	3 ± 0.1	8 ± 0.0
15-P	50 ± 1.6	24 ± 1.5	4 ± 0.0	17 ± 0.3	17 ± 0.0
15-N	9 ± 0.7	26 ± 1.2	1 ± 0.0	6 ± 0.2	12 ± 0.0
21-P	54 ± 1.9	22 ± 1.2	4 ± 0.1	19 ± 0.4	17 ± 0.1
21-N	9 ± 0.5	23 ± 1.7	1 ± 0.0	6 ± 0.1	13 ± 0.2
31-P	51 ± 2.3	21 ± 0.9	4 ± 0.4	21 ± 0.1	18 ± 0.0
31-N	15 ± 1.2	31 ± 1.5	0 ± 0.0	2 ± 0.0	10 ± 0.2
36-P	51 ± 2.1	18 ± 0.3	4 ± 0.0	22 ± 0.3	19 ± 0.0
36-N	15 ± 0.8	30 ± 1.1	0 ± 0.0	2 ± 0.0	10 ± 0.3

Mean value ± absolute deviation (n=2)

AmbientWBF: whole bran flour milled at ambient temperature. CryoWBF: whole bran flour obtained by cryogenic milling the AmbientWBF. L_{t125}: charging tube length of 125 cm. 15, 21, 31, 36: carrier gas velocity in m/s. –P: positively charged fraction. –N: negatively charged fraction.

The difference in enrichment is probably because of the different origins of the components. The AX stems mainly from the pericarp, whereas the β-glucans, starch and proteins are mostly from the aleurone layer and endosperm. Because AX also vastly occurs in the cell walls of aleurone layer and endosperm, the positively charged fraction also contained certain amount of AX. The results are in agreement with those of Hemery et al. (2011) and indicate that electrostatic separation of wheat bran is based on the histological structure of the bran. Particles from the pericarp tend to be charged oppositely from the particles originating from aleurone layer and endosperm. Hemery et al. hypothesized that the difference in cell walls might be the main factor influencing the charging of the

different bran particles. Besides that, the starch could also be a key component influencing the charging and separation process, because of its relatively large mass fraction and relatively small size, which makes it more likely to stick to different surfaces.

Optimization on single-step electrostatic separation

The particle size, carrier gas velocity and charging tube length are known to influence the charging of (agro-)materials and as a consequence the separation performance (Wang et al., 2014). Therefore, these parameters were varied to optimize the enrichment of AX.

Reducing particle size by cryogenic milling

Smaller particles have been found to take a relatively large charge, due to their larger specific surface area and their sensitivity towards gas flow pattern changes (Wang et al., 2014). Therefore, it is expected that separation is improved by reduction of the particle size, e.g. by cryogenic milling. However, Hemery et al. (2011) found that direct cryogenic milling of wheat bran did not lead to a better separation: more composite particles were obtained, probably all components exhibit similar mechanical properties at these low temperatures, and thus the fracture is through the tissues, instead of between them.

Therefore, milling was carried out in two consecutive steps. First ambient milling on wheat bran to obtain whole bran flour (AmbientWBF), and subsequently cryogenic milling was applied. Following this approach we expected similar dissociation of components for AmbientWBF and the flour after cryogenic milling (CryoWBF).

As can be observed in Figure 13, the particles were further reduced in size by cryogenic milling (D[4,3] from 210 µm to 110 µm). The smaller fraction of very fine particles (smaller than 10 µm) in CryoWBF could be due to the loss of starch and protein caused by the evaporation of liquid nitrogen during milling (Table 2). The charge measurement of AmbientWBF and CryoWBF (0.57±0.03 and 0.68±0.01 µC/g, respectively) showed that a smaller particle size resulted in

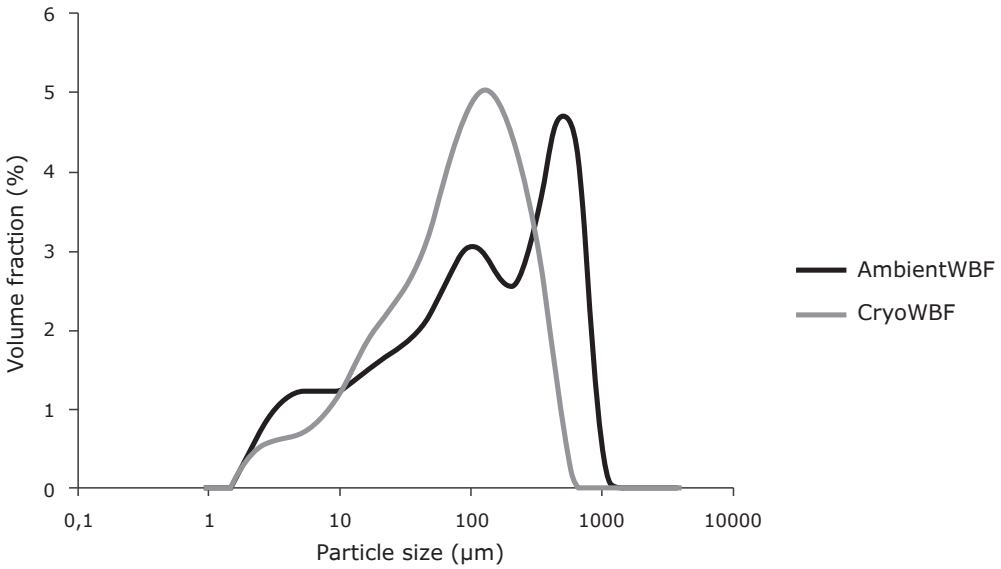

Figure 13. Particle size distribution of whole bran flour milled at ambient temperature (AmbientWBF) and whole bran flour obtained by cryogenic milling the AmbientWBF (CryoWBF).

increased charging as expected. However, the cryogenic milling did not improve the enrichment of AX as the AX content in Cryo-N was only 2% higher than it was in CryoWBF (Table 2), while the separation efficiency was lower than that of Ambient-N (11% comparing to 16%).

Therefore, the hypothesis that further reducing the particle size facilitates the enrichment of AX was not confirmed. This may be explained by an increase in the agglomeration behaviour of oppositely charged particles in the charging tube (Schönert et al., 1996). Oppositely charged particles tend to associate because of their coulombic interaction, which is more pronounced for smaller particles due to their higher specific charge, while external stresses are less likely to dissociate these small particles (Lam and Newton, 1992). Because the net charge of the CryoWBF was positive, the charge of the agglomerates is most likely dominated by the positively charged particles. As a consequence, the agglomerates are expected to end up in the positive fraction resulting in a higher yield of this fraction (Table 2).

Additionally, loss of starch and protein during cryogenic milling due to the generation of a large volume of gas by the evaporation of the liquid nitrogen, would change the type of particle-particle interactions and consequently lead to an insufficient charge of the other components (Forward et al., 2008).

To conclude, adding a cryogenic milling step after ambient milling of the wheat bran is not recommended, because further reduction of particle size did not improve the enrichment. The particle size and composition of the starting material should be optimized for sufficient opposite charging on the components and at the same time minimizing the agglomeration. Additionally, the usage of liquid nitrogen will increase the energy consumption of the whole dry fractionation process, which also makes cryogenic milling unfavourable.

Influence of carrier gas velocity

A higher carrier gas velocity was expected to promote the enrichment of AX because it increases the charging (Chen et al., 2014a; Wang et al., 2014), and also facilitate the breakdown of agglomeration. Five gas velocities were tested and the results are shown in Figure 14.

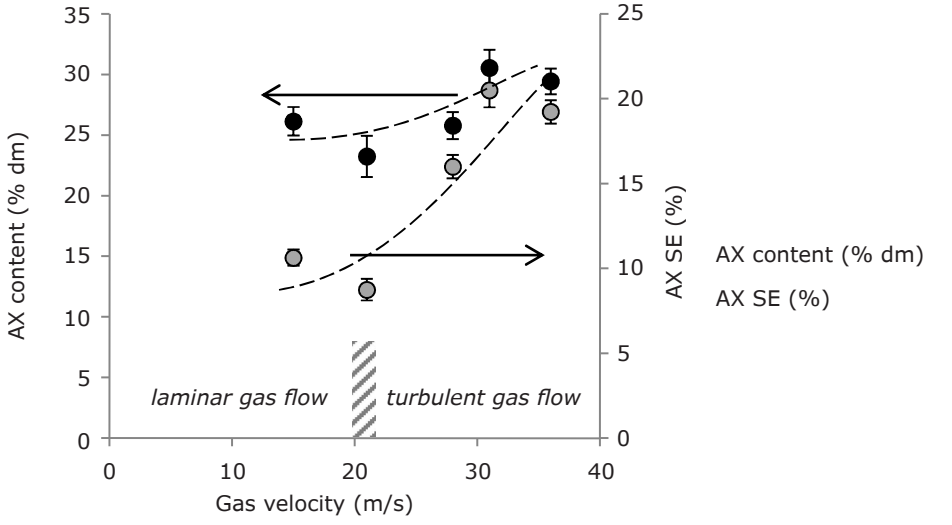

Figure 14. AX content and separation efficiency (SE) of the AX-enriched fraction as a function of carrier gas velocity. The error bars indicate the absolute deviation. Lines are to guide the eye.

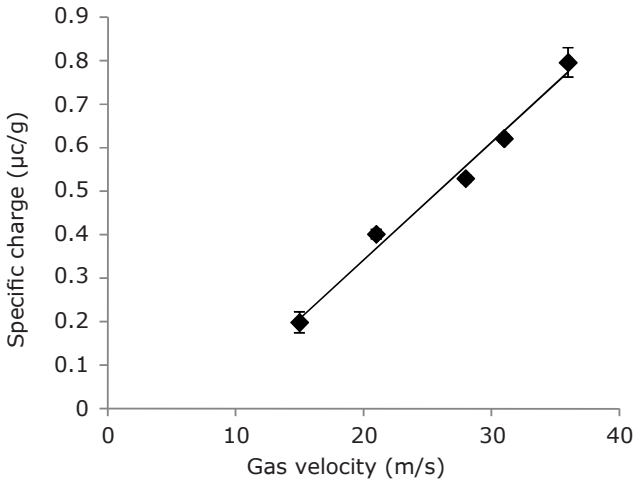

Figure 15. Specific charge of whole bran flour as a function of the carrier gas velocity. The error bars indicate the absolute deviation. The linear line is fitted to the data.

Figure 15 shows that the charge of the whole bran flour increased linearly with the gas velocity, with some offset. However, the change of the AX content and separation efficiency did not relate linearly to the gas velocity. Below 28 m/s, the gas velocity had no influence on the AX content in the negative fraction. An increase of 5% dry matter basis of AX content occurred when the gas velocity was increased to 31 m/s. However, increasing the gas velocity from 21 m/s to 28 m/s could already increase the separation efficiency from 10 % to 16%. Further increasing the gas velocity to 31 m/s gave another 5% increase in separation efficiency.

These results may be explained by the balance between formation and breakdown of agglomerates. As discussed before, the increased charge of particles leads to stronger coulombic interactions and thus more agglomeration of oppositely charged particles. On the one hand, increasing the gas velocity leads to a higher charge and thus an increased chance for agglomeration. On the other hand, a high gas velocity also contributes to break down of agglomerates (Schönert et al., 1996). Above 21 m/s, the gas flow in charging tube starts to transit from laminar to turbulent flow, which might enhance the net breakdown of agglomerates compared to low gas velocities. Therefore, fewer agglomerates may be formed and thus better separation is achieved. To conclude, higher carrier gas velocity is favoured to achieve a better enrichment of AX.

Influence of charging tube length

To verify the hypothesis that longer charging tube facilitates the separation of whole bran flour by increasing the charging of particles, a different length of charging tube was tested.

A shorter charging tube indeed gave a lower specific charge to the whole bran flour (0.46 ±0.00 μC/g), but it resulted in a higher AX content in the negative fraction (Table 2). This can again be explained by the formation of agglomerates in the charging tube. A longer charging tube increases the residence time of particles in the tube, which increases the chance for oppositely charged particles to meet each other and lead to more agglomerates. Due to the higher specific charge, these agglomerates would be difficult to break down in the electric field (Tilmatine et al., 2009).

Summary for the optimization of a single-step electrostatic separation

To summarize, simply increasing the charge of the particles is not enough to have a better separation. A higher charge of particles also leads to more agglomerates. Only if these agglomerates are broken down e.g. at increased gas velocities a better separation can be achieved. Based on the results above, the optimal settings for enriching the AX in this system was found as: whole wheat bran milled at ambient temperature as starting material, 125 cm charging tube, gas velocity of 31 m/s. This optimal condition was used during further experiments.

Combination of electrostatic separation and sieving

Hemery et al. (2011) suggested sieving the whole bran flour with a 50 μm sieve before electrostatic separation to remove the fine particles, which might improve the electrostatic separation performance. However, this may also change the composition of starting material, which might negatively influence the separation. To test both hypotheses, we combined electrostatic separation and sieving in different orders. AX enriched fractions were compared on their yield, AX content and separation efficiency (SE) (Figure 16).

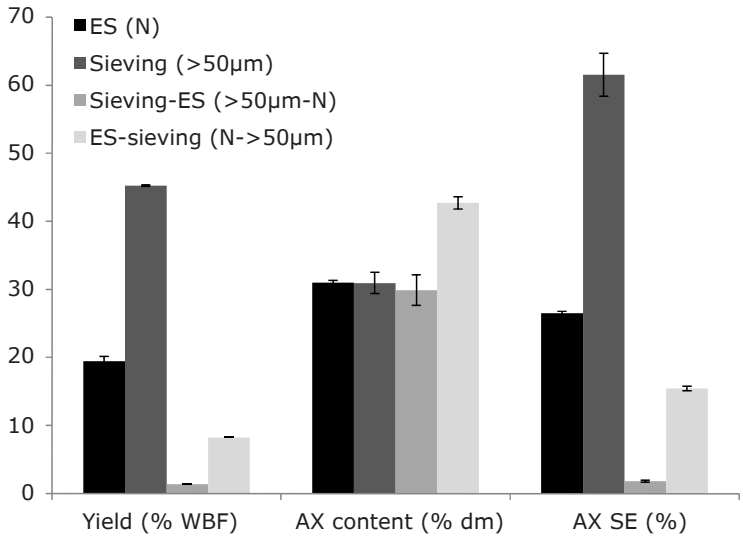

Figure 16. Yield, AX content and AX separation efficiency (SE) of enriched fractions obtained with: only electrostatic separation (N), only sieving (>50 µm), first sieving and then electrostatic separation (>50 µm-N), and first electrostatic separation and then sieving (N->50 µm). ES: electrostatic separation. The error bars indicate the absolute deviation.

With the optimized setting, electrostatic separation alone could enrich the AX from 23% to 30% dry matter basis in the negative fraction (N). The coarse fraction (>50 µm) obtained by sieving had a similar AX content. However, the separation efficiency of sieving was more than twice that of electrostatic separation, which is due to the different yield. As described before, the gravitational force drags particles to the bottom of the separation chamber before particles are attracted to the electrodes. Therefore the horizontal design of the lab-scale electrostatic separator resulted in a larger loss and thus low yield of the AX-enriched fraction (19%). During sieving, there was hardly any loss and 45% of the starting material ended up in the coarse fraction.

A sieving step before electrostatic separation did not further increase the AX content of fraction. In contrast, much lower separation efficiency was found due to the low yield in this fraction (1%), because sieving affected the composition of the starting material in a similar way as cryogenic milling. Fine particles, e.g. starch and protein, tend to be charged positively in electrostatic separation. Removing these particles by sieving is expected to affect the charging behaviour

due to different particle-particle interactions and as a result insufficient charging of the other components, especially of those that tend to take opposite charge, i.e. particles rich in AX.

A sieving step after the electrostatic separation resulted in a fraction with the highest AX content (43% dry matter basis) among the four compared fractions. The structure of the outer pericarp (brush hair, outer epidermis, hypodermis and parenchyma) and the inner pericarp (cross cells) were observed in this fraction by scanning electron microscopy (Figure 17). Because the seed coat and nucellar epidermis are firmly fused with the inner pericarp (Bechtel et al., 2009), they probably also end up in this fraction. Furthermore, almost no starch or protein was found, which confirms that this fraction contains mainly particles from outer pericarp and intermediate layer (inner pericarp, seed coat and nucellar epidermis).

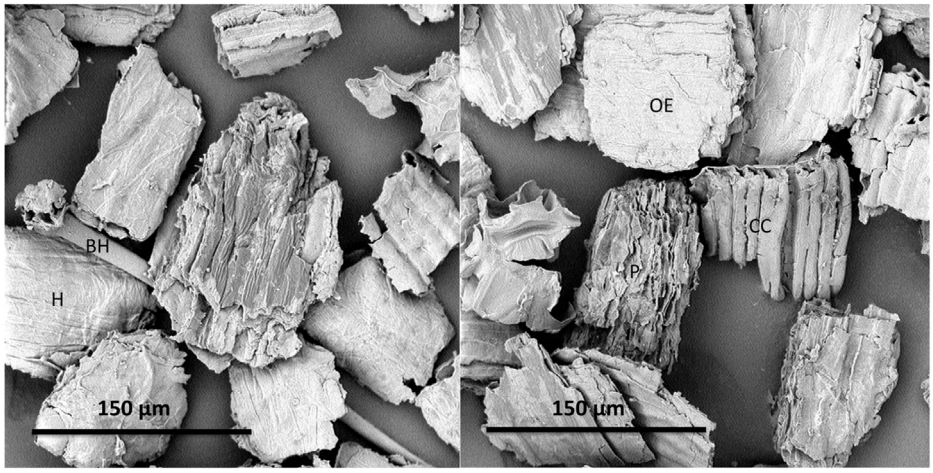

Figure 17. Scanning electron microscope (SEM) image of the AX-enriched fraction obtained with first electrostatic separation and then sieving. Structure of outer epidermis (OE), hypodermis (H), parenchyma (P), brush hair (BH) and cross cells (CC) can be distinguished.

The outer pericarp and intermediate layer together make up 51~54% of the bran weight (Barron et al., 2007; Hemery et al., 2009a), and therefore the maximum theoretical yield of this fraction is 51~54%. The resulting maximum theoretical AX content is then 35~47% dry matter basis based on the AX content of the outer pericarp and intermediate layer and is cultivar-dependent (Barron et al.,

2007; Benamrouche et al., 2002; Brillouet and Joseleau, 1987). Therefore, by adding a sieving step after the electrostatic separation, we were able to achieve the maximum theoretical AX content. The yield was relatively low (8%) due to the large loss caused by the horizontal set-up, but we expect that this can be amended by adjusting the system design: a vertical set-up is expected to provide higher yields.

Conclusions

Electrostatic separation of wheat bran was shown to be based on the histological structure of the bran. During triboelectric charging, particles from the aleurone layer and the endosperm take positive charge, whereas particles from the pericarp adopt a negative charge.

Because AX is mostly present in the pericarp, it was possible to enrich AX with electrostatic separation. Adding a cryogenic milling step after ambient milling did not improve the enrichment of AX, due to agglomeration of the smaller particles, and the overall negative change of the composition of starting material. Additionally, cryogenic milling is undesired for its high energy consumption.

A larger gas velocity improved the enrichment of AX because of the higher charging of the particles and avoiding agglomeration. A short tube was favoured, probably because of the short residence time in the charging tube, which reduce the risk of agglomeration of oppositely charged particles. Therefore, to optimize the enrichment of AX from wheat bran by electrostatic separation, it is important to sufficiently charge the particles while agglomeration is minimized. Combination of ambient milling, shorter charging tube and a high gas velocity was found optimal for AX enrichment. Single step electrostatic separation of wheat bran could increase the AX content from 23% to 30% dry matter basis, which is similar as can be achieved by sieving. However, in comparison to sieving, the yield of the enriched fraction was lower due to the horizontal design of the setup. This may be improved by switching from a horizontally to a vertically designed separator, which is also more practical.

Sieving the wheat four with a 50 μm sieve before the optimized single-step electrostatic separation did not improve the enrichment of AX: the removal of starch and protein changes the composition of the starting material and leads to different particle-particle interactions and thus less charging on particles rich in

AX. However, adding a sieving step with 50 µm sieve after the electrostatic step could effectively remove starch and protein and resulted in a fraction with an AX content of 43% dry matter basis, which is around the maximum theoretical AX content.

Acknowledgements

This research is supported by the Dutch Technology Foundation STW and the Institute for Sustainable Process Technology, ISPT through the DRYFRAC project (grant number 11399). The authors would like to thank their co-workers within the DRYFRAC project in Eindhoven, Korevaar and Padding, and the user committee for stimulating discussions on dry separation.

Charging and separation behaviour of gluten-starch mixtures assessed with a custom-built electrostatic separator

This chapter has been published as:

Wang, J., de Wit, M., Boom, R.M., Schutyser, M.A.I., (2015). Charging and separation behavior of gluten–starch mixtures assessed with a custom-built electrostatic separator. Separation and Purification Technology 152, 164-171.

Abstract

Electrostatic separation is a novel and sustainable process for dry separation of food ingredients. To establish guidelines for electrostatic separation, well-defined charging and separation experiments of model mixtures prepared from wheat gluten and starch were carried out. For this a custom-built bench-scale electrostatic separator was developed. Charging behaviour of mixtures improved with decreasing particle concentration and increasing gas flow rate, which was similar compared to charging behaviour of single materials. However, the charge of mixtures was not simply the sum of the charge of single materials because particle-particle interactions also largely influence the charging. Separation efficiencies for mixtures were found lower than could be expected on the basis of behaviour of single materials in the equipment. This was attributed to formation of agglomerates by particles having opposite charge, which was further confirmed by the observation that dispersibility of the mixtures was poorer than for the single materials. Agglomeration of particles during electrostatic separation can be minimized by using high gas flow velocity, low feed dosing and higher field strength.

Introduction

Dry fractionation has major advantages compared to wet fractionation of foods into ingredients due to its much lower energy consumption and retention of the native ingredient properties (Schutyser et al.; Schutyser and van der Goot, 2011). By combining fine milling and dry separation, dry fractionation separates the material into a fraction that is enriched and one that is depleted in a specific target component, such as protein or fibre (Pelgrom et al., 2015b). Conventionally air classification and sieving are used for the separation step; only recently electrostatic separation has been proposed for dry separation of food materials, although the general principle of electrostatic separation has been applied for decades in mining industries for separation of minerals and purification of coal (Bada et al., 2010; Ban et al., 1997; Cangialosi et al., 2008; Dwari et al., 2015; Li et al., 1999; Trigwell et al., 2003), and also for recycling of plastic waste (Bendimerad et al., 2009; Dodbiba et al., 2002; Inculet et al., 1998; Jeon et al., 2006; Tilmatine and Dascalescu, 2010; Wu et al., 2013; Younes et al., 2015).

Electrostatic separation based on triboelectric charging is found effective for separation of small particulates with small differences in conductivity (Higashiyama and Asano, 1998; Kelly and Spottiswood, 1989b). Triboelectric charging is achieved by entraining particles in a gas flow through a channel, where the particles collide with the walls of the channel and are charged. Subsequently, the charged particles are separated under the influence of an external electric field (Fraas and Balston, 1940; Haga, 1995; Kelly and Spottiswood, 1989c), as they are subjected to a force (F_e), which is the product of the charge on the particle (q_p) and the electric field strength (E). Therefore, the process parameters that influence the charging process and electric field, e.g. particle concentration, gas flow rate, applied voltage and distance between electrodes, influence the effectiveness of separation (Bada et al., 2010; Bendimerad et al., 2009; Cangialosi et al., 2008; Dwari et al., 2015; Gupta et al., 1993). While several studies have demonstrated the possibility of using electrostatic separation to

fractionate food ingredients, e.g. for the enrichment of aleurone layers and fibre-rich layers in different fractions, respectively, from wheat bran and oat bran (Brouns et al., 2012; Chen et al., 2014b; Dascalescu et al., 2010; Hemery et al., 2011; Remadnia et al., 2014; Sibakov et al., 2014; Stone and Minifie, 1988; Wang et al., 2015b), and for the enrichment of protein from legumes (Pelgrom et al., 2015a), the influence of process parameters such as particle concentration, gas flow and electric field on the electrostatic separation of food ingredients has not been systematically studied.

In our previous study, the triboelectric charging behaviour of a single material was investigated (Wang et al., 2014). However, the charging behaviour of a mixture is more complex because particle-particle interactions come into play (Bendimerad et al., 2009; Cangialosi et al., 2008; Forward et al., 2008; Schönert et al., 1996). Therefore, the study reported here aimed at elucidating the role of these interactions, and providing the directions for developing an electrostatic separation process for legumes and cereal. Representative model ingredient mixtures were prepared from purified wheat gluten and starch. Moreover, a custom bench-scale electrostatic separator was constructed, which allowed well-defined charging and separation experiments. The experiments were designed to evaluate the influence of several factors on charging and separation behaviour: the composition of mixture, powder dosing rate, gas flow rate, the applied voltage and the distance between two electrodes.

Materials and methods

Materials

Vital wheat gluten (D[4,3] = 67 μm, D[3,2] = 17 μm) was obtained from Roquette (France) with the following specifications: moisture 6% (w/w), protein 75~80% (w/w), starch 9% (w/w), cellulose <1% (w/w), fat 7% (w/w) and ash 1% (w/w). Wheat starch (D[4,3] = 29 μm, D[3,2] = 9 μm) was purchased from Sigma–Aldrich (Germany) with a moisture content of 10.1 ± 0.6% (w/w). No further drying of the materials was carried out because the moisture content of both materials is within the range that does not influence the charging process (Hemery et al., 2009b; Wang et al., 2014).

Model mixtures of wheat gluten and starch were prepared by mixing the individual components with a weight ratio of 1:9, 2:8, 3:7, 4:6, 5:5, 6:4, 7:3, 8:2 and 9:1. Because the protein content of wheat gluten is ~80%, the corresponding protein contents of the mixtures are 8%, 16%, 24%, 32%, 40%, 48%, 56%, 64% and 72%, respectively.

Bench-scale electrostatic separator

A vertical bench-scale electrostatic separator was constructed to carry out well-defined charging and separation experiments. It consists of four parts: feeding system, charging slit, separation chamber and collecting chamber (Figure 18). The feeding system allows independent control of the powder dosing rate and the carrier gas flow rate by introducing the gas flow in a special-designed unit below the outlet of a screw feeder. The screw feeder can accurately dose powder between 0.5 kg/h and 2.5 kg/h. In the transition unit the particles are dispersed by the gas flow and carried downwards to the charging slit. Inside the charging slit, the particles are charged by tribo-electrification due to particle-particle and particle-wall contact. The charging slit is made of aluminium and consists of

four parallel channels, all having the same dimension of 2.5 mm × 3 mm × 220 mm. After being charged, the particles then are entrained by the gas into the separation chamber, where an electric field is created between two oppositely placed electrodes. One electrode is supplied with a high positive voltage, while the other one is grounded. The two electrode plates were always kept parallel and only the distance between the electrodes was varied. The particles are deflected based on their charge: positively charged particles to the grounded electrode and negatively charged particles to the positive electrode. At the bottom of the separation chamber two filter bags are mounted to collect the positively charged fraction (PF) and negatively charged fraction (NF), respectively.

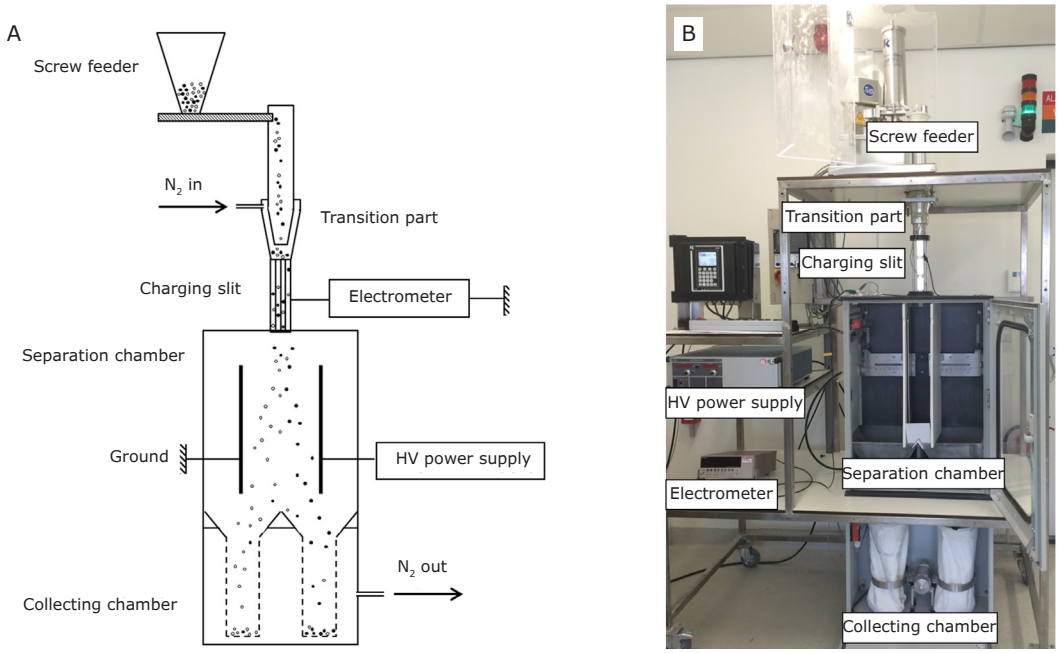

Figure 18. A) Schematic drawing and B) a picture of bench-scale electrostatic separator.

Charge measurement

An electrometer (Keithley Model 6215) was connected to the charging slit to measure the impact charge obtained by the slit, and hence of the particles colliding with the slit surface. The measurement and calculation of the specific particle charge, defined as the charge-to-mass ratio, was adapted from a previous study (Wang et al., 2014). All measurements were carried out in duplicate.

Separation experiment

Before each separation experiment, the entire system was flushed with dry nitrogen for safety reasons. The run time was adjusted for different powder dosing rates to allow 25 g of powder dosed for each experiment. Five parameters were varied: the gluten-to-starch weight ratio (1:9 – 9:1); the powder dosing rate (0.5 – 2.5 kg/h); the gas flow rate (5 – 30 L/min); the electric field strength (100 – 250 kV/m, by changing the applied voltage between 10 – 25 kV at a distance of 10 cm between the electrodes) and distance between the electrodes (10 – 25 cm). Only one parameter was varied at a time while the others were kept constant. From each experiment a positively charged fraction (PF, including the material deposited on the ground electrode and retained in the left collector) and a negatively charged fraction (NF, including the material deposited on the positive electrode and retained in the right collector) were collected, weighed and analysed on protein content. All the experiments were carried out in duplicate.

Separation behaviour was evaluated by determining protein concentrations, relative yield of the fractions and protein separation efficiency. Protein separation efficiency (*PSE*) is defined as the percentage of protein recovered in the target fraction from the protein in the starting material and is calculated by Eq. 4 (Schutyser and van der Goot, 2011).

$$PSE = \frac{Y_f \cdot P_f}{P_m} \qquad \text{(Eq. 4)}$$

where Y_f is the yield of the fraction, P_f is the protein concentration of the fraction and P_m is the protein concentration of starting material.

On the basis of the distribution behaviour of the individual components (wheat gluten or starch) in the equipment, separation behaviour of their mixture was predicted. This estimation neglected particle-particle interactions and thus the role of these interactions could be investigated. The predicted yield (Y_f^{pre}) and protein concentration (P_f^{pre}) were calculated as follows:

$$Y_f^{pre} = \frac{G_m \cdot Y_f^g + (100 - G_m) \cdot Y_f^s}{100} \qquad \text{(Eq. 5)}$$

$$P_f^{pre} = \frac{G_m \cdot Y_f^g \cdot P^g}{100 \cdot Y_f^{pr}} \quad \text{(Eq. 6)}$$

where G_m is the gluten content of the mixture, Y_f^g is the yield of the fraction when only gluten was used, Y_f^s is the yield of the fraction when only starch was used and P^g is the protein concentration of 'pure' wheat gluten.

Protein concentration

The protein concentration was analysed using Dumas analysis (Nitrogen analyser, FlashEA 1112 series, Thermo Scientific, Interscience). A conversion factor of N × 5.7 was used. All measurements were carried out in duplicate.

Dispersibility analysis

The dispersibility of powder was analysed according to the pressure titration method described by Pelgrom et al. (2014). The particle size distribution was measured at different dispersion pressures between 10 and 400 kPa, by using Mastersizer 2000 equipped with a Scirocco 2000 dry dispersion unit (Malvern Instruments, Worcestershire, UK). It was assumed that at the highest pressure (400 kPa) full dispersion is achieved, while at lower air pressures the particles do not fully disperse as they remain agglomerated, which results in a larger particle size. The dispersibility was expressed by the degree of de-agglomeration (*DDA*) calculated according to Eq. 7 (Jaffari et al., 2013).

$$DDA = \frac{D_{HP}}{D_P} \quad \text{(Eq. 7)}$$

where D_{HP} is the D_{50} at the highest dispersion pressure and D_P is the D_{50} at each dispersion pressure. A full dispersion is achieved when $DDA = 1$.

Results and discussion

Charging of isolated wheat gluten and starch

Because the bench-scale electrostatic separator allows independent control of the powder dosing rate and the carrier gas flow rate, it was possible to investigate the influence of the particle concentration in the charging slit and the gas flow rate independently. The particle concentration (v/v%) was calculated by assuming that the particles moved along at the same overall rate as the carrier gas. This assumption aims to make the calculation simple while keeping in mind that in charging slit the actual particle concentration can be higher than calculated, because the particles might move slower than the carrier gas due to collisions with the wall and possible electrostatic effect (Korevaar et al., 2014). At a constant gas flow rate, different particle concentrations were achieved by varying the powder dosing rate (0.5 – 2.5 kg/h). Because of the different particle densities for wheat gluten (1350 kg/m^3) and starch (1500 kg/m^3), the particle concentration at the same powder dosing rate is different for the two materials.

In Figure 19-A it can be observed that at a gas flow rate of 10 L/min, the specific charge of both gluten and starch slightly decreased with higher particle concentration in the charging slit. This can be explained by the decreased probability of particle-wall collisions due to the presence of more particles in the slit (Matsusaka et al., 2010; Watano, 2006). When we increased the gas flow rate from 10 L/min to 20 L/min at constant particle concentration of 0.12 v/v% by adjusting the powder dosing rate accordingly, the specific charge for both materials increased strongly (Figure 19-B). This can be explained by the increasing impact velocity when particles collide with the slit wall, which results in a larger contact surface and as a result higher charge obtained by the particle (Yamamoto and Scarlett, 1986). Furthermore, the transition from laminar to turbulent occurs around 20 L/min (Reynolds number ~2100) in the charging slit, which is expected to result in more collisions with the wall (Wang et al., 2014). In other words, the decrease in specific charge caused by high particle

concentration can be compensated by increasing the gas flow rate. Because of their influence on charging, particle concentration and gas flow rate are expected to be critical factors for electrostatic separation.

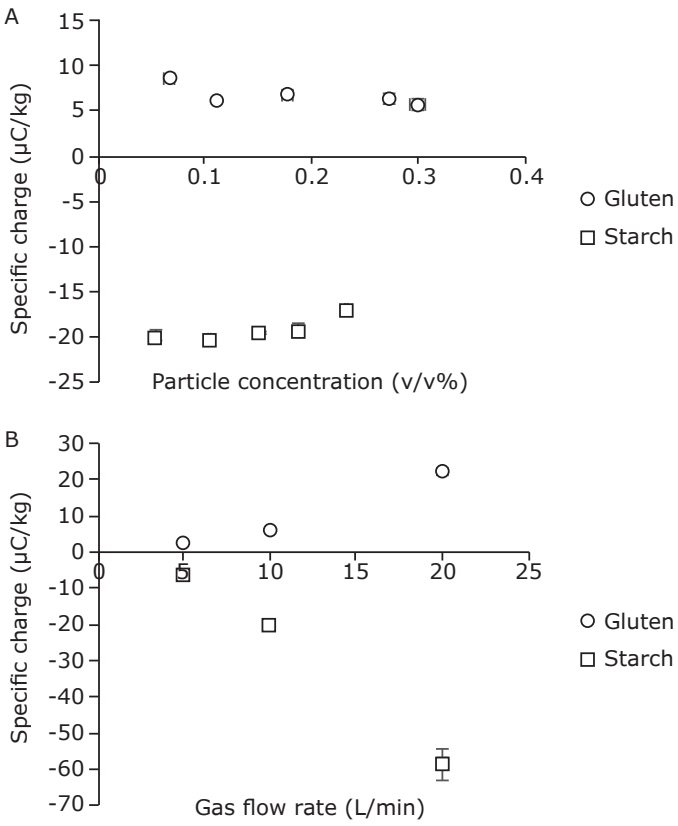

Figure 19. Charging of wheat gluten and starch A) as function of particle concentration in charging slit, with gas flow rate of 10 L/min; B) as function of gas flow rate, with particle concentration of 0.12 v/v%. The error bars indicate the absolute deviation.

Charging and separation of mixtures with different gluten to starch ratio

To investigate the influence of composition on charging and separation of binary mixture, a series of gluten-starch mixtures were prepared with gluten to starch weight ratio ranging from 1:9 to 9:1. Because the protein content of 'pure' wheat gluten is ~80%, the protein content of the mixtures ranged from 8% to 72%. Electrostatic separation was carried out with a dosing rate of 2.5 kg/h, a gas flow rate of 10 L/min, an applied voltage of 15 kV and a distance between the two electrodes of 10 cm. The same settings were also applied with only wheat gluten or starch as feed for predicting charging and separation behaviour of the mixtures.

Influence of the mixture composition on charging

The measured specific charge of the mixtures is plotted as a function of the initial protein content in Figure 20. A line was drawn for the predicted charge on the basis of the measured charge of wheat gluten and starch at the same conditions during single material experiments. A linear relation between the specific charge of the mixture and the gluten-to-starch ratio was assumed for this. The specific charge of all mixtures deviated from the predicted values, indicating that the charge of the mixture is not simply a sum of the charge of the two individual components and particle-particle interactions are important (Forward et al., 2008). Besides particle-wall collision, in practice collisions between gluten particles and starch granules contribute to charge exchange between the two materials. Subsequently, when the charged particles collide with the walls, the existing charge of the particles will influence the charge transferred to the wall differently from single-material system (Korevaar et al., 2014; Matsusaka et al., 2010; Watano, 2006). Furthermore, when charged gluten particles and starch granules contact with each other, they can agglomerate due to their opposite charge. This effect also influences the overall charging behaviour of the mixture. More quantitative explanation of the velocity and position of the particles during charging is reported in a separate paper (Korevaar et al., 2015).

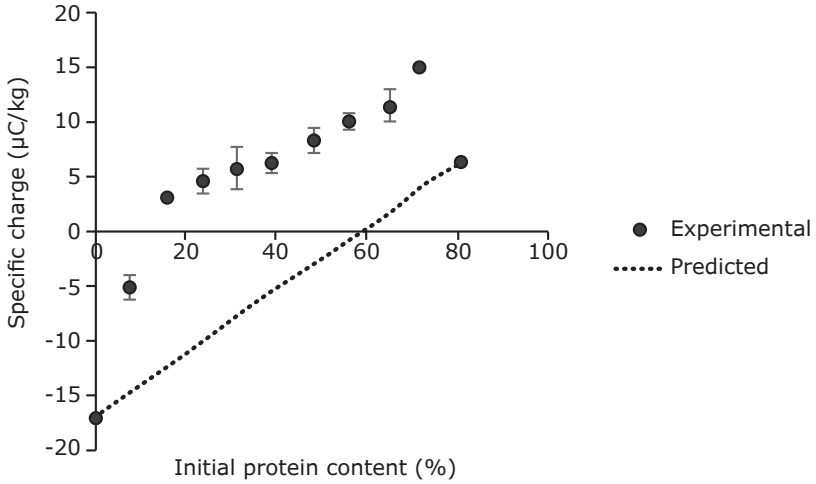

Figure 20. Specific charge of gluten-starch mixtures as a function of initial protein content, with powder dosing rate 2.5 kg/h and gas flow rate 10 L/min. The predicted line is calculated by assuming a linear relation between the charge of the mixture and the composition of the mixture. The error bars indicate the absolute deviation.

Influence of the mixture composition on separation

The yield of the positively charged fraction (PF) increased with increasing initial protein content, while the yield of the negative charged fraction (NF) decreased (Figure 21-A). This can be explained because gluten obtains a positive charge and thus is enriched in the positively charged fraction. With the increase of the initial protein content (gluten-to-starch ratio), more material took a positive charge and therefore the yield of the positively charged fraction increased. However, for mixtures with initial protein content lower than 65 %, the yield of the positively charged fraction was lower than the predicted value, along with a relative larger loss. This can be related to agglomeration and the poor dispersibility of those mixtures. As can be seen in Figure 22-A, the degree of de-agglomeration (*DDA*) decreased with decrease of the dispersion pressure for all powders, indicating that the low dispersion pressure was not sufficient to break the agglomerates formed by fine particles.

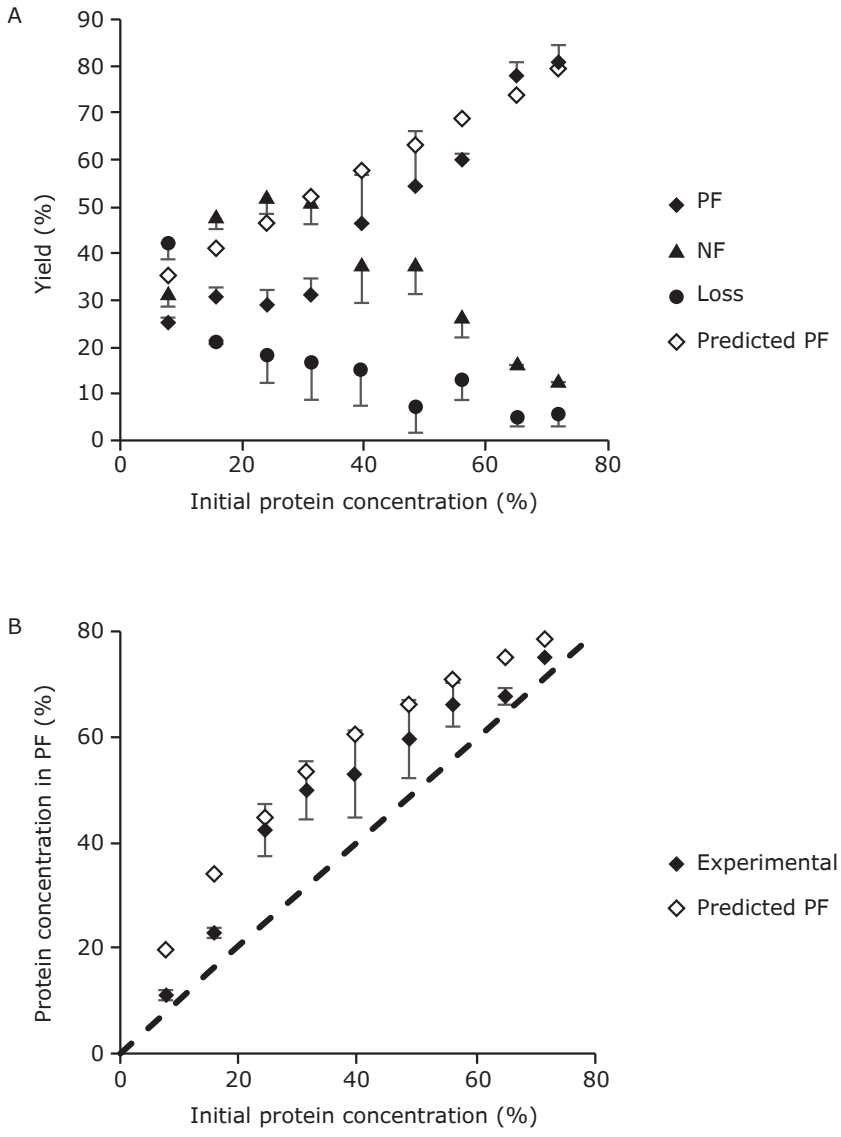

Figure 21. Separation of gluten-starch mixture at powder dosing rate 2.5 kg/h, gas flow rate 10 L/min, applied voltage 15 kV and distance between electrodes 10cm: A) Yield of the positively charged fraction (PF), the negatively charged fraction (NF) and the loss fraction (Loss) as a function of initial protein concentration and B) Protein concentration of the positively charged fraction (PF) as a function of the initial protein concentration. The dashed line indicates the initial protein concentration. The predicted values are calculated on the basis of results of only wheat gluten or starch at the same conditions. The error bars indicate the absolute deviation.

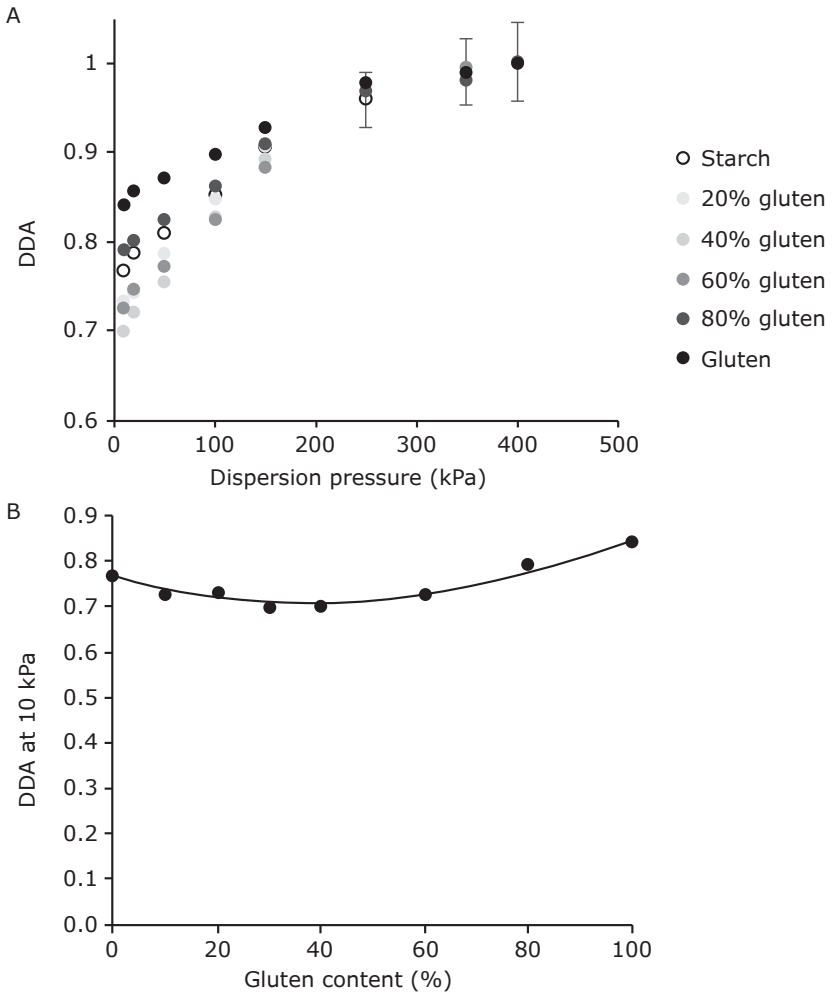

Figure 22. A) Degree of de-agglomeration (DDA) of gluten-starch mixtures as function of dispersion pressure and B) DDA at 10 kPa as a function of gluten content in the mixture. The line is drawn to guide the eye. The error bars indicate the absolute deviation.

Figure 22-B compares the *DDA* at 10 kPa for all powders. 'Pure' gluten has a higher DDA than pure starch (0.84 compared to 0.77), which may be a result of the lower cohesive forces between gluten particles due to their larger particle size and surface roughness (Figure 23) (Islam et al., 2005; Lam and Newton, 1992). The roughness reduces the effective contact area of the contact surfaces and therefore the cohesive force between particles (Islam et al., 2005; Rietema, 1991; Tsukada et al., 2004). Mixing gluten and starch together resulted in an initial decrease and then an increase of the *DDA*. This is not completely in

agreement with the findings of Dijkink et al. (2007) that the dispersibility of wheat starch-protein mixture increases with increasing protein content because of the better dispersibility of wheat protein. Our finding can be explained by the change in the attractive electrostatic forces between gluten particles and starch granules, and subsequent formation of agglomerates. Because both gluten and starch have considerably low moisture content and are probably further dried out by the dry carrier nitrogen gas, the main attractive force between the powders should be electrostatic forces and van der Waals forces (Lam and Newton, 1992). According to Horn and Smith (1992), the attractive forces between dissimilar surfaces caused by electrostatic charging can be two orders of magnitude larger than the van der Waals forces. With SEM pictures we observed agglomerates of gluten particles and starch granules (Figure 23-A). The more gluten was added to the mixture, the more agglomerates are formed and as a result the lower the dispersibility is. Only when the gluten is the predominant type of particle in the mixture, the dispersibility of the mixture is determined by the dispersibility of gluten and increased with further increase of the gluten content.

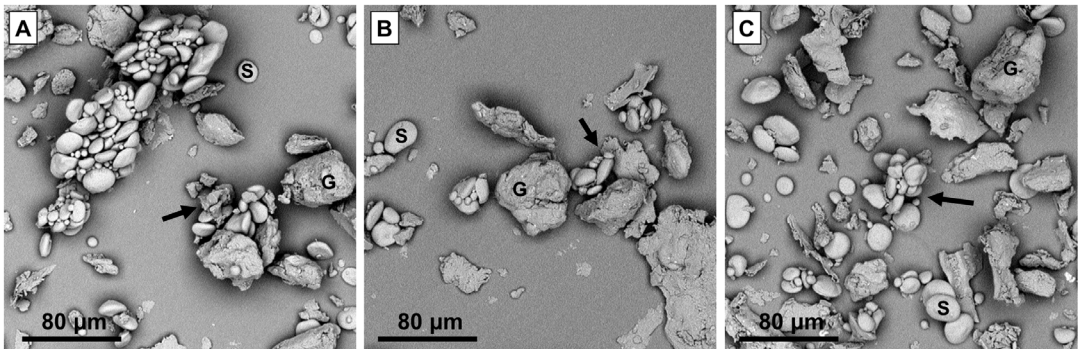

Figure 23. Scanning electron microscope (SEM) images of A) a 6:4 gluten-starch mixture, B) positively charged fraction (PF) from the 6:4 gluten-starch mixture and C) negatively charge fraction (NF) from the 6:4 gluten-starch mixture. Arrows indicate the agglomerates formed by starch (S) and gluten (G).

The protein concentrations of the positively charged fraction is plotted as a function of the initial protein content in Figure 21-B. Protein was enriched in the positively charged fraction for all the mixtures. However, for most mixtures the protein enrichment did not reach the predicted value. This again may be due to particle-particle interactions and as a result of agglomeration of oppositely charged particles (Gupta et al., 1993; Schönert et al., 1996). After agglomeration,

the net charge on the particle cluster is partly neutralized. An agglomerate rich in gluten will have a slight positive charge and one rich in starch will have a slight negative charge. As a result the agglomerates may move to either electrode (Figure 23-B and C), depending on their composition, which results in a poor separation. The attractive electrostatic force between the oppositely charged particles is so strong that the agglomerates will not break easily by the electric field or by subsequent collisions (Gupta et al., 1993). The low protein enrichment for mixtures with low initial protein content (1:9 and 2:8) can be explained in this way. Only at higher gluten contents, the clusters will become positively charged, and thus predominantly end up in the positively charged fraction. The protein enrichment for mixtures with high gluten to starch ratio (8:2 and 9:1) was almost zero, since the initial protein content of the mixture was already close to the maximum, and not much further enrichment can be obtained. Concluding, to achieve a good separation, the mixture should exhibit high dispersibility and sufficient charging of the individual species should be achieved.

The influence of operating conditions on the separation of gluten-starch mixture

Since the particle-particle interactions are expected to play an important role in both the charging and the separation of gluten-starch mixture, operating conditions that can reduce agglomeration or counteract the effect of agglomeration are expected to improve the separation. Therefore, influences of particle concentration, gas glow rate, electric field strength and distance between the electrodes on the separation behaviour of a 1:1 gluten-starch mixture were studied. For all the experiments the specific charge of the mixture was online measured.

Particle concentration

Similarly to the single-material system, the specific charge of the mixture decreases strongly with increasing particle concentration (Figure 24-A) due to the decreased possibility of particle-wall collision. Similar influence was also observed for mixtures of different minerals (Ban et al., 1997; Cangialosi et al., 2008; Li et al., 1999).

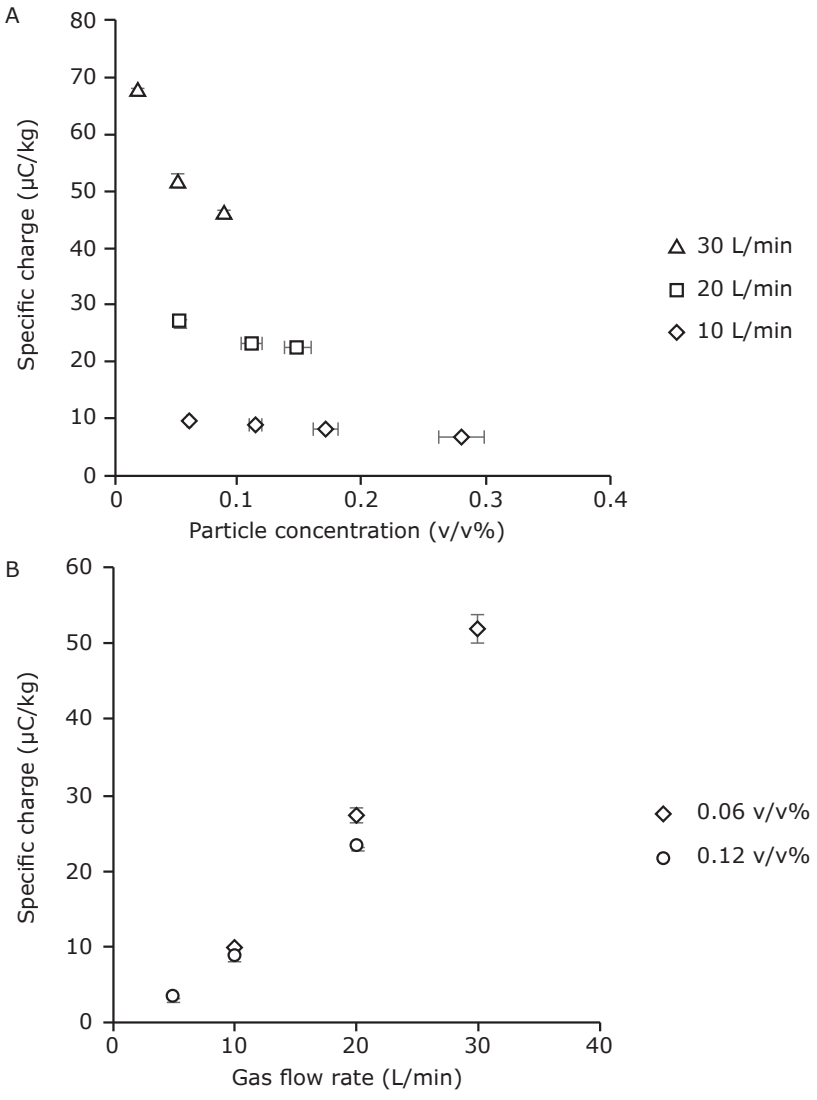

Figure 24. Specific charge of 1:1 mixture as a function of A) particle concentration in the charging slit and B) gas flow rate. Error bars indicate the absolute deviation.

With a gas flow rate of 10 L/min, an applied voltage of 15kV and a distance between the electrodes of 10cm, four powder dosing rates (0.5 kg/h, 1 kg/h, 1.5 kg/h and 2.5 kg/h) were applied. Both the yield and protein separation efficiency of the positively charged fraction (PF) decreased with increasing powder dosing rate (Figure 25-A and E). This may be explained by the net result of a decreasing specific charge and an increasing space charge effect in the electric field (Cangialosi et al., 2008).

The space charge effect is the shielding effect caused by charged particles. When charged particles approach the electrode with an opposite charge, the charge on the electrode is shielded by the charge on the particles and as a result the electric field strength is reduced. As a consequence, the electrostatic force sensed by the particles will be lower (Cangialosi et al., 2008). In our case, starch particles take more charge than gluten particles, and therefore starch particles have a larger influence on the space charge (Li et al., 1999). As a consequence, the gluten particles will experience a lower electrostatic force, resulting in a lower yield and separation efficiency.

Gas flow rate

Gas flow rate had a similar impact on the specific charge of mixtures as on single materials (Figure 24-B). Higher gas flow rate results in a higher impact velocity and turbulence when it is higher than 20 L/min (Reynolds number ~2100), and therefore a higher specific charge.

Because the decrease in specific charge caused by high particle concentration can be compensated by increasing the gas flow rate, higher gas flow rate is expected to improve the yield and protein separation efficiency as well. Figure 25-F shows that the separation efficiency of protein does increase with increasing gas flow rate from 10 L/min to 30 L/min while the particle concentration was kept constant at 0.12 v/v% by adjusting the powder dosing rate accordingly, applied voltage was kept at 15 kV and the distance between electrodes were kept at 10 cm. In addition to the positive influence on the specific charge of particles, a higher gas flow also results in a shorter residence time of particles in both charging slit and electric field, which may reduce the degree of agglomeration and the influence of space charge (Cangialosi et al., 2008).

A higher gas flow rate also results in a larger loss (Figure 25-B). This was caused by the circulation of gas in the separation chamber when the flow is high, which distributed fine particles across the separation chamber resulting in more loss.

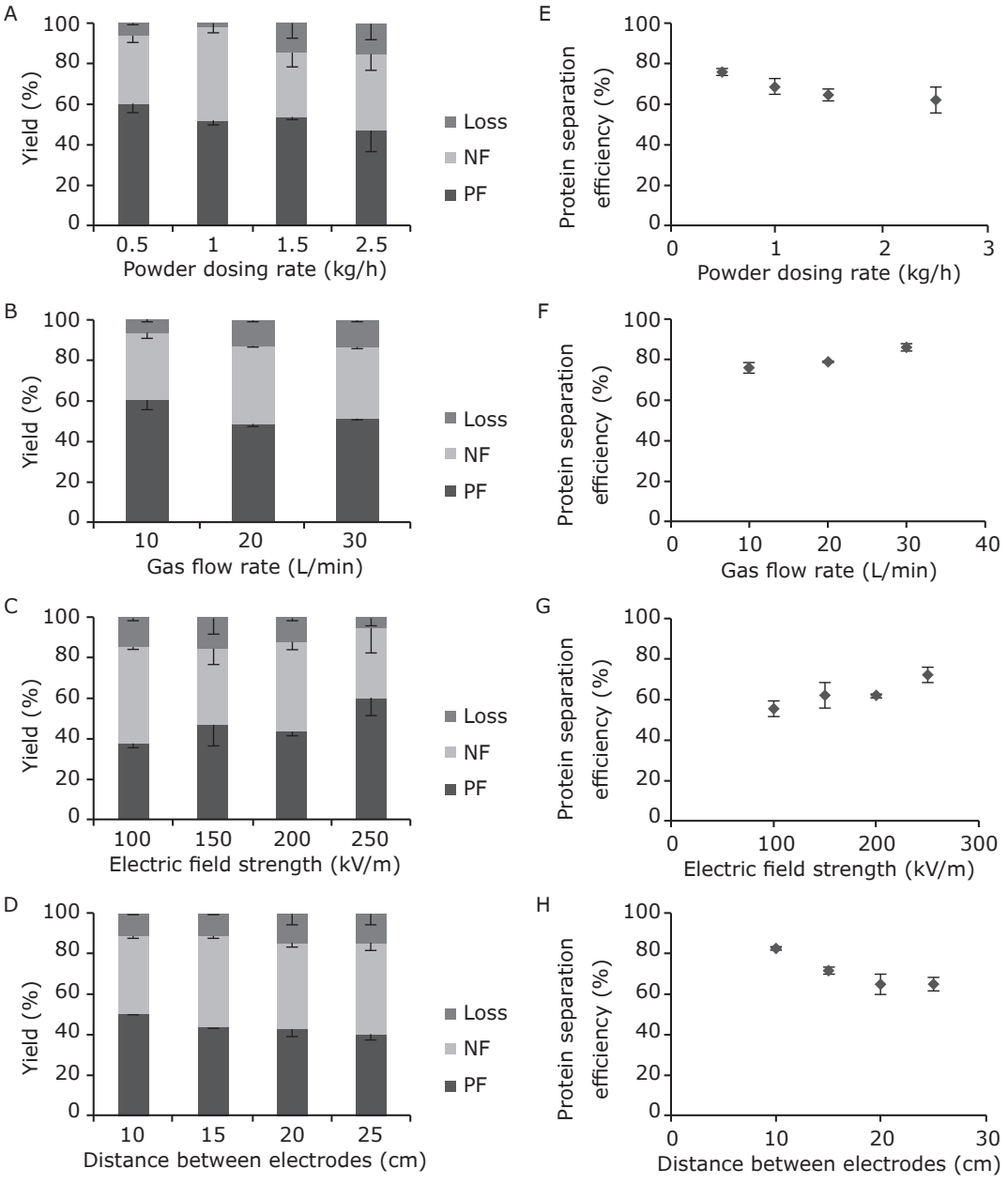

Figure 25. Separation of a 1:1 gluten-starch mixture: yield of positively charged fraction (PF), negatively charged fraction (NF) and loss fraction (Loss) as function of A) particle concentration, B) gas flow rate, C) electric field strength and D) distance between two electrodes; protein separation efficiency of positively charged fraction (PF) as function of E) particle concentration, F) gas flow rate, G) electric field strength and H) distance between two electrodes. The error bars indicate the absolute deviation.

Electric field strength

Electric field strength was varied between 100 – 250 kV/m by changing the applied voltage to the electrode between 10 – 25 kV while keeping the distance between the electrodes at 10cm. The powder dosing rate and gas flow rate were also kept constant at 2.5 kg/h and 10 L/min, respectively. An increase in the electric field strength gives a higher yield and higher protein separation efficiency (Figure 25-C and G). This indicates that at lower electric field strengths, not all particles can be captured by the field.

Distance between electrodes

Calin et al. (2008) mentioned in their study that charged particles which collide with the electrode may bounce back and end up in the "wrong" fraction. Furthermore, Cangialosi et al. (2008) found that charged particles that are deposited on the electrode might exchange charge with the electrode, become oppositely charged, and rebound to the other electrode. Therefore, with the same electric field strength, more distance between the two electrodes is expected to positively influence the separation of the mixture because it allows more particles to fall into the collector without contacting the electrode. To test this hypothesis, separation of a 1:1 mixture was done with the distance varied from 10 to 25 cm while the powder dosing rate, gas flow rate and electric field were fixed at 2.5 kg/h, 10 L/min and 1 kV/cm, respectively. However, in contrast to the hypothesis, both yield and separation efficiency of the positively charged fraction decreased with increasing distance between electrodes (Figure 25-D and H). This may be explained by the reduced gas flow between the electrodes, which resulted in a longer residence time of particles in the electric field. As a consequence, the chance for agglomeration and the effect of space charge increased, which negatively influences the separation.

To summarize, lower powder dosing rate, higher gas flow rate, higher voltage on electrode and shorter distance between two electrodes enhanced separation of the 1:1 gluten to starch mixture.

Conclusions

A custom-built electrostatic separator was used to investigate the influence of various parameters on electrostatic separation of gluten and starch particles. Results showed that the specific charge of both gluten and starch increased with decreasing particle concentration in the charging slit and with increasing gas flow rate. To a certain degree, the loss of specific charge with increasing concentration can be compensated for by using a larger gas flow rate.

The net charge of gluten-starch mixtures is not simply a sum of the charge of the two individual components, indicating that particle-particle interactions play an important role during the charging of the mixture. The yield of the positively charged fraction increased with the initial protein content. For all the mixtures, protein was enriched in the positively charged fraction, but the enrichment was not as high as predicted. We hypothesize that the poorer separation is due to the formation of agglomerates between positively and negatively charged particles. This was supported by the fact that the dispersibility for mixtures of the two components was lower compared to the individual components.

During electrostatic separation of a mixture, it is important to find the optimal condition that charges the particles sufficiently, but avoids the agglomeration between oppositely charged particles, and reduces the space charge effect. This can be achieved by a combination of lower dosing rate, higher gas flow rate and higher electric field strength. However, it is important to realize that a lower dosing rate and higher gas flow rate will result in low throughput and high costs for the gas flow, while high electric field strength may result in electric discharge between the electrodes and has to be avoided at all times.

Acknowledgements

This research is supported by the Dutch Technology Foundation STW and the Institute for Sustainable Process Technology, ISPT through the DRYFRAC project (grant number 11399). The authors would like to thank their co-workers within the DRYFRAC project in Eindhoven, Korevaar and Padding, and the user committee for stimulating discussions on dry separation.

Lupine protein enrichment by milling and electrostatic separation

This chapter has been published as:

Wang, J., Zhao, J., de Wit, M., Boom, R.M., Schutyser, M.A.I., (2015). Lupine protein enrichment by milling and electrostatic separation. Innovative Food Science & Emerging Technologies.

Abstract

Lupine seeds are an excellent source of plant protein. We here report on dry fractionation by combining milling and electrostatic separation providing an alternative to wet extraction of protein from lupine seeds. Relatively coarse milling was preferred as this provides sufficient detached protein bodies with less agglomeration of particles. After a single separation step a fraction with a protein content 57.3 % dry matter basis was obtained. After three successive steps protein content was increased further to 65.0 % dry matter basis. By extra milling and recycling the fractions with comparable protein content as the flour, yield was improved without compromising protein content. A final fraction with a protein content 65.1 % dry matter basis and yield of 6% was obtained, which means 10% of protein in the flour was recovered. Based on our findings an optimized scheme for protein enrichment from lupine seeds by combining milling and electrostatic separation is proposed.

Introduction

The quickly growing world population requires a rapid increase in the production of protein-rich foods (Bruinsma, 2009). The production of animal protein is intensive in the use of resources, such as land, water, nutrients and especially valuable plant proteins (Aiking, 2011). Including those plant proteins directly in the human diet would be more sustainable. Lupine recently has gained attention as a 'novel' plant protein ingredient source for foods because of its high protein content in seeds (38 – 40 g/100 g dry seeds) (Hove, 1974; Lqari et al., 2002) and its ability to grow in temperate climates and different soil types (Maxted et al., 2001). With these characteristics, lupine represents a significant alternative to soybean. Therefore, lupine protein has been investigated for its emulsifying, foaming and gelling properties etc. (Berghout et al., 2015a; Berghout et al., 2015c; Lqari et al., 2002; Pelgrom et al., 2014; Pollard et al., 2002; Pozani et al., 2002) and has been explored as additive to food/feed products, e.g. baking product, processed meat product and fish meal (Alamanou et al., 1996; Dervas et al., 1999; Draganovic et al., 2014; Drakos et al., 2007; Papavergou et al., 1999).

Protein exists in lupine seeds mostly in the form of protein bodies (Figure 26). The protein bodies have sizes between 5 and 25 μm (Le Gal and Rey, 1986), with a protein content of 73 g/100 g protein bodies (Plant and Moore, 1983). Other main cellular components in lupine seeds are carbohydrates including fibre and soluble sugars (43 – 48 g/100 g dry seeds) and lipids (7 – 10 g/100 g dry seeds) (Lqari et al., 2002; Sujak et al., 2006). Conventional extraction of protein from seeds involves large quantities of organic solvent and water to remove the lipids and soluble carbohydrates (Alamanou and Doxastakis, 1995; Jayasena et al., 2011). Furthermore, the drying step afterwards is energy intensive. Aqueous fractionation that skips the defatting step was proven to be a more sustainable method (Berghout et al., 2014; Berghout et al., 2015b; Jung, 2009), but still cannot avoid the large consumption of water and energy because a drying step

is still needed. Alternatively, dry fractionation by combining proper milling and air classification consumes no water and hardly any energy and has resulted in functional protein enriched fractions (Pelgrom et al., 2014; Schutyser et al.; Schutyser and van der Goot, 2011).

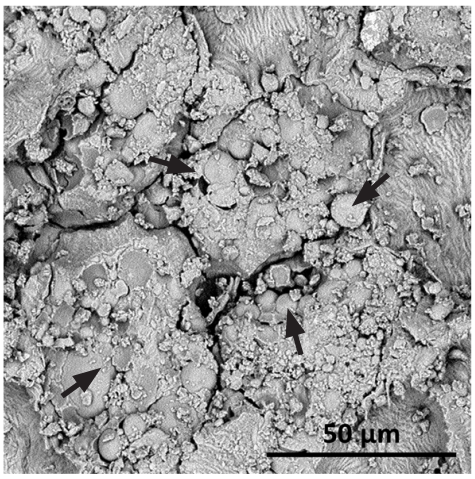

Figure 26. Scanning electron microscope (SEM) image of a section of lupine seed. Arrows indicate the protein bodies (PB).

A disadvantage of dry fractionation is the low purity obtained, compared to wet fractionation. By applying milling and air classification to lupine seeds, the protein content in the fine fraction could reach a maximum 59 % dry matter basis, with a yield of 6 – 10% (Pelgrom et al., 2014). The main cause for this low purity was the presence of fine fibre fragments in the fine fraction (Pelgrom et al., 2014). Intensive milling not only opens the cellular structure and detaches the protein bodies from other cellular components, but also breaks fibre fragments to smaller sizes. Because air classification is based on particle size and density, these fine fibre fragments then accumulate in the fine fraction and reduce the overall protein content. Therefore, to improve the purity and yield of protein enriched fraction obtained by dry fractionation, a separation process based on a different driving force is needed.

Recently, electrostatic separation based on triboelectric charging and subsequent separation of particles in an electric field was explored as an alternative to dry separate food materials (Brouns et al., 2012; Chen et al., 2014b; Hemery et al., 2011; Pelgrom et al., 2015a; Sibakov et al., 2014; Stone and Minifie, 1988;

Wang et al., 2015b). Due to their different tribo-electrostatic properties, different materials such as protein and fibre, charge either positively or negatively when sliding along a surface made of another material. Pelgrom et al. (2015a) applied electrostatic separation as a post-treatment to further increase the protein content of the fractions obtained by air classification. It was observed that electrostatic separation could deliver lupine protein enriched fractions (protein concentration of ~59 % dry matter basis) not only from the fine fraction, but also directly from the coarse fraction and whole flour.

Pelgrom et al. (2015a) carried out an explorative study on a lab-scale electrostatic separator described by Wang et al. (2015b), but the influence of milling conditions on the separation performance was not considered. Proper milling is crucial to obtain good separation, because the cellular components need to be disassociated from each other and the particles need to be small enough to take sufficient charge, but at the same time the particles may not be too small to avoid risk of agglomeration of the particles (Lam and Newton, 1992; Wang et al., 2015a). Moreover, milling also exposes the lipids, which promotes the agglomeration by liquid bridging between particles (Pelgrom et al., 2014).

Therefore, the current study aims to produce protein enriched fractions from lupine using a custom-built bench-scale electrostatic separator that allows better defined experiments (Wang et al., 2015a). Lupine flours with different particle size distributions obtained by impact milling were used to investigate the influence of milling conditions on electrostatic separation. After establishing the optimal milling conditions, a single-step electrostatic separation was carried out with different carrier gas flow rates. Subsequently, multiple-step electrostatic separations were explored based on the optimal conditions from the single-step process to further increase protein enrichment. Furthermore, methods that could increase both the purity and yield were tested to fully optimize the separation. Finally, an optimised scheme is proposed for lupine by electrostatic separation.

Materials and methods

Preparation of lupine flour

Dry lupine seeds, *Lupinus angustifolius L.*, were purchased from L.I. Frank (Twello, The Netherlands). To obtain lupine flour, the seeds were first pre-milled with a pin mill (LV 15M, Condux-Werk, Wolfgang bei Hanau, Germany). The grits were then further milled to flour with a ZPS50 impact mill (Hosokawa- Alpine, Augsburg, Germany). The air flow was 80 m^3/h and the impact mill speed was fixed at 8000 rpm. The classifier wheel speed was 2500, 4000, 6000 or 8000 rpm to obtain flours with different particle size distributions. The moisture content of the flours was in the range of 8 – 10 %, a range of values assumed to provide no difference in charging behaviour (Wang et al., 2014). Therefore, the flours were used directly for electrostatic separation without further drying. All flours and fractions were stored at -20 °C in sealed containers.

Electrostatic separation

The electrostatic separation experiments were carried out with a custom-built separator described previously in large detail (Wang et al., 2015a). For each single-step electrostatic separation experiment, ~25 g of lupine flour was dosed by the screw feeder into the system with a dosing rate of 1.25 kg/h. The flow rate of the carrier nitrogen gas was set at 10, 20 or 30 L/min. The electric field strength applied was kept at 200 kV/m by applying a voltage of 20 kV to the positive electrode and keeping the distance between the electrodes at 10 cm. From each experiment four fractions were obtained: one from the ground electrode, labelled ‘GE’, one from the positive electrode labelled ‘PE’, one from the collecting filter bag below the ground electrode labelled ‘GC’ and one from the collecting filter bag below the positive electrode labelled ‘PC’. According to the study of Pelgrom et al. (2015a), lupine protein takes positive charge and will be deflected towards the ground electrode. Therefore the fractions GE and GC are expected to be protein enriched.

For multiple-step electrostatic separation experiments (Figure 27), ~ 400 g of lupine flour was used for each experiment. The other parameters were set according to the optimal settings established during the single-step experiments. After the first electrostatic separation step, the fraction GE (relabelled as 'GE1') was subject to another electrostatic separation and again resulted in four fractions: GE2, PE2, GC2 and PC2. Then a third electrostatic separation was carried out with the fraction GE2 and yielded another four fractions: GE3, PE3, GC3 and PC3. Depending on the amount of fraction GE3 and its purity, more steps of electrostatic separation could be done yielding four fractions from each step. All fractions were analysed on yield and protein content.

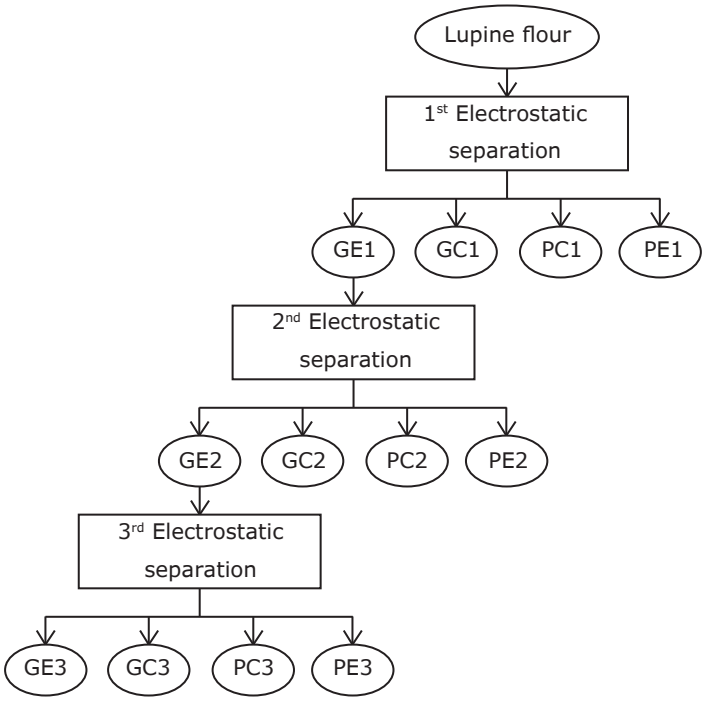

Figure 27. Scheme of multiple-step electrostatic separation. 'GE', 'GC', 'PC' and 'PE' are the fractions from the ground electrode, the filter bag below the ground electrode, the filter bag below the positive electrode and the positive electrode, respectively. The number indicates from which step the fractions are obtained.

Particle size distribution

The particle size distributions of the samples were determined by laser diffraction using a Mastersizer 2000 in combination with the Scirocco 2000 dry dispersion unit (Malvern Instruments Worcestershire, UK). All measurements were performed in duplicate.

Protein content

The protein content was analysed with Dumas analysis (Nitrogen analyser, FlashEA 1112 series, Thermo Scientific, Interscience). A conversion factor of N × 6.25 was used (El-Adawy et al., 2001). All measurements were performed in duplicate.

Results and discussion

Influence of milling condition on electrostatic separation

To investigate the influence of milling conditions on electrostatic separation, the classifier wheel speed was varied (2500, 4000, 6000 and 8000 rpm) during impact milling while keeping the air flow and mill speed constant at 80 m^3/h and 8000 rpm, respectively. Subsequently, the obtained flours were subjected to electrostatic separation with a dosing rate of 1.25 kg/h, a gas flow rate of 10 L/min, an applied voltage of 20 kV and a distance of 10 cm between the two electrodes. For the analysis on yield and protein content, fractions GE and GC, PE and PC were combined, respectively, as a positively charged fraction (GE+GC) and a negatively charged fraction (PE+PC) according to the method described in our previous study (Wang et al., 2015a). The positively charged fraction was expected to be protein enriched (Pelgrom et al., 2015a).

The particle size of the milled flour decreased with increasing classifier wheel speed (Figure 28). This is because at a constant air flow, a higher classifier wheel speed will increase the residence time of particles in the mill and lead to more extensive milling of the particles (Pelgrom et al., 2014). All the four flours contained a reasonable amount of particles smaller than 25 µm, especially the one milled at 8000 rpm ($D_{0.9}$ = 23.6 ± 4.2 µm), which indicates the existing of detached protein bodies (5 – 25 µm). The yields of all flours were lower than 100% (Table 3), and decreased with increasing classifier wheel speed due to more fouling (loss of material) on the inner walls of the mill caused by the smaller particle size and the more exposed lipid (Pelgrom et al., 2014). The protein content of the flour milled at 8000 rpm was higher than the other flours (Table 3). At this speed, all the particles including fibre-rich ones were milled down to very small sizes, which resulted in more fibre-rich particles lost in the mill (fouling) compared to other flours.

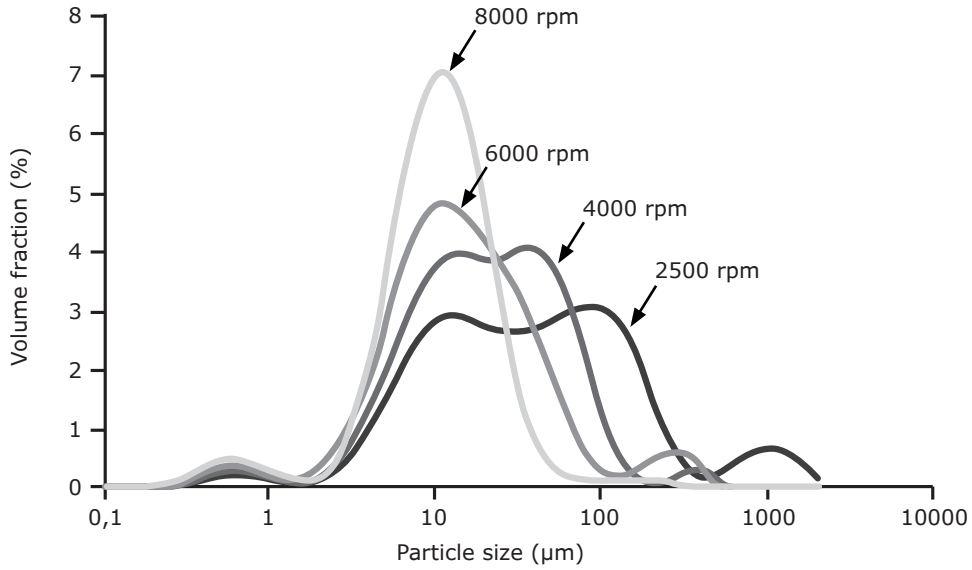

Figure 28. Particle size distribution of lupine flours milled at various classifier wheel speeds.

Table 3. Yield and protein content of the flours milled at different classifier wheel speeds and their fractions obtained by electrostatic separation.

Classifier wheel speed during milling (rpm)	Milling Yield (g/100 g grits)	Protein content flour (g/100 g dry solids)	Protein content GE+GC (g/100 g dry solids)	Protein content PE+PC (g/100 g dry solids)	Yield GE+GC (g/100 g flour)
2500	90.5 ± 3.5	40.5 ± 0.3	43.5 ± 1.6	34.8 ± 1.2	62.0 ± 1.4
4000	72.1 ± 4.2	42.0 ± 0.9	44.8 ± 0.8	38.0 ± 2.8	60.6 ± 3.4
6000	68.4 ± 3.0	43.0 ± 2.1	46.0 ± 1.0	35.3 ± 0.6	60.7 ± 0.2
8000	52.1 ± 2.2	55.5 ± 0.9	54.6 ± 1.0	53.2 ± 1.2	69.1 ± 2.9

Mean value ± absolute deviation (n=2)

After electrostatic separation, similar protein enrichment (~7%) in the positively charge fraction (GE+GC) was found for the flours milled at 2500, 4000 and 6000 rpm, whereas no enrichment was found for the flour milled at 8000 rpm (Table 3). This is counterintuitive, because the more intensive milling would be expected to promote the electrostatic separation by breaking the cell structure more completely and releasing more protein bodies. However, the finer particles and more exposed lipids obtained by the intensive milling lead to extensive agglomeration of the primary particles and thus yield poor separation (Lam and

Newton, 1992; Pelgrom et al., 2014; Wang et al., 2015a). Therefore, instead of more intensive milling, an optimal milling that balances the dissociation of cellular components and the avoidance of agglomerates is required for a successful electrostatic separation.

Although the protein enrichments were similar for the three flours that were milled less intensively, classifier wheel speed at 2500 rpm had the highest milling yield and thereby the least overall loss of the whole process. Furthermore, less intensive milling consumes less energy. Therefore, 2500 rpm was determined as the optimal classifier wheel speed and the flour milled under this condition was used for all the following experiments.

The enrichment of protein was found less than observed on lab-scale by Pelgrom et al. (43.5 % compared to 59 % dry matter basis) (Pelgrom et al., 2015a). This may be caused by the different collecting methods. Pelgrom et al. collected only the samples deposited on the electrode, whereas in the work reported here, the samples were collected from the electrodes and the filter bags and combined into one fraction. The fraction from the ground electrode (GE) is considered most enriched in protein, because particles with higher protein content take more positive charge and thus experience a stronger electrostatic force towards the electrode (Hemery et al., 2011; Wang et al., 2015a). Particles with somewhat lower protein content, especially larger composite particles, will end up in the filter bag below the electrode, which results in a lower protein enrichment of the fraction in the filter bag than that collected from the electrode. Therefore, for following single-step electrostatic separation experiments, fractions collected from the electrodes and filter bags were analysed individually.

Single-step electrostatic separation

During electrostatic separation, the gas flow rate is the most crucial factor, since it determines the charging of the particles, and the degree of agglomeration of the particles (Wang et al., 2015a). Therefore, three different carrier gas flow rates (10, 20 and 30 L/min) were assessed for electrostatic separation of lupine flour milled at 2500 rpm classifier wheel speed, while the other parameters were kept constant.

Table 4 shows that increasing the gas flow rate from 10 to 20 L/min resulted in an increase in the protein content of enriched fraction (GE) while the yield was similar. The protein content was now comparable with the finding of Pelgrom et al. (2015a) (57.3 % compared to 59 % dry matter basis), which confirms that the protein was mostly enriched in the fraction on the ground electrode. The fraction on the positive electrode was protein depleted while the two fractions from the filter bags had comparable protein content as the flour. Further increasing the gas flow to 30 L/min did not improve the enrichment. These results may be explained by the balance between formation and breakdown of agglomerates (Wang et al., 2015a). Higher gas flow rates lead to stronger charging of the particles (Wang et al., 2014) which results in stronger coulomb interactions between positively and negatively charged particles, and thus the formation of agglomerates. At the same time, the larger inertial forces that are associated with particles moving in a faster gas flow facilitates the de-agglomeration as well (Schönert et al., 1996). We hypothesize that equilibrium between the formation and breakdown of agglomerates was reached at 20 L/min.

Since 20 L/min and 30 L/min gas flow rates gave very similar enrichment, 20 L/min was selected as the optimal gas flow and used for all following experiments.

Table 4. Yield and protein content of the fractions obtained by electrostatic separation at varying carrier gas flow rate. The lupine flour was milled at classifier wheel speed 2500 rpm

Carrier gas flow rate (L/min)	Protein content GE (g/100 g dry solids)	Protein content PE (g/100 g dry solids)	Protein content GC (g/100 g dry solids)	Protein content PC (g/100 g dry solids)	Yield GE (g/100 g flour)	Yield PE (g/100 g flour)
10	50.7 ± 3.1	37.1 ± 0.4	41.5 ± 1.6	38.6 ± 2.2	13.6 ± 4.2	17.1 ± 5.0
20	57.3 ± 3.4	34.1 ± 0.9	40.5 ± 0.8	40.0 ± 2.8	13.6 ± 2.3	30.7 ± 4.3
30	57.2 ± 2.0	34.4 ± 1.4	42.6 ± 1.0	38.9 ± 0.6	14.2 ± 2.5	30.0 ± 5.3

Mean value ± absolute deviation (n=2)

Multiple-step electrostatic separation

Three-step electrostatic separation

A three-step electrostatic separation was carried out with the optimal setting as identified from the single-step electrostatic separation experiments, to further increase the protein enrichment. Because of the relatively low yield of the protein enriched fraction (GE) from single-step separation, more flour (~ 400 g) was used for the experiment.

After three electrostatic separation steps the protein content was found to increase from 51.4 to 65.0 g/100 g solids (Figure 29–A), which is 15% more than with air classification. The enrichment of protein from the first step was lower compared to the single-step experiment (51.4 compared to 57.3 g/100 g solids in the enriched fraction). This is caused by the different amount of flour used for each experiment. Much more flour was used as starting material for the multiple-step experiment than the single-step one. Although the experiment was paused a number of times to allow collection of samples from the electrodes, generally the multiple-step experiment ran for longer time and more powder deposited on the electrodes. The coverage of the electrode by the samples negatively affects the electric field strength by shielding (Cangialosi et al., 2008), which explains that in this case the first step of the multiple-step separation was less efficient than a single-step separation.

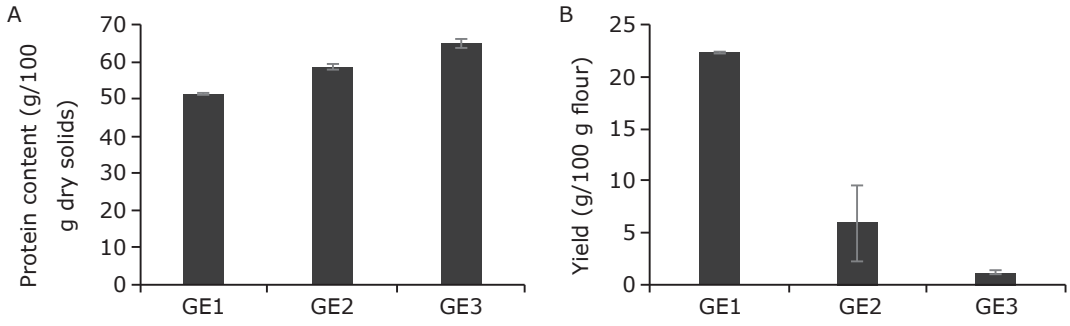

Figure 29. A) Protein content and B) yield of the protein enriched fractions GE1, GE2 and GE3 obtained from the 1st, 2nd and 3rd electrostatic separation of lupine flour. The error bars indicate the absolute deviation.

The increase in protein content was accompanied by a large decrease in the yield (Figure 29–B). Recycling of the unused fractions in the filter bags (GC and PC) was therefore explored to improve the yield.

Yield improvement by recycling the fractions in filter bags

To improve the yield of protein enriched fraction from each electrostatic separation step, the fractions from the filter bags (GC and PC) were combined as one fraction and returned to the feeder. Four recycling passes were done for the first electrostatic separation which yielded four protein enriched fractions from each recycling: GE1-R1, GE1-R2, GE1-R3 and GE1-R4. As shown in Figure 30–A, the yield was almost doubled after four recycling passes. However, the protein content slightly decreased with more passes (Figure 30–B). This could be described by a simple model assuming that a fraction (F) of the protein in lupine flour will never be recovered in the enriched fraction (e.g., because it is attached to particles that consist mainly of other components), and per recycle pass a certain fraction (f) of the protein will be extracted. Therefore, after n passes the protein recovery (P_n) defined as the fraction protein recovered from the starting material is calculated by Eq. 8.

$$P_n = 1 - (F + (1 - F) (1 - f)^n) \qquad \text{(Eq. 8)}$$

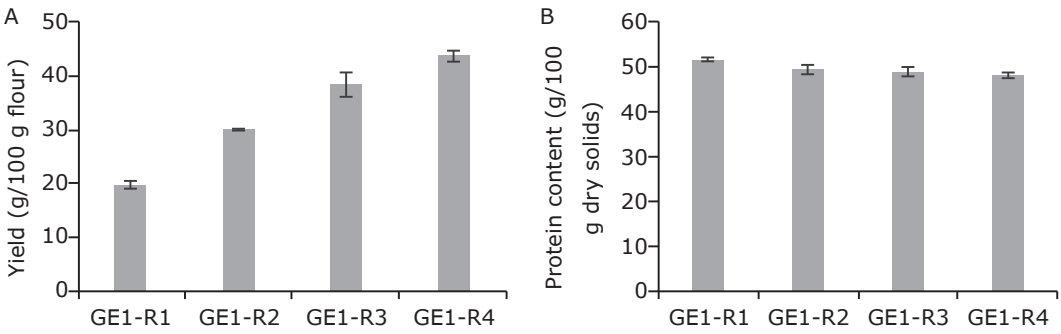

Figure 30. A) Yield and B) protein content of the protein enriched fractions GE1-R1, GE1-R2, GE1-R3 and GE1-R4 obtained from the 1st electrostatic separation of lupine flour with 1, 2, 3, and 4 times recycling of the fractions from filter bags (GC+PC). The error bars indicate the absolute deviation.

Figure 31 shows that the model fits the experimental data well with parameter values F=0.41 and f=0.40. The protein recovery is not linearly related to the recycling pass number, therefore with increase in the yield there is always a decrease in purity.

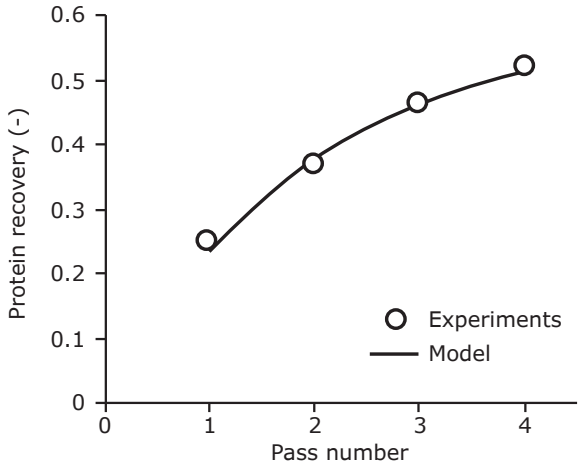

Figure 31. Fitting of Eq. 8 to experimental data of protein recovery of the first electrostatic separation step with four recycling passes.

Similar results were also found for following steps with recycling. Because of the improved yield from each step, the effect of more steps was explored. After five separation steps, the protein content of the enriched fraction reached 65.0 % dry matter basis, but again with a very low yield.

To illustrate the trade-off between the yield and the protein content of the enriched fraction for all separation steps, the yield was plotted as a function of the protein content for all the enriched fractions obtained by the multiple-step experiments (Figure 32). All the data points from the three-step electrostatic separation and the five-step electrostatic separation with recycling combine into one curve. We expect that this is because there is a distribution of particles having different compositions. The particles that have the most protein are isolated first since they will charge the most. Those particles having less protein will charge less, and will be only collected in the next recycles.

This hypothesis implies that the current process has reached its limit to separate protein from other lupine cellular components. Without changing the material properties or milling procedure, e.g. breaking the cell structure more and releasing

more detached protein bodies, an increase in the yield will be accompanied by a decrease in the protein content and vice versa.

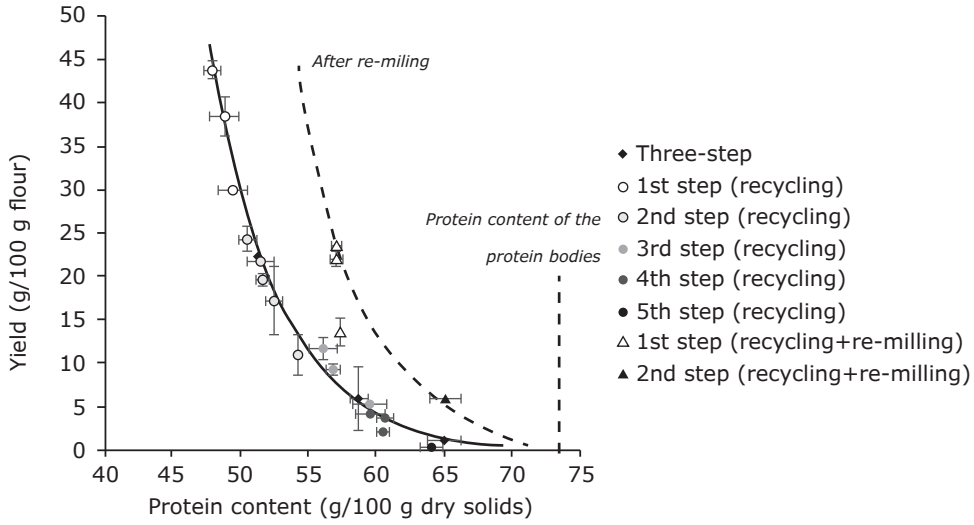

Figure 32. Relation between the yield and protein content of the protein enriched fraction by electrostatic separation. The lines are to guide the eye. The error bars indicate the absolute deviation. The uninterrupted curve represents the single- and multistep separations; the interrupted curve represents the performance with re-milling of the fractions collected in the filter bags.

Re-milling on the fractions in filter bags to improve both yield and purity

The hypothesis formulated above implies that re-milling of the fractions collected in the filter bags may improve the subsequent separation, if we can fracture particles into smaller ones that contain different amounts of protein, by this re-milling. In previous section we showed that direct fine milling did not result in good separation due to agglomeration of small particles. However most of fine particles were already extracted by the first pass, and thus we expected less problem in agglomeration when re-milling the fraction in filter bags.

Therefore, the fraction from the filter bags was milled at a classifier wheel speed of 4000 rpm to break the larger composite particles and release more detached protein bodies. The $D_{0.5}$ of the fraction was reduced from 126 ± 5.0 µm to 15.6 ± 0.4 µm. Similar as for the original flour a significant loss (~35 g/100 g fraction) occurred during the intensive milling, which was included in the calculation of

the overall fraction yield. Moreover, to reduce the shielding effect by the particles deposited on the electrodes, the experiment was paused more frequently to remove the particles from the electrodes.

After the first electrostatic separation, with one time re-milling and recycling, the yield of the protein enriched fraction was almost doubled (23.6 compared to 13.6 g/100 g flour) while the protein content was maintained around 57.3 % dry matter basis. In Figure 32, we see that the performance coincides with a curve ('After re-milling') that is substantially shifted to higher yields and purities. After a second electrostatic separation, a fraction with a protein content of 65.1 % dry matter basis and yield of 6 g/100 g flour was obtained. This means a recovery of 10% protein in lupine flours.

Compared to milling the whole lupine flour directly at a higher intensity, the step-wise milling and electrostatic separation is also less energy intensive and has less overall loss due to the smaller amount of material subjected to the more intensive milling.

Proposed scheme for protein enrichment from lupine seeds by milling and electrostatic separation

Based on all above results, we propose a scheme of protein enrichment from lupine seeds by combining milling and electrostatic separation (Figure 33). The lupine seeds are first milled down, to such size that enough protein bodies are detached from other cellular components, while the particles are not too fine to induce too much agglomeration. Subsequently, the flour is separated into three fractions. The fraction deposited on the ground electrode (GE) is enriched in protein while the fraction on the positive electrode (PE) is protein depleted. All flour that is not collected on the electrodes is now combined as one fraction (FB) and re-milled and recycled.

Then the protein enriched fraction from the first step can be used to carry out one or more subsequent electrostatic separation steps, optionally combined with re-milling and recycling as well, depending on the required protein content and yield of the final fraction.

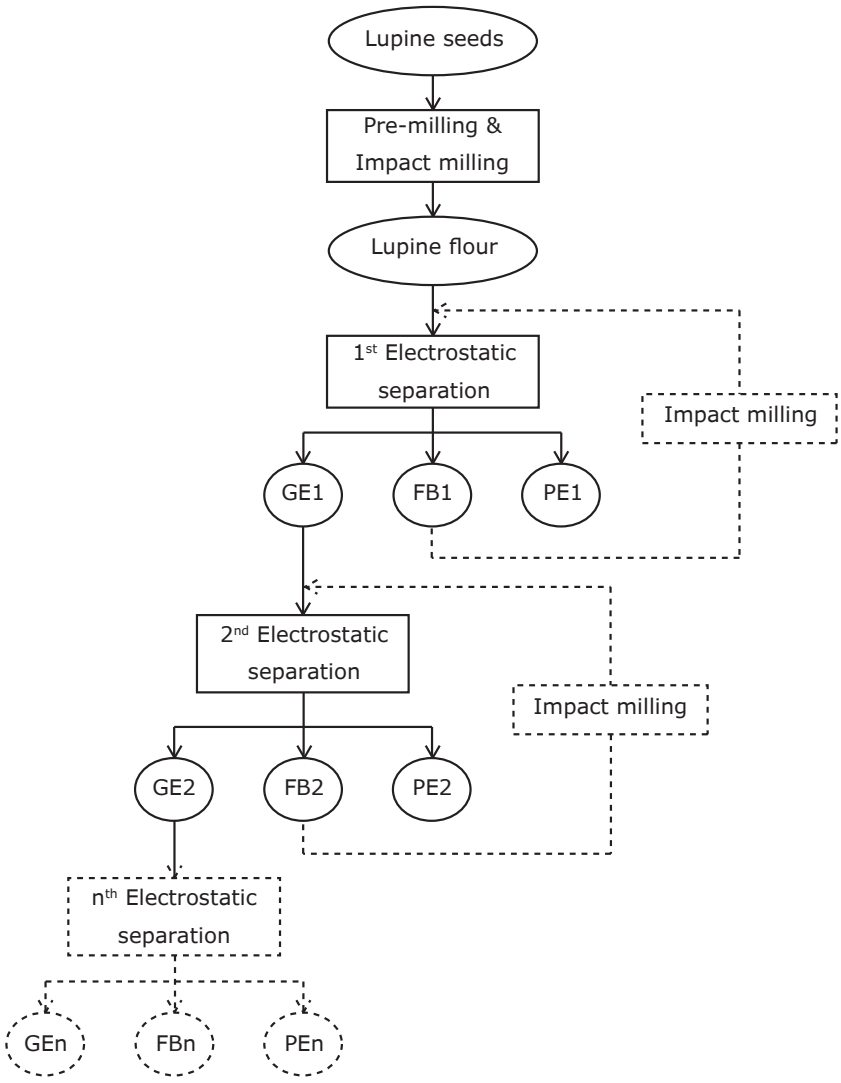

Figure 33. The proposed scheme for protein enrichment from lupine seeds by combined milling and electrostatic separation. 'GE', 'PE' and 'FB' are the fractions from the ground electrode, the positive electrode and the filter bags, respectively. The number indicates from which step the fractions are obtained.

Conclusions

Dry concentration of lupine protein was achieved using milling and subsequent electrostatic separation. Proper milling of the lupine flour was found to be essential for successful protein enrichment by electrostatic separation. Instead of more intensive milling, a relatively coarse milling step provides better electrostatic separation by releasing sufficient detached protein bodies, while avoiding excessive agglomeration. Protein was enriched in the fraction deposited on the ground electrode, while the fraction on the positive electrode was protein depleted. The two fractions collected in the filter bags were comparable to the flour in protein content. With optimal settings of single-step electrostatic separation, a fraction with protein content of 57.3 % dry matter basis could be obtained.

The protein content could be further increased by applying a multiple-step electrostatic separation process. After three separation steps, a fraction with protein content of 65.0 % dry matter basis was obtained, which is 15% better than obtained by air classification. The yield of the protein enriched fraction was further increased by recycling the fractions from the filter bags, but this was accompanied by a decrease in protein content and vice versa. The yields and purities were shown to follow a single master curve. A significant shift towards better yield and purities was achieved by re-milling the flour that was not collected on the electrodes. A final fraction with a protein content of 65.1 % dry matter basis and a yield of 6 g/100 g flour was obtained, which recovered 10% of the protein in the flour.

Based on the results for milling, single-step and multiple-step electrostatic separation, a process scheme for protein enrichment from lupine seeds is proposed by combining milling and electrostatic separation, which can provide both high purities and yields for lupine protein concentrates.

Acknowledgements

This research is supported by the Dutch Technology Foundation STW and the Institute for Sustainable Process Technology, ISPT through the DRYFRAC project (grant number 11399). The authors would like to thank their co-workers within the DRYFRAC project in Eindhoven, Korevaar and Padding, and the user committee for stimulating discussions on dry separation.

Dietary fibre enrichment from defatted rice bran by dry fractionation

This chapter has been submitted as:

Wang, J., Suo, G., de Wit, M., Boom, R.M., & Schutyser, M.A., (2016). Dietary fibre enrichment from defatted rice bran by dry fractionation.

Abstract

Rice bran is a plentiful, nutritious and under-valued co-product from rice finishing. Defatted rice bran is an excellent source of dietary fibre. The mostly used lab-scale method to extract dietary fibre is not very efficient; dry fractionation is a more energy efficient alternative at larger scales. Three separation routes were studied: two-step electrostatic separation, sieving and a combination of electrostatic separation and sieving. All yielded fibre-enriched fractions with similar yield (20 – 21 % of the rice bran flour) and purity (67 – 68 % dry matter basis), which recovered 42 – 48% of the fibre from the original rice bran flour. The enriched fractions obtained by a two-step electrostatic separation process contained more small particles compared to the other two, which resulted in different hydration properties and oil binding capacity. Compared to the total dietary fibre extracted by the enzymatic-gravimetric method, the enriched fractions by dry fractionation have a similar water retention capacity and oil bind capacity. This suggests that the fibre-enriched fractions by dry fractionation can be applied in foods and provide similar technological properties and physiological effects as the wet-extracted dietary fibre does.

Introduction

Rice is a staple food for more than half of the world's population (Childs, 2004). The annual global production of paddy rice in 2013 was 740.9 million metric tons (FAOSTAT, 2015). The bulk of the rice is consumed as white rice (Childs, 2004), yielding annually approx. 60 million metric tons of rice bran as a co-product from rice milling, of which the major part is underutilized as animal feed or discarded directly (Orthoefer and Eastman, 2004).

Rice bran consists of several layers, i.e. the pericarp, testa (seed coat), nucellus and aleurone layers. During rice milling, a small portion of the starchy endosperm may also end up in the bran fraction (Shibuya and Iwasaki, 1985). Rice bran contains a relatively high amount of oil (17.4 – 22.9 g / 100 g dry bran), protein (14.0 – 18.1 g / 100 g dry bran) and dietary fibre (27.0 g / 100 g dry bran) (Abdul-Hamid and Luan, 2000; Chinma et al., 2015; Kahlon and Chow, 2000; Orthoefer and Eastman, 2004). Furthermore, it is also rich in micronutrient, e.g. vitamins and trace minerals (Saunders, 1985). The primary product from rice bran is rice bran oil because of its high nutritional value (Friedman, 2013; Lakkakula et al., 2004; Orthoefer and Eastman, 2004). After oil extraction, the residual defatted rice bran can be further valorised for dietary fibre production (Abdul-Hamid and Luan, 2000; Daou and Zhang, 2011, 2014; Nandi and Ghosh, 2015).

Dietary fibre from rice bran mainly contains cellulose, lignin and hemicellulose, of which the main part is insoluble (Chinma et al., 2015; Elleuch et al., 2011). Insoluble dietary fibres promote human health by supporting the growth of the intestinal microflora, increase the faecal bulk and decrease the intestinal transit (Foschia et al., 2013). Furthermore, the dietary fibre includes components such as ferulic acid, which exert beneficial health effects to the human intestine and provide antioxidant activity (Daou and Zhang, 2011; Mod et al., 1978; Vitaglione et al., 2008). Dietary fibre from rice bran has a very high water- and

oil-absorption capacity (Abdul-Hamid and Luan, 2000; Daou and Zhang, 2014; Nandi and Ghosh, 2015), indicating its potential for preparing food products, e.g. gluten-free bread, pasta and meat product, to avoid syneresis and modify the food structure, and to stabilize high-fat food (Chinma et al., 2015; Choi et al., 2009; Elleuch et al., 2011; Hu et al., 2009; Kaur et al., 2012; Sairam et al., 2011; Saunders, 1985).

Currently an AOAC enzymatic-gravimetric method for analysing dietary fibre (Prosky et al., 1988) is most often applied with modification to extract dietary fibre from rice bran on smaller scales (Abdul-Hamid and Luan, 2000; Bunzel et al., 2003; Daou and Zhang, 2011; Nandi and Ghosh, 2015). The defatted rice bran is first digested with heat-stable α-amylase, protease and amyloglucosidase at 100 °C, 60 °C and 60 °C, respectively, to remove the starch and protein. Then four volumes of 95% ethanol are added to precipitate the soluble dietary fibre. After precipitation the mixture is filtered and the residue is washed and oven-dried to obtain the total dietary fibre.

This procedure is energy inefficient, generates solvent (ethanol) emissions and uses expensive enzymes, which makes it unsuitable for larger-scale production. In the present study, a dry fractionation process by combining milling and dry separation methods, e.g. sieving and electrostatic separation, is applied, which is more efficient in terms of water and energy consumption, and does not need any solvents. An additional benefit of the latter methods is that the native properties of the materials are retained (Pelgrom et al., 2013a; Schutyser and van der Goot, 2011).

The combination of milling and electrostatic separation is effective to fractionate wheat bran and oat bran into fibre-rich and fibre-depleted fractions (Chen et al., 2014b; Hemery et al., 2011; Sibakov et al., 2014; Wang et al., 2015b). The separation is based on the histological structure of the bran. Different layers of the bran are dissociated from each other and broken down to small particles by milling. Then the particles are tribocharged by passing through a tube by entrainment in a gas. Because of the difference in composition, fragments from different layers obtain different charges which then enables subsequent separation under the influence of an external electric field (Wang et al., 2015b).

The pericarp that is fibre-rich was enriched in negatively charged fractions, whereas the other components, e.g. starch, protein and aleurone cells, were enriched in the positively charged fractions. Applying a different separation method, e.g. sieving or air classification, additional to electrostatic separation can further improve the enrichment (Sibakov et al., 2014; Wang et al., 2015b). Since rice bran has a similar histological structure as wheat and oat bran, a similar separation by dry fractionation is expected.

The aim of this study was therefore to investigate the possibility of enriching dietary fibre from defatted rice bran by dry fractionation. First we analysed the arabinoxylans content of hand-isolated bran layers to find the maximum theoretical purity can be reached by dry fractionation. Arabinoxylans were chosen to represent the dietary fibre because it is the main hemicellulose from rice bran (Mod et al., 1978; Shibuya and Iwasaki, 1985). We determined the relation between the arabinoxylans content and total dietary fibre content by analysing both contents for different samples obtained after fractionation. Two-step electrostatic separation, sieving and a combination of electrostatic separation and sieving were applied, respectively, to the finely milled defatted rice bran flour. Then the fibre-enriched fractions from different processes were compared for yield and purity. Finally, we analysed the functional properties, e.g. swelling capacity (SC), water retention capacity (WRC) and oil binding capacity (OBC), of the fibre-enriched fractions to explore the potential of the enriched fractions as ingredient for food preparation.

Materials and methods

Material

Brown rice (*Oryza sativa L.*) was purchased from Windkorenmolen De Vlijt (the Netherlands).

Hand-isolation of pericarp, aleurone layer and starchy endosperm

After removing the germ and grain ends, the brown rice was soaked in water for 12 hours to reduce the adhesion between different layers. Then the grain was cut into two pieces by a razor-blade, and the pericarp and aleurone layer were peeled off gently by using a tweezer and a scalpel. Starchy endosperm was scraped off from the peeled part by a scalpel. The isolated tissues were defatted using acetone with a material to solvent ratio 1:8. After drying in an oven at 50 °C, the tissues were analysed for arabinoxylans content.

Preparation of defatted rice bran flour (DRBF)

Crude rice bran was obtained by milling (pearling) the brown rice with a Grain Testing Mill (Satake, Japan). The germ and broken grains were removed by sieving the crude bran with an 800 µm sieve. The obtained rice bran was about 10% of the brown rice weight. The rice bran was then defatted by using petroleum ether with a material-to-solvent ratio 1:6 for 24 hours to stabilize the bran. After defatting, the bran was milled using a pin mill (Hosokawa Alpine, type 100 UPZ, Augsburg, Germany) at ambient temperature at a speed of 22,000 rpm, air flow of 75 m^3/h. The obtained defatted rice bran flour (DRBF) was stored in a -20 °C freezer until use.

Separation of DRBF by electrostatic separation and sieving

Electrostatic separation of the defatted rice bran flour (DRBF) was done with a custom-designed bench-scale separator described in a previous study (Wang et al., 2015a), with the following settings: dosing rate of DRBF 2 kg/h, flow rate of the carrier nitrogen gas 20 L/min, the applied voltage to the positive electrode 20 kV and the distance between the electrodes 10 cm. From each experiment four fractions were obtained: one from the ground electrode (GE), one from the positive electrode (PE), one from the collecting filter bag below the ground electrode (GC) and one from the collecting filter bag below the positive electrode (PC) (Figure 34).

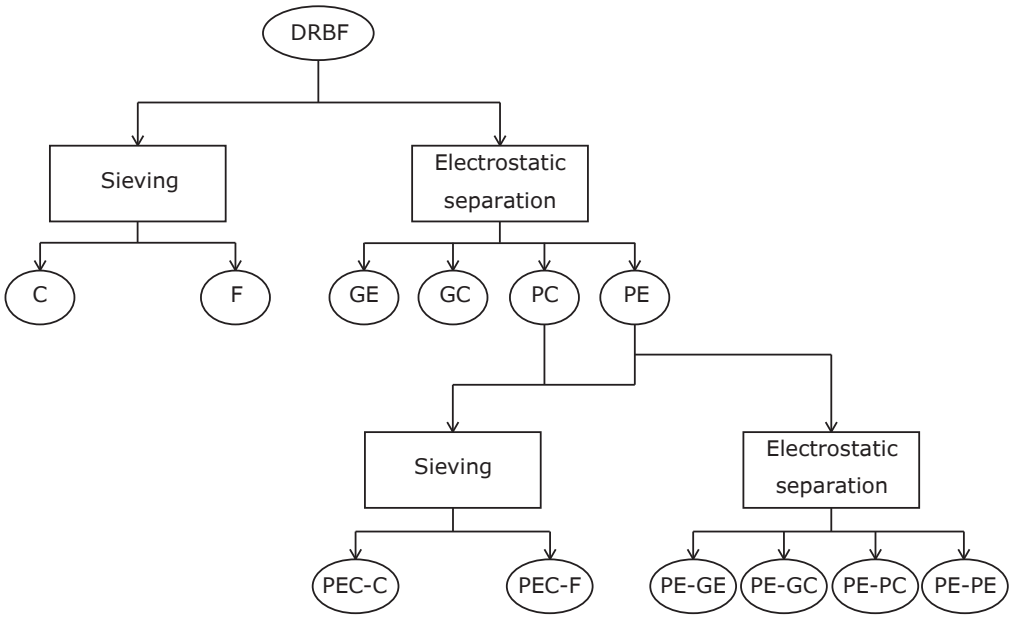

Figure 34. Scheme of dry separation of defatted rice bran flour (DRBF) by electrostatic separation and sieving. 'GE', 'GC', 'PC' and 'PE' are the fractions from the first-step electrostatic separation, from the ground electrode, the filter bag below the ground electrode, the filter bag below the positive electrode and the positive electrode, respectively. 'PE-GE', 'PE-GC', 'PE-PC' and 'PE-PE' are the fractions obtained from the second-step electrostatic separation from the ground electrode, the filter bag below the ground electrode, the filter bag below the positive electrode and the positive electrode, respectively. 'C' and 'F' are the coarse and fine fractions, respectively, from direct sieving of DRBF. 'PEC-C' and 'PEC-F' are the coarse and fine fractions, respectively, obtained by sieving the mixtures of PE and PC.

For two-step electrostatic separation, the fraction PE was subjected to a second separation step which yielded another four fractions (PE-GE, PE-GC, PE-PE and PE-PC). For the combination of electrostatic separation and sieving, fractions PE and PC were mixed and used for sieving, yielding a course fraction (PEC-C) and a fine fraction (PEC-F). Sieving was done using an air jet sieve (Alpine200 LS-N, Hosokawa-Alpine, Augsburg, Germany) with a 50 µm sieve at 4000 Pa for 2 min. Direct sieving of the DFRB yielded two fractions: coarse (C) and fine (F). The 50 µm sieve was chosen based on the particle size distribution of the DRBF (Figure 35). The two large and clear peaks indicate that the DFRB contains materials with different grinding behaviour, which is likely a result of their different biochemical compositions.

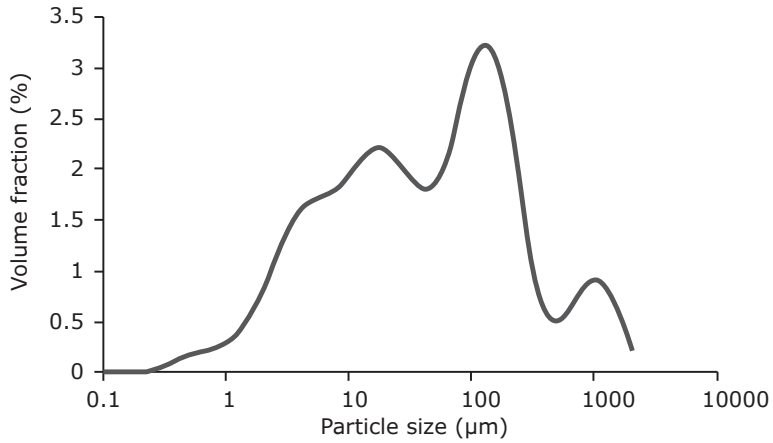

Figure 35. Particle size distribution of defatted rice bran flour (DRBF).

Biochemical analyses

The dry matter content was determined by drying 2 g in an oven at 105 °C overnight. The ash content was determined according to AACC method 08-12. The total starch content and total dietary fibre content were measured according to AACC method 76-13 and AOAC Method 991.43 (AACC, 2000), respectively, using Megazyme kits (Megazyme International Ireland Ltd., Ireland). The protein content was analysed using Dumas analysis (Nitrogen analyser, FlashEA 1112 series, Thermo Scientific, Interscience) with a conversion factor of N × 5.95 (Shih, 2004). The arabinoxylans content was analysed as described in a previous study (Wang et al., 2015b) by using a modified phloroglucinol method (Douglas, 1981). All measurements were done in duplicate.

Swelling capacity (SC), water retention capacity (WRC) and oil binding capacity (OBC)

The swelling capacity is defined as the ratio of the volume occupied by the wetted sample after equilibration to the actual sample weight (Raghavendra et al., 2004) and was determined according to Robertson et al. (2000). About 200 mg sample was accurately weighted. With the known dry matter content, the dry sample weight (m_d) was calculated. The sample was then hydrated in 10 mL distilled water in a calibrated cylinder at room temperature for 18 h. Then the volume occupied by the sample was recorded (V_s). The SC was calculated as:

$$SC = \frac{V_s}{m_d} \quad \text{(Eq. 9)}$$

The water retention capacity (WRC) is defined as the amount of water that remains bound to the hydrated fibre after the application of a specific external force, e.g. centrifugation (Raghavendra et al., 2004). According to Robertson et al. (2000), About one gram of sample with known dry matter content was accurately weighted for the dry sample weight (m_d). The sample was hydrated in 30 mL distilled in a centrifuge tube at room temperature. After 18 h, the sample was centrifuged at 3000 g for 20 min. Then the supernatant was decanted and the residue was weighted (m_{rw}). The WRC was calculated as:

$$WRC = \frac{m_{rw}}{m_d} \quad \text{(Eq.10)}$$

The oil binding capacity (OBC) was determined according to Raghavendra et al. (2006). About 500 mg of sample with known dry matter content was accurately weighted for the dry sample weight (m_d). The sample was mixed with 10 mL refined sunflower oil in a centrifuge tube. It was allowed to equilibrate overnight at room temperature and then centrifuged at 10000 g for 30 min. Then the supernatant was decanted and the residue was weighted (m_{ro}). OBC was calculated as:

$$OBC = \frac{m_{ro}}{m_d} \quad \text{(Eq.11)}$$

Results and discussions

Distribution of arabinoxylans in different layers of rice bran

The distribution of arabinoxylans in rice bran determines the maximum achievable purity that can be obtained by dry fractionation, as the method does not molecularly disrupt the tissue, but rather fragments it on a larger scale and then isolates the fragments. Thus, the concentration of arabinoxylans in the rice bran sets the maximum achievable purity. The pericarp, aleurone layer and starchy endosperm were hand-isolated (Figure 36) and analysed on their arabinoxylans content.

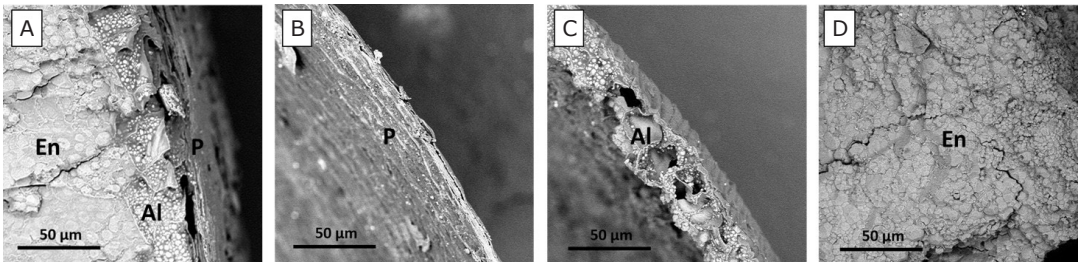

Figure 36. Scanning electron microscope (SEM) images of A) section of brown rice; B) hand-isolated pericarp (P); C) hand-isolated aleurone layer (Al) and D) hand-isolated starchy endosperm (En).

Though it is difficult to see from the SEM images, it is probable that the testa and nucellus are attached to the pericarp and aleurone layer, respectively. These two tissues are fused to the surrounding tissues, whereas the bond between the testa and nucellus tends to be weak; therefore the tissues may separate at the junction between those two (Bechtel and Pomeranz, 1977).

The arabinoxylans content in the pericarp was the highest among the three hand-isolated tissues, whereas there was no arabinoxylans detected in the starchy endosperm (Table 5). A similar distribution of arabinoxylans was found in

wheat bran (Barron et al., 2007; Swennen et al., 2006; Wang et al., 2015b). The arabinoxylans-enriched fraction from wheat bran by electrostatic separation was found to contain fragments mainly from pericarp (Wang et al., 2015b). Because of the similarity in histological structure and arabinoxylans distribution in rice bran and wheat bran, a fraction rich in arabinoxylans is also expected from rice bran by electrostatic separation. Thus the arabinoxylans content of the pericarp (26.7 ± 3.3 % dry matter basis) is considered as the maximum achievable purity of the arabinoxylans-enriched fraction.

Table 5. Arabinoxylans content of hand-isolated pericarp, aleurone layer and starchy endosperm from brown rice.

Hand-isolated tissue from brown rice	Arabinoxylans content (% dry matter basis)
Pericarp	26.7 ± 3.3
Aleurone layer	13.2 ± 1.2
Starchy endosperm	ND

Mean value ± absolute deviation (n=2)

ND: Not detected

Separation of DRBF by electrostatic separation and sieving

After milling, the defatted rice bran flour (DRBF) was separated by three different routes: two-step electrostatic separation, sieving or a combination of electrostatic separation and sieving (Figure 34). Obtained fractions were analysed on yield and biochemical composition.

Because the analysis of the arabinoxylans content is much less time-consuming than the total dietary fibre analysis, we analysed several fractions with different compositions on both arabinoxylans and total dietary fibre contents to find the relation between the two. As Figure 37 shows, the total dietary fibre content is proportional to the arabinoxylans content. With this linear relation, we can find the total dietary fibre content by using the measured arabinoxylans content (Table 6). Furthermore, the maximum achievable purity of dietary fibre that can be enriched by dry fractionation could also be calculated based on the arabinoxylans content of pericarp and contributes about 86.2 % dry matter basis.

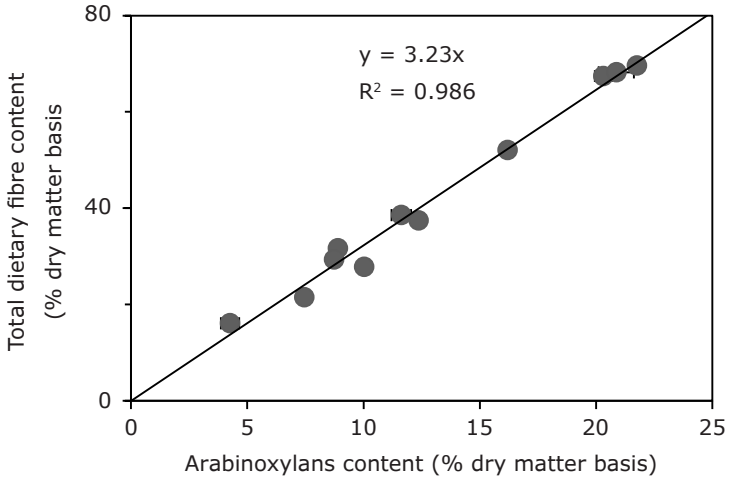

Figure 37. Total dietary fibre content as a function of arabinoxylans content of different fractions from DRBF by dry fractionation. The error bars indicate the absolute deviation.

Table 6. Yield and biochemical composition of fractions obtained by dry fractionation of DRBF

Name Fraction	Yield (% of DRBF)	Arabinoxylans (% dry matter basis)	Total dietary fibre (% dry matter basis)	Protein (% dry matter basis)	Starch (% dry matter basis)	Ash (% dry matter basis)
DRBF	-	8.9 ± 0.4	31.7 ± 0.3	16.2 ± 0.0	36.7 ± 0.3	8.9 ± 0.1
GE	24.9 ± 0.8	5.2 ± 0.1	16.8*	17.1 ± 0.2	53.0 ± 1.8	9.3 ± 0.1
PE	44.3 ± 0.7	16.1 ± 0.8	52.1*	14.6 ± 0.3	25.1 ± 1.1	4.9 ± 0.0
GC	8.4 ± 1.0	7.9 ± 0.7	25.7*	17.1 ± 0.0	37.5 ± 0.4	9.1 ± 0.1
PC	9.6 ± 0.3	8.0 ± 0.8	25.8*	15.6 ± 0.1	36.7 ± 0.2	8.5 ± 0.0
PE-GE	4.6 ± 1.1	12.0 ± 0.3	38.8*	15.8 ± 0.0	36.8 ± 1.1	7.7 ± 0.0
PE-PE	20.5 ± 0.3	20.8 ± 0.4	67.1*	12.5 ± 0.5	5.3 ± 0.2	3.6 ± 0.1
PE-GC	7.5 ± 0.2	9.9 ± 0.1	32.0*	15.0 ± 0.2	33.1 ± 0.0	6.5 ± 0.0
PE-PC	9.8 ± 0.6	10.8 ± 0.5	35.0*	13.4 ± 0.2	31.2 ± 0.2	5.3 ± 0.0
C	22.4 ± 0.0	20.3 ± 0.7	67.5 ± 0.4	14.0 ± 0.1	10.1 ± 0.4	3.6 ± 0.0
F	71.4 ± 0.0	7.5 ± 0.1	21.5 ± 0.1	16.4 ± 0.0	45.0 ± 0.7	8.0 ± 0.1
PEC-C	20.3 ± 0.0	20.9 ± 0.0	68.2 ± 0.8	13.5 ± 0.0	7.6 ± 1.3	3.6 ± 0.0
PEC-F	28.5 ± 0.0	10.0 ± 0.0	27.8 ± 0.1	15.4 ± 0.0	42.9 ± 1.3	7.5 ± 0.0

Mean value ± absolute deviation (n=2)

*: Value calculated by using the linear relation between the total dietary fibre and arabinoxylans content (Figure 37)

After one-step electrostatic separation, fibre was enriched into the fraction PE while starch was enriched into the fraction GE. This indicates that the fibre-rich fragments took negative charge and were deflected towards the positively charged electrode under the influence of the electric field, whereas the starch took positive charge and was deflected into the opposite direction. This result is in line with the results of electrostatic separation on other brans (Hemery et al., 2011; Sibakov et al., 2014; Wang et al., 2015b). A second electrostatic separation on the fraction PE further increased the fibre content from 52.1% dry matter basis to 67.1% dry matter basis, which is more than double of the fibre content in DRBF (31.7% dry matter basis). Additionally, this fraction (PE-PE) contains less ash and protein, and especially much less starch compared to the other fractions. SEM picture of the fraction (Figure 38-A) confirms that it contains mainly fragments from the pericarp. However, there are also some empty aleurone cells and pieces of starchy endosperm, which explains why the maximum achievable purity of fibre was not yet reached.

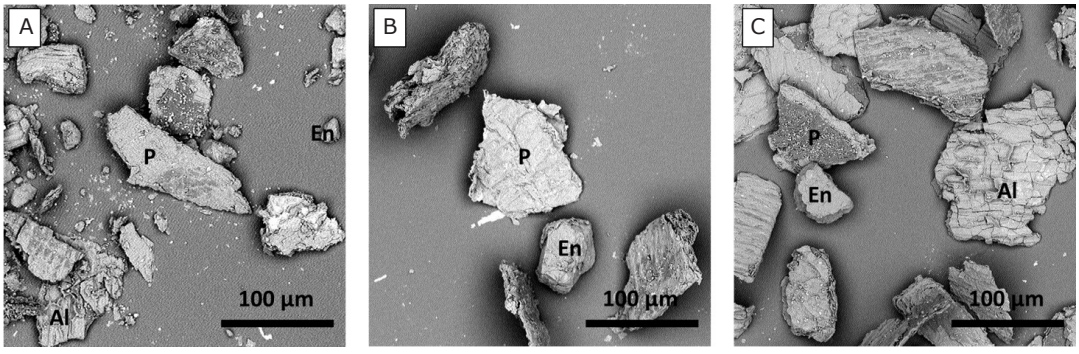

Figure 38. Scanning electron microscope (SEM) images of A) fraction PE-PE; B) fraction C and C) fraction PEC-C. P, Al, and En indicate the pericarp, empty aleurone cell and piece of starchy endosperm, respectively.

Direct sieving of the DRBF enriched fibre in the coarse fraction (C) provided similar yields and purities compared to the two-step electrostatic separation (PE-PE). Similarly, pericarp was the main source of the fragments appearing in this fraction (Figure 38-B). Larger pieces of starchy endosperm were also observed here. Moreover, the combination of a single electrostatic separation step and sieving yielded a fraction (PEC-C) resembling the coarse fraction C, with similar yield and biochemical composition. Also this fraction contains empty aleurone cells and pieces from starchy endosperm (Figure 38-C).

Though the yield and composition of the three enriched fractions are similar, they differ in their particle size distribution (Figure 39). The two coarse fractions C and PEC-C have identical particle size distribution whereas the faction PE-PE contains more small particles ($D_{0.1}$ = 20.7 µm compared to $D_{0.1}$ = 63.4 µm). This indicates that the milling broke fragments from both the outer layers and the starchy endosperm into fine particles. Because electrostatic separation in principle separates particles on their charge and not on their size, small particles with high fibre content also end up in the enriched fraction. This different particle size can influence the functional properties of the fractions, as discussed in the next section.

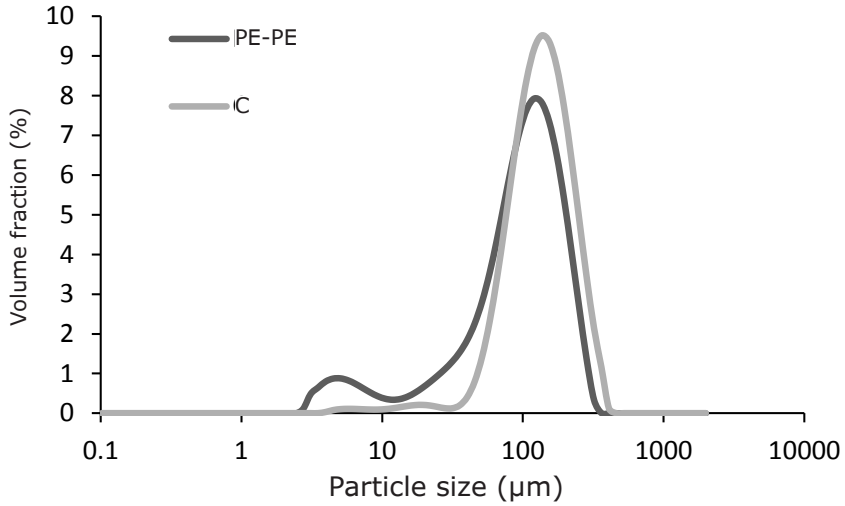

Figure 39. Particle size distribution of fibre enriched fractions obtained by different separation processes. PE-PE: negatively charged fraction obtained by two-step electrostatic separation; C: coarse fraction obtained from direct sieving of DRBF.

All three processes recovered 42 – 48% of the fibre from DRBF. Removing the starch and empty aleurone cells by adding more electrostatic separation steps may further increase the fibre content, however at the mean time the yield will become lower. This trade-off between the yield and purity needs to be considered.

Functional properties of enriched fractions

The technological and physiological functional properties of dietary fibre in food systems are attributed to their physicochemical properties such as swelling capacity (SC), water retention capacity (WRC) and oil binding capacity (OBC) (Chinma et al., 2015; Elleuch et al., 2011). To demonstrate the possible application of the fibre-enriched fraction in food, the fractions were analysed on SC, WRC and OBC, and compared with the original flour DRBF and the total dietary fibre extracted by the wet enzymatic-gravimetric method (TDF wet-extracted). The rough chemical composition of TDF wet-extracted was found to be similar as found by Abdul-Hamid and Luan (2000): total dietary fibre content 65.0 ± 0.0 % dry matter basis, protein content 15.1 ± 0.3 % dry matter basis and ash content 16.3 ± 0.1 % dry matter basis.

Compared to the original flour DRBF, all three fibre-enriched fractions had a higher SC, WRC and OBC (Table 7). This is because the dietary fibre is the main contributor to these functional properties (Chinma et al., 2015; Foschia et al., 2013). The fibre content of the enriched fractions is more than double of that of the original flour, therefore a much higher SC, WRC and OBC could be expected.

Table 7. Swelling capacity (SC), water retention capacity (WRC) and oil binding capacity (OBC) of defatted rice bran flour (DRBF), fibre-enriched fractions from DRBF by different separation routes, and total dietary fibre extracted by using enzymatic-gravimetric method (TDF wet-extracted).

Name Fraction	SC (mL/g)	WRC (g/g)	OBC (g/g)	TDF content (% dry mater basis)
DRBF	4.4 ± 0.4	1.9 ± 0.0	3.1 ± 0.0	31.7 ± 0.3
PE-PE	7.8 ± 0.1	4.7 ± 0.1	6.7 ± 0.2	67.1*
C	9.3 ± 0.0	4.5 ± 0.0	5.4 ± 0.2	67.5 ± 0.4
PEC-C	9.3 ± 0.0	4.7 ± 0.2	5.1 ± 0.0	68.2 ± 0.8
TDF wet-extracted	9.2 ± 0.3	4.1 ± 0.0	5.5 ± 0.3	65.0 ± 0.0

Mean value ± absolute deviation (n=2)

*: Value calculated by using the linear relation between the total dietary fibre and arabinoxylans content (Figure 37)

The functional properties of the two coarse fractions (C and PEC-C) are similar, whereas the SC of the fraction PE-PE is lower while its OBC is higher than the others. Since the composition of these three fractions are quite similar, the difference in particle size distribution would be the main reason for the different functional properties (Sangnark and Noomhorm, 2003).

More polydispersity results in a higher bulk density, therefore a smaller packing volume and less SC as a result (Raghavendra et al., 2004). The differences in WRC and OBC could be due to the increased surface area and the damaged fibre matrix. Reducing the particle size would on the one hand increase the surface area and allow more surface interaction with water or oil. However, on the other hand, the fibre matrix can be damaged during size reduction, which reduces the water or oil entrapment by the physical structure (Raghavendra et al., 2004; Wang et al., 2013). Contradictory results were found when comparing different studies (Cadden, 1987; Sangnark and Noomhorm, 2003; Wang et al., 2013), which indicates that the balance between having more surface area and maintaining sufficient physical structure of the fibre is important for having good WRC and OBC.

All three enriched fractions have similar or even better WRC and OBC compared to the total dietary fibre extracted by the wet process, which means that these fractions can provide similar technological properties to the food system and physiological effect on human health. The high WRC indicates the potential of using the enriched fractions as a functional ingredient to prevent syneresis, modify viscosity and texture, and reduce calories of formulated food products (Chau et al., 2007). Furthermore the enriched fractions can have a positive effect on gut health, increase stool weight and potentially slow down the digestion process and the rate of nutrient absorption (Takahashi et al., 2009). The good OBC of the fractions indicates the potential for application of the fractions in high-fat food.

Conclusions

The maximum achievable fibre content that can be achieved by dry fractionation was determined as 86.2 % on a dry matter basis, by analysing the arabinoxylans content of hand-isolated tissues and using the linear relation between the fibre content and arabinoxylans content.

Enrichment of dietary fibre from defatted rice bran was achieved by combing milling and different dry separation processes. All three tested separation routes produced fibre-enriched fractions with similar yield (20 – 21 % of the milled flour) and fibre content (67 – 68 % dry matter basis), which recovered 42 – 48 % of the fibre from the original flour. The enriched fractions mainly contained fragments from the pericarp. Removing the trace of starchy endosperm and empty aleurone cells may further increase the fibre content, but the trade-off between the purity and yield needs to be considered.

The enriched fraction obtained by two-step electrostatic separation contained more small particles compared to the enriched fractions obtained by the other two separation routes involving sieving. This is a consequence of using different driving forces in the two separation methods. The different particle size distributions of the enriched fractions resulted in different functional properties. The fraction obtained by two-step electrostatic separation featured a lower swelling capacity and a higher oil binding capacity than the other two. The balance between having more surface area and maintaining sufficient physical structure of the fibre is important for good functional properties.

The enriched fractions had similar hydration properties and oil binding capacity when compared to the total dietary fibre extracted by the enzymatic-gravimetric method. This suggests that the fibre-enriched fractions by dry fractionation can be applied in foods and provide similar technological properties and physiological effects as the wet-extracted dietary fibre does.

Acknowledgements

This research is supported by the Dutch Technology Foundation STW and the Institute for Sustainable Process Technology, ISPT through the DRYFRAC project (grant number 11399). The authors would like to thank their co-workers within the DRYFRAC project in Eindhoven, Korevaar and Padding, and the user committee for stimulating discussions on dry separation.

General discussion

Abstract

Rice bran is a plentiful, nutritious and under-valued co-product from rice finishing. Defatted rice bran is an excellent source of dietary fibre. The mostly used lab-scale method to extract dietary fibre is not very efficient; dry fractionation is a more energy efficient alternative at larger scales. Three separation routes were studied: two-step electrostatic separation, sieving and a combination of electrostatic separation and sieving. All yielded fibre-enriched fractions with similar yield (20 – 21 % of the rice bran flour) and purity (67 – 68 % dry matter basis), which recovered 42 – 48% of the fibre from the original rice bran flour. The enriched fractions obtained by a two-step electrostatic separation process contained more small particles compared to the other two, which resulted in different hydration properties and oil binding capacity. Compared to the total dietary fibre extracted by the enzymatic-gravimetric method, the enriched fractions by dry fractionation have a similar water retention capacity and oil bind capacity. This suggests that the fibre-enriched fractions by dry fractionation can be applied in foods and provide similar technological properties and physiological effects as the wet-extracted dietary fibre does.

Introduction

Modern water-based processes for food ingredient production aim at high purity and consume copious amounts of water, chemicals and energy. Furthermore, harsh conditions such as high temperatures and pH shifts can lead to a loss of the native functional properties of components. The increased awareness on sustainability in food production chain is a major driver for research on dry fractionation, as it uses hardly any water, consumes less energy and retains the native functionality of the ingredients. Conventional dry fractionation combines milling with air classification or sieving, which separate particles based on their different particles sizes and/or densities. In this thesis, a recent dry separation process called electrostatic separation was explored, which relies on electrostatic forces for separation. Although the potential of electrostatic separation to fractionate agro-materials has been demonstrated, the effectiveness in terms of purity and yield and the influence of process parameters on charging and separation of food ingredients were not yet systematically studied. Therefore, the objective of this thesis was to gain better understanding of the charging and separation behaviour of model and agro-materials, provide insight in the critical factors for successful electrostatic separation and explore the potential of this separation method to different agro-materials. This chapter summarizes the main findings and proposes two general schemes for protein enrichment and fibre enrichment. Subsequently the challenges to achieve successful electrostatic separation and up-scaling are discussed. Finally, the chapter ends with an outlook for future research.

Discussion of main findings

Electrostatic separation consists of two steps: triboelectric charging of the particles and subsequent separation of the particles in an electric field. The driving force is the electrostatic force, which is the product of the charge on the particles and the electric field strength. The charging step is critical to the effectiveness of the separation and is influenced by many factors such as the chemical, physical and electrical properties of particle and contact surface, number of impacts, velocity and angle of the impact and environmental conditions such as temperature and relative humidity. Consequently, we characterized the charging behaviour of single-component particles in nitrogen gas flowing through aluminium tubes with a lab-scale electrostatic separator in **chapter 2**, where polystyrene particles and wheat gluten were used as model particles. Higher gas velocities led to a larger specific charge by increasing the normal component of impact velocity. Smaller particles gained more specific charge than larger ones because of their higher surface-to-volume ratio and their sensitivity towards gas flow pattern changes. Longer charging tube allowed more contacts between the particles and the wall and therefore resulted in higher specific charge. The relative humidity of the nitrogen gas flow within the range 0 – 60% had no influence on the charging of both model particles.

Even though the charging behaviour of single-component particles can provide insight on critical parameters for electrostatic separation, the charging and separation of a real mixture is complex because particle-particle interactions cone into play. Therefore, in **chapter 4** we elucidated the role of these interactions by investigating the charging and separation of model gluten-starch mixtures with a custom-built bench-scale electrostatic separator. As hypothesized, the net charge of gluten-starch mixtures was not simply a sum of the charge of the two individual components, indicating that particle-particle interactions play an important role. We also hypothesized that the formation of agglomerates between oppositely charged particles influenced the separation negatively,

which was corroborated by the fact that the dispersibility for mixtures of the two components was lower compared to that of individual components. We found that it is important to find the optimal condition that provides sufficient charge to charges, but avoids agglomeration between oppositely charged particles. This could be achieved by a combination of lower dosing rate and higher gas flow rate.

Based on the findings with model systems (**chapter 2** and **chapter 4**), we explored the possibility of applying electrostatic separation to different agro-materials for food ingredient production in **chapter 3**, **chapter 5**, and **chapter 6**, respectively. **Chapter 3** demonstrated the potential of using electrostatic separation to enrich arabinoxylans from wheat bran with the lab-scale electrostatic separator. A combination of larger particle size, higher gas velocity and shorter charging tube was preferred for separation, because it sufficiently charged the particles while agglomeration was minimized. Electrostatic separation while using the optimum setting achieved a similar enrichment in arabinoxylans (from 23% to 30% dry matter basis) as sieving does. However, the combination of electrostatic separation and sieving further improved the enrichment and resulted in a fraction with an arabinoxylans content of 43% dry matter basis, which is around the maximum achievable purity can be reached by dry fractionation.

Because rice bran has similar structure to wheat bran, we expected a similar separation and explored this in **chapter 6**, where a custom-built bench-scale electrostatic separator was used. Enrichment of the dietary fibre from defatted rice bran was achieved by combing milling and different dry separation processes. All three tested separation routes produced fibre-enriched fractions with similar yield (20 – 21 % of the milled flour) and fibre content (67 – 68 % dry matter basis), which recovered 42 – 48 % of the fibre from the original flour. The enriched fractions obtained by a two-step electrostatic separation process contained more small particles compared to the other two, which resulted in different swelling and oil binding capacity. Compared to the total dietary fibre extracted by the enzymatic-gravimetric method, the enriched fractions by dry fractionation had a similar water retention capacity and oil binding capacity. This suggests that the fibre-enriched fractions by dry fractionation can be applied in foods and provide similar technological properties and physiological effects as the wet-extracted dietary fibre does.

Differently from cereal brans, legumes are interesting because of their high protein content. In **chapter 5** we reported on dry fractionation by combining milling and electrostatic separation providing an alternative to wet extraction of protein from lupine seeds. Proper milling of the lupine flour was found to be essential for successful protein enrichment by electrostatic separation. Relatively coarse milling was preferred because it sufficiently disclosed protein bodies from the matrix, while avoiding poor dispersibility of the powder due to too small particle sizes. With the optimal settings of single-step electrostatic separation, a fraction with 57.3 g/100 g dry solids could be obtained. The protein content was further improved after two more separation steps. A fraction with 65.0% dry matter basis was obtained, which is 15% higher than obtained by air classification. The yield of the protein enriched fraction was further increased by recycling the fractions from the filter bags, but this was accompanied by a decrease in protein content and vice versa. A significant shift towards better yield and purities was achieved by re-milling the flour that was not collected on the electrodes. A final fraction with a protein content of 65.1% dry matter basis and a yield of 6% was obtained, which recovered 10% of the protein in the original flour.

Two schemes for protein enrichment from legumes and fibre enrichment from brans

Based on the findings we propose two dry fractionation schemes for protein enrichment from legumes and fibre enrichment from brans (Figure 40). For legumes, impact milling is effective to break the cellular structure and release individual protein bodies. Multiple-step electrostatic separation is suggested, with the option of re-milling and recycling of the middle fraction from each step to improve the yield (**chapter 5**). For starch-rich legumes such as pea, an air classification step is needed to remove the starch before electrostatic separation, because starch and protein tend to be charged with the same polarity and end up in the same fraction (Pelgrom et al., 2015a). For brans, pin milling is used because it can separate the different layers. Fibres can be enriched by sieving, multiple-step electrostatic separation, or a combination of electrostatic separation and sieving. The similar effectiveness of sieving and electrostatic separation is because the pericarp (rich in fibre) is more elastic and more difficult to break down into smaller particles compared to the aleurone layer and the starchy endosperm. As a result, most of the pericarp fragments are larger in size after pin milling and are enriched in the coarse fraction by sieving. However, the fibre-enriched fractions obtained by electrostatic separation also contain small particles, which can provide different functional properties (**chapter 6**). Therefore, according to the type of application that is targeted, one can decide which separation route is most suitable for enriching fibre from brans.

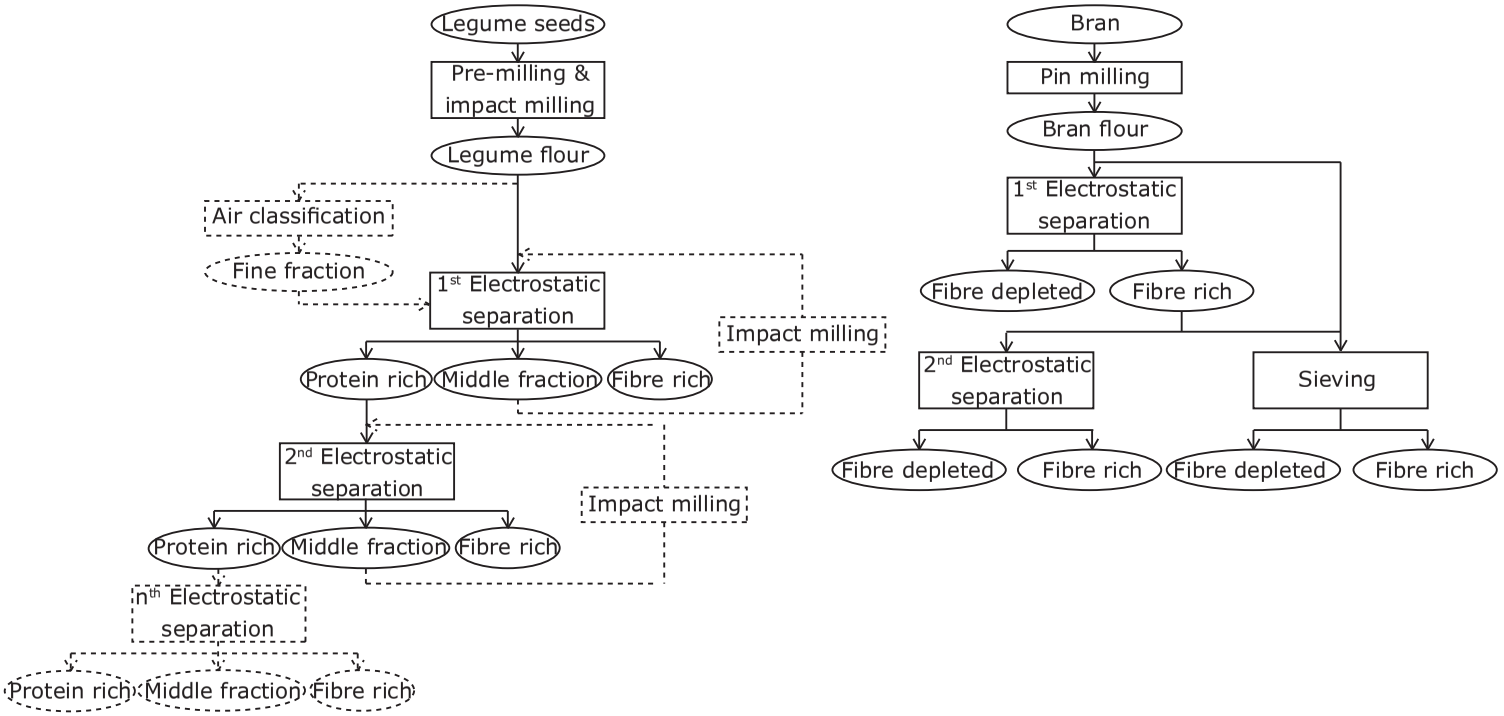

Figure 40. Dry fractionation scheme for A) enriching protein from legume and B) enriching fibre from bran.

Key factors to a successful electrostatic separation for food ingredient production from agro-material

Based on the findings, we concluded that there are three key factors that need to be fulfilled to obtain successful electrostatic separation for an agro-material:

1) Sufficient dissociation of structures during milling to enable separation;
2) Different charging behaviour of the target component versus that of the other components;
3) Optimal balance between sufficient charging and absence of agglomeration due to poor dispersibility or too high opposite charges.

Sufficient dissociation of different components

Electrostatic separation separates particles that have different compositions, based on their different charges. Therefore, a sufficient dissociation of different substructures from the complex raw material is a prerequisite for a successful electrostatic separation. For example, the different layers of cereal bran needs to be separated from each other for achieving fibre enrichment (**chapter 3** and **chapter 6**), protein bodies need to be detached from other cellular compounds of lupine seeds to allow enrichment of protein (**chapter 5**).

To achieve sufficient dissociation of different substructures, the milling should match the structural and mechanical properties of the material. For bran particles, separation between different layers is more important than reduction of the particle sizes. Therefore, pin milling, which is considered relatively coarse milling compared to jet milling and impact milling, was found most suitable for milling bran particles. It separates the pericarp and aleurone layers due to their different elastoplasticities and rupture energies (Chen et al., 2013). In contrast, for legume seeds a finer milling is needed to break the particles down to the size

equivalent to the size of protein bodies, e.g. 5 – 25 μm for lupine, to allow the detachment of protein bodies from other cellular components. Impact milling was here found the most effective method. However, the milling should not be too fine because this will lead to poor dispersibility of the fine powder, which hinders subsequent separation. Besides choosing the right milling method, some pre-treatment, e.g. defatting and adjusting the moisture content and temperature of the material, may also help the dissociation of the components (Pelgrom et al., 2015a).

Concluding, to achieve sufficient dissociation of different components, a thorough understanding of the morphology, composition and grinding behaviour of the agro-material is needed, which should be the basis of the selection of the milling methods. Pre-treatment may be carried out to facilitate this process.

Different charge of the targeted component versus that of the others

Electrostatic separation can only be achieved if the charges taken by the targeted components are different (ideally in polarity, but at least in the amount of charge) from the others. Using bran as an example, by contacting with aluminium, the pericarp fragments (rich in fibre) became negatively charged while the aleurone layers (rich in protein) and starchy endosperm became positively charged (**chapter 3** and **chapter 6**). This allowed the separation of fibre from the other components. However, enrichment of protein from the bran with the same method would not be successful. Similarly, applying electrostatic separation directly to full pea flour could not enrich protein, because both starch and protein took positive charge by contacting with aluminium and ended up in the same fraction (Pelgrom et al., 2015a). Enrichment of protein from lupine was successful because lupine seed contains no starch and the two main components, protein and fibre, were charged oppositely (**chapter 5**).

Most agro-materials contain mainly starch, protein and fibre. According to our findings, the protein and starch in native state often charge with the same polarity by contacting with aluminium, whereas fibre charges oppositely. To separate protein from starch, a different charging material that can charge protein and

starch oppositely is needed. Based on the tendency in charge polarity, a simple triboelectric series of starch, protein, fibre and aluminium can be made (Table 8). The order of starch and protein is not clear because the absolute amount of charge obtained by each component could not be measured. The charging material should be chosen from the materials above aluminium in the list, e.g. glass or nylon (Adams, 1987).

Table 8. Triboelectric series

	This thesis	Adams (1987)
Positive	Starch (Protein)	Hand
↑	Protein (Starch)	Asbestos
↑	Aluminium	Rabbit fur
↑	Fibre	Glass
↑		Mica
↑		Hair
↑		Nylon
↑		Wool
↑		Pb
↑		Silk
↑		Aluminium
↑		Paper
↑		Cotton
↑		Steel
↑		Wood
↑		Hard rubber
↑		Cu
↑		Ag
↑		Sulphur
↑		Polyester
↑		Styrene
↑		Polyethylene
↑		Polypropylene
↑		PVC
↑		Silicon
Negative		Teflon

As alternative to using a different charging material, one can also change the collecting method to allow separate collection of particles charged with the same polarity but having different absolute charge. In this thesis we aimed to collect two fractions: a positively charged fraction and a negatively charged fraction. However, it is logical to think that particles with higher charge will be deflected more and deposited earlier onto the electrode. Therefore, the electrode may be divided into several parts along the gas-powder flow direction. Samples collected from the different parts of the electrode may have different compositions. Alternatively, instead of two collectors under the electrodes, more collectors can be placed. The fraction from the collector on the side is expected to contain higher charged particles, while the collector closer to the middle contains less charged particles (Higashiyama and Asano, 1998).

Balance between sufficient charging and avoiding agglomeration

Generally, a high dispersibility of the powder and absence of agglomeration is important for all types of dry fractionation. This is particularly crucial for electrostatic separation, because the separation needs particles to take sufficient charge, which in turn increases the risk of agglomeration by oppositely charged particles. Therefore, a balance between sufficient charging and avoiding agglomeration is key for successful electrostatic separation.

Smaller particles, a longer charging tube, a higher gas velocity and a lower dosing rate were found to be favourable to obtain increased particle charging (**chapter 2** and **chapter 4**). Nevertheless, the effects of these parameters on agglomeration are not the same. Smaller particles are more prone to agglomerate because of the stronger attractive forces (Lam and Newton, 1992), while the pneumatic force acting on the particles due to the flow, and which may disrupt the agglomerates, is less. A longer charging tube may also lead to more agglomeration by increasing the residence time of particles in the tube and therefore the chance for oppositely charged particles to meet each other. In contrast, the higher gas velocity and lower dosing rate were both found to decrease the chance for agglomeration, by decreasing the residence time of particles and the particle concentration. However, a lower dosing compared to the gas flow will impact the productivity of the process; for large-scale application, one would need the throughput of particles to be as high as possible.

Therefore, optimal milling is again important, which yields sufficient dissociation of different components, but still provides a powder that can be well dispersed in the gas. Second, the length of the charging tube/channel needs to be optimized. For a given particle size and charging tube length, agglomeration can be minimized by using a lower dosing rate and higher gas velocity. However, it is important to realize that a lower dosing rate and higher gas flow rate will result in lower throughput and thus higher costs.

A conceptual design for scaling-up

Compared to the lab-scale electrostatic separator used in **chapter 2** and **chapter 3**, the custom-built bench-scale separator presented in **chapter 4 – 6** had increased feed capacity (~500 g compared to 5 g) with lower losses (~10% compared to ~35%). However, the bench-scale separator is still batch-wise and materials from the electrodes need to be manually collected once in a while during a trial. Therefore the electrostatic separation process needs to be further optimized for scaling-up to industrial production.

Rotating belt electrode for automated sample collection

During our study on protein enrichment from lupine flour, we found that the fraction on the electrode is the most enriched, and not the fractions collected from the collector bags. Therefore instead of collecting fractions from the collector, we collected the fraction from the electrodes. However, to collect the sample the trial needs to be interrupted several times. The interval between manual handling should not be too long, because else the powder deposited on the electrode may decrease the electric field strength by a shielding effect and result in poor separation (**chapter 5**). Therefore, automated sample collection with rotating drum electrodes or rotating belt electrodes is suggested (Chinma et al., 2015). To preserve a specific distance between the electrodes, which is important for a homogeneous electric field, and to limit the space needed for the system, several drums have to be used in series (Figure 41-B), or rotating belts can be used (Figure 41-A), because it occupies less space and allows better adjustment of the angle and distance between the two electrodes. The metal electrode then remains as it is and is connected with the high voltage power supply. A conveyor belt made of a thin layer of PTFE (Teflon) then moves over the electrodes, covering the inner side (the side facing the other electrode) of the metal plate. The belt is rotated with two rollers. At the lower part of the belt a brush or knife scrapes off the particles deposited on the belt. The particles fall into a collector bin right below the electrode.

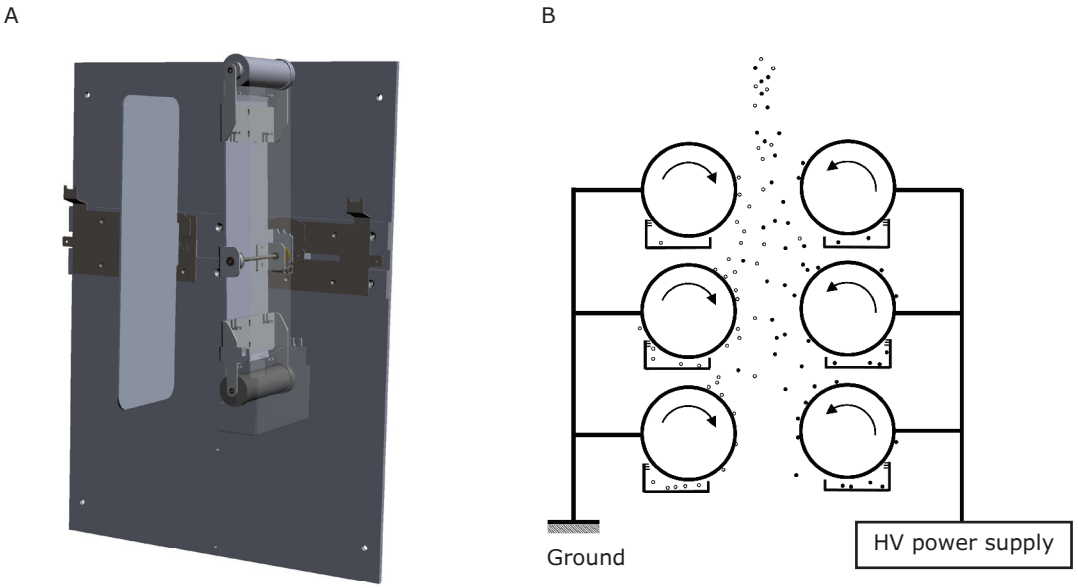

Figure 41. A) Rotating belt electrode – adaptation on the bench-scale electrostatic separator and B) a set of drum electrodes

For scaling-up without the constraints of the current set up one could also opt for a set of drum electrodes (Figure 41-B), which is probably easier to construct. One recent study also proposed a combination of a drum electrode and a belt electrode (Remadnia et al., 2014). However, this set-up does not have gas-assisted flow, which is important for dispersing fine powders. Furthermore, the charging applied in this set up relies on induction charging rather than on triboelectric charging.

Extend or adapt the design of the transition part to optimise powder dispersion

Dispersion of the powder particles was found critical to separate very fine powders in the current set-up, as this resulted sometimes in blockage above the charging slit. This might be improved by extension of the transition part above the charging slit in order to enhance dispersion of particles in the gas. Alternatively, the design may be adapted, for example by introducing a swirl to enhance the mixing of gas and particles.

More generally, to better disperse the particles, a completely different design of the charging device might be considered. For example, the use of a fluidized bed (Abdul-Hamid and Luan, 2000) may enhance dispersion of small particles in the gas.

Safety evaluation

The risk of dust explosions is always of great concern in food industry, because dry powders such as sugar, starches and flours may explode at critically high enough concentrations (Childs, 2004). Actually electrostatic charging during powder handling is known as a potential hazard that can lead to dust explosion (Shibuya and Iwasaki, 1985). Therefore, it is important to evaluate the explosion hazards for electrostatic separation to provide useful information about risks and possible measures to prevent explosion.

A dust explosion may occur when three main factors are satisfied simultaneously (Childs, 2004): 1) The combustible dust must be dispersed in air while contained within a volume; 2) The concentration of dispersed dust must be above the minimum explosive concentration; 3) An ignition source with sufficient density and total energy to initiate the combustion wave must be present.

During electrostatic separation, particles need to be dispersed in the carrier gas. The particle concentration in the bench-scale system is normally about 1000 g/m^3, which is much higher than the minimum explosive concentration for food powders (45 – 85 g/m^3). Furthermore, discharge between the high-voltage electrode and charged particles can occur, which results in sparks. Therefore, there is a potential risk of dust explosion during electrostatic separation.

To prevent explosion, eliminating one the three factors mentioned above would be sufficient. In our case, dispersion of particles in carrier gas is needed, as well as the high voltage on the electrodes. Besides, the particle concentration should not be too low because a reasonable throughput of the process is required. As a result, the left option is to reduce the availability of oxygen. To achieve this, we applied nitrogen gas instead of normal air for dispersing the powders and fully fill the set-up with nitrogen before running an experiment. For scaling-up, the

costs for using large amounts of nitrogen gas need to be considered, which can be reduced by recycling and reusing the gas.

Conclusion and outlook for future research

To conclude, the work reported in this thesis has given us insight in the key factors for successful electrostatic separation by providing better understanding of the charging and separation behaviour of model and agro-materials. The work demonstrated the potential of applying this separation method for functional ingredient production from different agro-materials and also gave directions for further improvement and scaling-up.

Future research should be directed towards understanding fracture behaviour and optimal milling behaviour of the material to be separated. Better insight on optimal dispersion of fine powders in gas could support improving the design of the current electrostatic separator as this is a bottleneck in the current set up. Next, a triboelectric series for agro-materials could be constructed for better selection of charging materials that enable electrostatic separation of more components. Finally, studying functional and nutritional properties of enriched fractions could enhance further development and application of this sustainable technology in manufacturing of food ingredients.

References

Abdul-Hamid, A., Luan, Y.S., (2000). Functional properties of dietary fibre prepared from defatted rice bran. Food Chemistry 68(1), 15-19.

Adams, C.K., (1987). *Nature's Electricity*. Tab Books.

Aguilera, J.M., Levi, G., Karel, M., (1993). Effect of water content on the glass transition and caking of fish protein hydrolyzates. Biotechnology Progress 9(6), 651-654.

Aiking, H., (2011). Future protein supply. Trends in Food Science & Technology 22(2–3), 112-120.

Alamanou, S., Bloukas, J.G., Paneras, E.D., Doxastakis, G., (1996). Influence of protein isolate from lupin seeds (Lupinus albus ssp. Graecus) on processing and quality characteristics of frankfurters. Meat Science 42(1), 79-93.

Alamanou, S., Doxastakis, G., (1995). Thermoreversible size selective swelling polymers as a means of purification and concentration of lupin seed proteins (Lupinus albus ssp. Graecus). Food Hydrocolloids 9(2), 103-109.

Bada, S.O., Tao, D., Honaker, R.Q., Falcon, L.M., Falcon, R.M.S., (2010). A study of rotary tribo-electrostatic separation of south african fine coal. International Journal of Coal Preparation and Utilization 30(2-5), 154-172.

Bailey, A.G., (1984). Electrostatic phenomena during powder handling. Powder Technology 37(1), 71-85.

Bailey, A.G., (1993). Charging of solids and powders. Journal of Electrostatics 30(0), 167-180.

Bailey, A.G., Smedley, C.J.A., (1991). The impact charging of polymer particles. Advanced Powder Technology 2(4), 277-284.

Ban, H., Li, T.X., Hower, J.C., Schaefer, J.L., Stencel, J.M., (1997). Dry triboelectrostatic beneficiation of fly ash. Fuel 76(8), 801-805.

Barron, C., Surget, A., Rouau, X., (2007). Relative amounts of tissues in mature wheat (Triticum aestivum L.) grain and their carbohydrate and phenolic acid composition. Journal of Cereal Science 45(1), 88-96.

Bechtel, D.B., Abecassis, J., Shewry, P.R., Evers, A.D., (2009). CHAPTER 3: Development, structure, and mechanical properties of the wheat grain, *WHEAT: Chemistry and Technology*. AACC International, Inc., pp. 51-95.

Bechtel, D.B., Pomeranz, Y., (1977). Ultrastructure of the mature ungerminated rice (Oryza sativa) caryopsis. The caryopsis coat and the aleurone cells. American Journal of Botany 64(8), 966-973.

Benamrouche, S., Crônier, D., Debeire, P., Chabbert, B., (2002). A chemical and histological study on the effect of (1-->4)-β-endo-xylanase treatment on wheat bran. Journal of Cereal Science 36(2), 253-260.

Bendimerad, S., Tilmatine, A., Ziane, M., Dascalescu, L., (2009). Plastic wastes recovery using free-fall triboelectric separator. International Journal of Environmental Studies 66(5), 529-538.

Berghout, J.A.M., Boom, R.M., van der Goot, A.J., (2014). The potential of aqueous fractionation of lupin seeds for high-protein foods. Food Chemistry 159, 64-70.

Berghout, J.A.M., Boom, R.M., van der Goot, A.J., (2015a). Understanding the differences in gelling properties between lupin protein isolate and soy protein isolate. Food Hydrocolloids 43, 465-472.

Berghout, J.A.M., Marmolejo-Garcia, C., Berton-Carabin, C.C., Nikiforidis, C.V., Boom, R.M., van der Goot, A.J., (2015b). Aqueous fractionation yields chemically stable lupin protein isolates. Food Research International 72, 82-90.

Berghout, J.A.M., Venema, P., Boom, R.M., van der Goot, A.J., (2015c). Comparing functional properties of concentrated protein isolates with freeze-dried protein isolates from lupin seeds. Food Hydrocolloids 51, 346-354.

Bergmans, M.E.F., Beldman, G., Gruppen, H., Voragen, A.G.J., (1996). Optimisation of the selective extraction of (glucurono)arabinoxylans from wheat bran: Use of barium and calcium hydroxide solution at elevated temperatures. 23(3), 235-245.

Bettge, A.D., Morris, C.F., (2007). Oxidative gelation measurement and influence on soft wheat batter viscosity and end-use quality. Cereal Chemistry Journal 84(3), 237-242.

Bilgiçli, N., Ibano□lu, S., Herken, E.N., (2007). Effect of dietary fibre addition on the selected nutritional properties of cookies. 78(1), 86-89.

Bohm, A., Bogoni, C., Behrens, R., Otto, T., (2003). Method for the extraction of aleurone from bran, *Buhler AG, US Patent Application Publication*.

Brillouet, J.-M., Joseleau, J.-P., (1987). Investigation of the structure of a heteroxylan from the outer pericarp (beeswing bran) of wheat kernel. Carbohydrate research 159(1), 109-126.

Brouns, F., Hemery, Y., Price, R., Anson, N.M., (2012). Wheat aleurone: Separation, composition, health aspects, and potential food use. Critical Reviews in Food Science and Nutrition 52(6), 553-568.

Bruinsma, J., (2009). The resource outlook to 2050, *Expert meeting on how to feed the world in*, pp. 1-33.

Bunzel, M., Ralph, J., Kim, H., Lu, F., Ralph, S.A., Marita, J.M., Hatfield, R.D., Steinhart, H., (2003). Sinapate dehydrodimers and sinapate−ferulate heterodimers in cereal dietary fiber. Journal of Agricultural and Food Chemistry 51(5), 1427-1434.

Cadden, A.-M., (1987). Comparative effects of particle size reduction on physical structure and water binding properties of several plant fibers. Journal of Food Science 52(6), 1595-1599.

Calin, L., Mihalcioiu, A., Das, S., Neamtu, V., Dragan, C., Dascalescu, L., Iuga, A., (2008). Controlling particle trajectory in free-fall electrostatic separators. IEEE Transactions on Industry Applications 44(4), 1038-1044.

Cangialosi, F., Notarnicola, M., Liberti, L., Stencel, J.M., (2008). The effects of particle concentration and charge exchange on fly ash beneficiation with pneumatic triboelectrostatic separation. Separation and Purification Technology 62(1), 240-248.

Cao, L., Liu, X., Qian, T., Sun, G., Guo, Y., Chang, F., Zhou, S., Sun, X., (2011). Antitumor and immunomodulatory activity of arabinoxylans: A major constituent of wheat bran. 48(1), 160-164.

Carter, P.A., Cassidy, O.E., Rowley, G., Merrifield, D.R., (1998). Triboelectrification of fractionated crystalline and spray-dried lactose. Pharmacy and Pharmacology Communications 4(2), 111-115.

Chau, C.-F., Wang, Y.-T., Wen, Y.-L., (2007). Different micronization methods significantly improve the functionality of carrot insoluble fibre. Food Chemistry 100(4), 1402-1408.

Cheftel, J.C., Kitagawa, M., Quéguiner, C., (1992). New protein texturization processes by extrusion cooking at high moisture levels. Food Reviews International 8(2), 235-275.

Chen, Z., Liu, F., Wang, L., Li, Y., Wang, R., Chen, Z., (2014a). Tribocharging properties of wheat bran fragments in air–solid pipe flow. Food Research International 62(0), 262-271.

Chen, Z., Wang, L., Wang, R., Li, Y., Chen, Z., (2014b). Triboelectric separation of aleurone cell-cluster from wheat bran fragments in nonuniform electric field. Food Research International 62(0), 111-120.

Chen, Z., Zha, B., Wang, L., Wang, R., Tian, Y., (2013). Dissociation of aleurone cell cluster from wheat bran by centrifugal impact milling. 54(1), 63-71.

Childs, N.W., (2004). CHAPTER 1: Production and utilization of rice, *RICE: Chemistry and Technology*. American Association of Cereal Chemists, Inc., pp. 1-23.

Chinma, C.E., Ramakrishnan, Y., Ilowefah, M., Hanis-Syazwani, M., Muhammad, K., (2015). Properties of cereal brans: A review. Cereal chemistry 92(1), 1-7.

Choi, Y.-S., Choi, J.-H., Han, D.-J., Kim, H.-Y., Lee, M.-A., Kim, H.-W., Jeong, J.-Y., Kim, C.-J., (2009). Characteristics of low-fat meat emulsion systems with pork fat replaced by vegetable oils and rice bran fiber. Meat Science 82(2), 266-271.

Daou, C., Zhang, H., (2011). Physico-chemical properties and antioxidant activities of dietary fiber derived from defatted rice bran. Advance Journal of Food Science and Technology 3(5), 339-347.

Daou, C., Zhang, H., (2014). Functional and physiological properties of total, soluble, and insoluble dietary fibres derived from defatted rice bran. Journal of Food Science and Technology 51(12), 3878-3885.

Dascalescu, L., Dragan, C., Bilici, M., Beleca, R., Hemery, Y., Rouau, X., (2010). Electrostatic basis for separation of wheat bran tissues. Industry Applications, IEEE Transactions on 46(2), 659-665.

Dascalescu, L., Urs, A., Bente, S., Huzau, M., Samuila, A., (2005). Charging of mm-size insulating particles in vibratory devices. Journal of Electrostatics 63(6–10), 705-710.

Dervas, G., Doxastakis, G., Hadjisavva-Zinoviadi, S., Triantafillakos, N., (1999). Lupin flour addition to wheat flour doughs and effect on rheological properties. Food Chemistry 66(1), 67-73.

Dijkink, B.H., Speranza, L., Paltsidis, D., Vereijken, J.M., (2007). Air dispersion of starch–protein mixtures: A predictive tool for air classification performance. Powder Technology 172(2), 113-119.

Dodbiba, G., Shibayama, A., Miyazaki, T., Fujita, T., (2002). Electrostatic separation of the shredded plastic mixtures using a tribo-cyclone. Magnetic and Electrical Separation 11(1-2), 63-92.

Douglas, S.G., (1981). A rapid method for the determination of pentosans in wheat flour. Food Chemistry 7(2), 139-145.

Draganovic, V., Boom, R.M., Jonkers, J., van der Goot, A.J., (2014). Lupine and rapeseed protein concentrate in fish feed: A comparative assessment of the techno-functional properties using a shear cell device and an extruder. Journal of Food Engineering 126, 178-189.

Drakos, A., Doxastakis, G., Kiosseoglou, V., (2007). Functional effects of lupin proteins in comminuted meat and emulsion gels. Food Chemistry 100(2), 650-655.

Dwari, R.K., Mohanta, S.K., Rout, B., Soni, R.K., Reddy, P.S.R., Mishra, B.K., (2015). Studies on the effect of electrode plate position and feed temperature on the tribo-electrostatic separation of high ash Indian coking coal. Advanced Powder Technology 26(1), 31-41.

Eilbeck, J., Rowley, G., Carter, P.A., Fletcher, E.J., (1999). Effect of materials of construction of pharmaceutical processing equipment and drug delivery devices on the triboelectrification of size-fractionated lactose. Pharmacy and Pharmacology Communications 5(7), 429-433.

El-Adawy, T.A., Rahma, E.H., El-Bedawey, A.A., Gafar, A.F., (2001). Nutritional potential and functional properties of sweet and bitter lupin seed protein isolates. Food Chemistry 74(4), 455-462.

Elleuch, M., Bedigian, D., Roiseux, O., Besbes, S., Blecker, C., Attia, H., (2011). Dietary fibre and fibre-rich by-products of food processing: Characterisation, technological functionality and commercial applications: A review. Food Chemistry 124(2), 411-421.

Esposito, F., Arlotti, G., Maria Bonifati, A., Napolitano, A., Vitale, D., Fogliano, V., (2005). Antioxidant activity and dietary fibre in durum wheat bran by-products. Food Research International 38(10), 1167-1173.

FAOSTAT, (2015). Food and Agriculture Organization of the United Nations, FAOSTAT online database.

Finnie, S.M., Bettge, A.D., Morris, C.F., (2006). Influence of cultivar and environment on water-soluble and water-insoluble arabinoxylans in soft wheat. Cereal Chemistry Journal 83(6), 617-623.

Forward, K.M., Lacks, D.J., Sankaran, R.M., (2008). Triboelectric charging of granular insulator mixtures due solely to particle−particle interactions. Industrial & Engineering Chemistry Research 48(5), 2309-2314.

Foschia, M., Peressini, D., Sensidoni, A., Brennan, C.S., (2013). The effects of dietary fibre addition on the quality of common cereal products. Journal of Cereal Science 58(2), 216-227.

Fraas, F., Balston, O.C., (1940). Electrostatic separations of solids. Industrial & Engineering Chemistry 32(5), 600-604.

Friedman, M., (2013). Rice brans, rice bran oils, and rice hulls: composition, food and industrial uses, and bioactivities in humans, animals, and cells. Journal of Agricultural and Food Chemistry 61(45), 10626-10641.

Gajewski, A., (1989). Measuring the charging tendency of polysterene particles in pneumatic conveyance. Journal of Electrostatics 23(0), 55-66.

Garcia, A.L., Otto, B., Reich, S.C., Weickert, M.O., Steiniger, J., Machowetz, A., Rudovich, N.N., Mohlig, M., Katz, N., Speth, M., Meuser, F., Doerfer, J., Zunft, H.J.F., Pfeiffer, A.H.F., Koebnick, C., (2006). Arabinoxylan consumption decreases postprandial serum glucose, serum insulin and plasma total ghrelin response in subjects with impaired glucose tolerance. 61(3), 334-341.

Gaudin, A., Mora, R.G., (1958). Study of electrical concentration of minerals, *Massachusetts Institute of Technology. Dept. of Metallurgy*.

Greenley, R.Z., Brandrup, J., Immergut, E., (1989). Polymer handbook. Polymer Handbook, 267-274.

Gupta, R., Gidaspow, D., Wasan, D.T., (1993). Electrostatic separation of powder mixtures based on the work functions of its constituents. Powder Technology 75(1), 79-87.

Haga, K., (1995). Applications of the electrostatic separation technique, in: J.S.Chang, A.J. Kelly, Crowley, J.M. (Eds.), *Handbook of Electrostatic Processes.* Marcel Dekker, New York.

Hemery, Y., Holopainen, U., Lampi, A.-M., Lehtinen, P., Nurmi, T., Piironen, V., Edelmann, M., Rouau, X., (2011). Potential of dry fractionation of wheat bran for the development of food ingredients, part II: Electrostatic separation of particles. Journal of Cereal Science 53(1), 9-18.

Hemery, Y., Lullien-Pellerin, V., Rouau, X., Abecassis, J., Samson, M.-F., Åman, P., von Reding, W., Spoerndli, C., Barron, C., (2009a). Biochemical markers: Efficient tools for the assessment of wheat grain tissue proportions in milling fractions. Journal of Cereal Science 49(1), 55-64.

Hemery, Y., Rouau, X., Dragan, C., Bilici, M., Beleca, R., Dascalescu, L., (2009b). Electrostatic properties of wheat bran and its constitutive layers: Influence of particle size, composition, and moisture content. Journal of Food Engineering 93(1), 114-124.

Hemery, Y., Rouau, X., Lullien-Pellerin, V., Barron, C., Abecassis, J., (2007). Dry processes to develop wheat fractions and products with enhanced nutritional quality. Journal of Cereal Science 46(3), 327-347.

Higashiyama, Y., Asano, K., (1998). Recent progress in electrostatic separation technology. Particulate Science and Technology 16(1), 77-90.

Horn, R.G., Smith, D.T., (1992). Contact electrification and adhesion between dissimilar materials. Science 256(5055), 362-364.

Hove, E.L., (1974). Composition and protein quality of sweet lupin seed. Journal of the Science of Food and Agriculture 25(7), 851-859.

Hu, G., Huang, S., Cao, S., Ma, Z., (2009). Effect of enrichment with hemicellulose from rice bran on chemical and functional properties of bread. Food Chemistry 115(3), 839-842.

Inculet, I.I., Castle, G.S.P., Brown, J.D., (1998). Electrostatic separation of plastics for recycling. Particulate Science and Technology 16(1), 91-100.

Islam, N., Stewart, P., Larson, I., Hartley, P., (2005). Surface roughness contribution to the adhesion force distribution of salmeterol xinafoate on lactose carriers by atomic force microscopy. Journal of Pharmaceutical Sciences 94(7), 1500-1511.

Jaffari, S., Forbes, B., Collins, E., Barlow, D.J., Martin, G.P., Murnane, D., (2013). Rapid characterisation of the inherent dispersibility of respirable powders using dry dispersion laser diffraction. International Journal of Pharmaceutics 447(1–2), 124-131.

Jayasena, V., Chih, H., Nasar-Abbas, S., (2011). A practical and economical approach to efficient isolation of lupin protein. Food Australia 63(7), 306-309.
Jeon, H.-S., Park, C.-H., Kim, B.-G., Park, J.-K., (2006). Development of triboelectrostaic separation technique for recycling of final waste plastic. Geosystem Engineering 9(1), 21-24.

Jung, S., (2009). Aqueous extraction of oil and protein from soybean and lupin: a comparative study. Journal of Food Processing and Preservation 33(4), 547-559.

Kahlon, T.S., Chow, F.I., (2000). In vitro binding of bile acids by rice bran, oat bran, wheat bran, and corn bran. Cereal Chemistry Journal 77(4), 518-521.

Kalichevsky, M.T., Jaroszkiewicz, E.M., Blanshard, J.M.V., (1992). Glass transition of gluten. 1: Gluten and gluten—sugar mixtures. International Journal of Biological Macromolecules 14(5), 257-266.

Kaur, G., Sharma, S., Nagi, H.P.S., Dar, B., (2012). Functional properties of pasta enriched with variable cereal brans. Journal of Food Science and Technology 49(4), 467-474.

Kelly, E.G., Spottiswood, D.J., (1989a). The theory of electrostatic separations: A review Part I. Fundamentals. Minerals Engineering 2(1), 33-46.

Kelly, E.G., Spottiswood, D.J., (1989b). The theory of electrostatic separations: A review part II. Particle charging. Minerals Engineering 2(2), 193-205.

Kelly, E.G., Spottiswood, D.J., (1989c). The theory of electrostatic separations: A review part III. The separation of particles. Minerals Engineering 2(3), 337-349.

Korevaar, M.W., Padding, J.T., Deen, N.G., Wang, J., de Wit, M., Schutyser, M.A.I., Kuipers, J.A.M., (2015). Hybrid PIV/PTV measurements of velocity and position distributions of gas-conveyed particles in small, narrow channels. AIChE Journal 61(11), 3616-3627.

Korevaar, M.W., Padding, J.T., Van der Hoef, M.A., Kuipers, J.A.M., (2014). Integrated DEM–CFD modeling of the contact charging of pneumatically conveyed powders. Powder Technology 258(0), 144-156.

Kwetkus, B.A., (1998). Particle triboelectrification and its use in the electrostatic separation process. Particulate Science and Technology 16(1), 55-68.

Lakkakula, N.R., Lima, M., Walker, T., (2004). Rice bran stabilization and rice bran oil extraction using ohmic heating. Bioresource Technology 92(2), 157-161.

Lam, K.K., Newton, J.M., (1992). Influence of particle size on the adhesion behaviour of powders, after application of an initial press-on force. Powder Technology 73(2), 117-125.

Le Gal, M.F., Rey, L., (1986). The reserve proteins in the cells of mature cotyledons ofLupinus albus var.Lucky. I. Quantitative ultrastructural study of the protein bodies. Protoplasma 130(2-3), 120-127.

Li, T.X., Ban, H., Hower, J.C., Stencel, J.M., Saito, K., (1999). Dry triboelectrostatic separation of mineral particles: a potential application in space exploration. Journal of Electrostatics 47(3), 133-142.

Livsmedelsverk, S., (1987). Livsmedelstabeller, *European Food Composition Tables in Translation*. Springer, pp. 105-115.

Lqari, H., Vioque, J., Pedroche, J., Millán, F., (2002). Lupinus angustifolius protein isolates: chemical composition, functional properties and protein characterization. Food Chemistry 76(3), 349-356.

Maes, C., Delcour, J.A., (2001). Alkaline hydrogen peroxide extraction of wheat bran non-starch polysaccharides. Journal of Cereal Science 34(1), 29-35.
Maes, C., Delcour, J.A., (2002). Structural characterisation of water-extractable and water-unextractable arabinoxylans in wheat bran. Journal of Cereal Science 35(3), 315-326.

Matsusaka, S., Ghadiri, M., Masuda, H., (2000). Electrification of an elastic sphere by repeated impacts on a metal plate. Journal of Physics D: Applied Physics 33(18), 2311.

Matsusaka, S., Maruyama, H., Matsuyama, T., Ghadiri, M., (2010). Triboelectric charging of powders: A review. Chemical Engineering Science 65(22), 5781-5807.

Matsuyama, T., Šupuk, E., Ahmadian, H., Hassanpour, A., Ghadiri, M., (2009). Analysis of tribo-electric charging of spherical beads using distinct element method. AIP Conference Proceedings 1145(1), 127-130.

Matsuyama, T., Yamamoto, H., (1994). Charge transfer between a polymer particle and a metal plate due to impact. Industry Applications, IEEE Transactions on 30(3), 602-607.

Matsuyama, T., Yamamoto, H., (1995). Electrification of single polymer particles by successive impacts with metal targets. Industry Applications, IEEE Transactions on 31(6), 1441-1445.

Maxted, N., Bennett, S., Cowling, W., (2001). Lupins (Lupinus L.), *Plant Genetic Resources of Legumes in the Mediterranean*. Springer Netherlands, pp. 191-206.

Mazumder, M.K., Sims, R.A., Biris, A.S., Srirama, P.K., Saini, D., Yurteri, C.U., Trigwell, S., De, S., Sharma, R., (2006). Twenty-first century research needs in electrostatic processes applied to industry and medicine. Chemical Engineering Science 61(7), 2192-2211.

Mendis, M., Simsek, S., (2014). Arabinoxylans and human health. Food Hydrocolloids 42, Part 2(0), 239-243.

Mod, R.R., Conkerton, E.J., Ory, R.L., Normand, F.L., (1978). Hemicellulose composition of dietary fiber of milled rice and rice bran. Journal of Agricultural and Food Chemistry 26(5), 1031-1035.

Nandi, I., Ghosh, M., (2015). Studies on functional and antioxidant property of dietary fibre extracted from defatted sesame husk, rice bran and flaxseed. Bioactive Carbohydrates and Dietary Fibre 5(2), 129-136.

Nandini, C.D., Salimath, P.V., (2001). Carbohydrate composition of wheat, wheat bran, sorghum and bajra with good chapati/roti (Indian flat bread) making quality. 73(2), 197-203.

Nguyen, T., Nieh, S., (1989). The role of water vapor in the charge elimination process for flowing powders. Journal of Electrostatics 22(2), 213-227.

Nomura, T., Satoh, T., Masuda, H., (2003). The environment humidity effect on the tribo-charge of powder. Powder Technology 135–136(0), 43-49.

Orthoefer, F.T., Eastman, J., (2004). CHAPTER 19: Rice bran and oil, *RICE: Chemistry and Technology*. American Association of Cereal Chemists, Inc., pp. 569-593.

Papavergou, E.J., Bloukas, J.G., Doxastakis, G., (1999). Effect of lupin seed proteins on quality characteristics of fermented sausages. Meat Science 52(4), 421-427.

Parker, M.L., Ng, A., Waldron, K.W., (2005). The phenolic acid and polysaccharide composition of cell walls of bran layers of mature wheat (Triticum aestivum L. cv. Avalon) grains. Journal of the Science of Food and Agriculture 85(15), 2539-2547.

Pelgrom, P.J.M., Berghout, J.A.M., van der Goot, A.J., Boom, R.M., Schutyser, M.A.I., (2014). Preparation of functional lupine protein fractions by dry separation. LWT - Food Science and Technology 59(2, Part 1), 680-688.

Pelgrom, P.J.M., Vissers, A.M., Boom, R.M., Schutyser, M.A.I., (2013a). Dry fractionation for production of functional pea protein concentrates. Food Research International 53(1), 232-239.

Pelgrom, P.J.M., Wang, J., Boom, R.M., Schutyser, M.A.I., (2015a). Pre- and post-treatment enhance the protein enrichment from milling and air classification of legumes. Journal of Food Engineering 155(0), 53-61.

Pelgrom, P.M., Boom, R., Schutyser, M.I., (2015b). Method development to increase protein enrichment during dry fractionation of starch-rich legumes. Food and Bioprocess Technology 8(7), 1495-1502.

Pelgrom, P.M., Schutyser, M.I., Boom, R., (2013b). Thermomechanical morphology of peas and its relation to fracture behaviour. Food and Bioprocess Technology 6(12), 3317-3325.

Plant, A.R., Moore, K.G., (1983). The protein, lipid and carbohydrate composition of protein bodies from Lupinus angustifolius seeds. Phytochemistry 22(11), 2359-2363.

Pollard, N.J., Stoddard, F.L., Popineau, Y., Wrigley, C.W., MacRitchie, F., (2002). Lupin flours as additives: dough mixing, breadmaking, emulsifying, and foaming. Cereal Chemistry Journal 79(5), 662-669.

Pozani, S., Doxastakis, G., Kiosseoglou, V., (2002). Functionality of lupin seed protein isolate in relation to its interfacial behaviour. Food Hydrocolloids 16(3), 241-247.

Prosky, L., Asp, N.G., Schweizer, T.F., DeVries, J.W., Furda, I., (1988). Determination of insoluble, soluble, and total dietary fiber in foods and food products: interlaboratory study. 71(5), 1017-1023.

Raghavendra, S.N., Ramachandra Swamy, S.R., Rastogi, N.K., Raghavarao, K.S.M.S., Kumar, S., Tharanathan, R.N., (2006). Grinding characteristics and hydration properties of coconut residue: A source of dietary fiber. Journal of Food Engineering 72(3), 281-286.

Raghavendra, S.N., Rastogi, N.K., Raghavarao, K.S.M.S., Tharanathan, R.N., (2004). Dietary fiber from coconut residue: effects of different treatments and particle size on the hydration properties. European Food Research and Technology 218(6), 563-567.

Ramseyer, D.D., Bettge, A.D., Morris, C.F., (2011). Endogenous and enhanced oxidative cross-linking in wheat flour mill streams. Cereal Chemistry Journal 88(2), 217-222.

Remadnia, M., Kachi, M., Messal, S., Oprean, A., Rouau, X., Dascalescu, L., (2014). Electrostatic separation of peeling and gluten from finely ground wheat grains. Particulate Science and Technology 32(6), 608-615.

Rietema, K., (1991). *The dynamics of fine powders*. Springer Science & Business Media.

Robertson, J.A., De Monredon, F.D., Dysseler, P., Guillon, F., Amadò, R., Thibault, J.F., (2000). Hydration properties of dietary fibre and resistant starch: A European collaborative study. LWT - Food Science and Technology 33(2), 72-79.

Rowley, G., (2001). Quantifying electrostatic interactions in pharmaceutical solid systems. International Journal of Pharmaceutics 227(1–2), 47-55.

Rowley, G., Mackin, L.A., (2003). The effect of moisture sorption on electrostatic charging of selected pharmaceutical excipient powders. Powder Technology 135–136(0), 50-58.

Sairam, S., Gopala Krishna, A.G., Urooj, A., (2011). Physico-chemical characteristics of defatted rice bran and its utilization in a bakery product. Journal of Food Science and Technology 48(4), 478-483.

Sangnark, A., Noomhorm, A., (2003). Effect of particle sizes on functional properties of dietary fibre prepared from sugarcane bagasse. Food Chemistry 80(2), 221-229.

Saunders, R.M., (1985). Rice bran: Composition and potential food uses. Food Reviews International 1(3), 465-495.

Schönert, K., Eichas, K., Niermöller, F., (1996). Charge distribution and state of agglomeration after tribocharging fine particulate materials. Powder Technology 86(1), 41-47.

Schooneveld-Bergmans, M.E.F., Beldman, G., Voragen, A.G.J., (1999). Structural features of (glucurono)arabinoxylans extracted from wheat bran by barium hydroxide. Journal of Cereal Science 29(1), 63-75.

Schutyser, M.A.I., Pelgrom, P.J.M., van der Goot, A.J., Boom, R.M., (2015). Dry fractionation for sustainable production of functional legume protein concentrates. Trends in Food Science & Technology 45(2), 327-335.

Schutyser, M.A.I., van der Goot, A.J., (2011). The potential of dry fractionation processes for sustainable plant protein production. Trends in Food Science & Technology 22(4), 154-164.

Shaw, P.E.C.F.p.d.N., (1917). Experiments on tribo-electricity. I. The tribo-electric series. Proceedings of the Royal Society of London. Series A, Containing Papers of a Mathematical and Physical Character 94(656), 16-33.

Shibuya, N., Iwasaki, T., (1985). Structural features of rice bran hemicellulose. Phytochemistry 24(2), 285-289.

Shih, F.F., (2004). CHAPTER 6: Rice proteins, *RICE: Chemistry and Technology*. American Association of Cereal Chemists, Inc., pp. 143-162.

Shiiba, K., Yamada, H., Hara, H., Okada, K., Nagao, S., (1993). Purification and characterization of two arabinoxylans from wheat bran. Cereal chemistry 70(2), 209-214.

Sibakov, J., Abecassis, J., Barron, C., Poutanen, K., (2014). Electrostatic separation combined with ultra-fine grinding to produce β-glucan enriched ingredients from oat bran. Innovative Food Science & Emerging Technologies 26(0), 445-455.

Stevens, D.J., McDermott, E.E., Pace, J., (1963). Isolation of endosperm protein and aleurone cell contents from wheat, and determination of their amino-acid composition. Journal of the Science of Food and Agriculture 14(5), 284-287.

Stone, B., Morell, M.K., (2009). CHAPTER 9: Carbohydrates, WHEAT: Chemistry and Technology. AACC International, Inc., pp. 299-362.

Stone, B.A., Minifie, J., (1988). Separation of fiber material. Google Patents.
Sujak, A., Kotlarz, A., Strobel, W., (2006). Compositional and nutritional evaluation of several lupin seeds. Food Chemistry 98(4), 711-719.

Swennen, K., Courtin, C.M., Lindemans, G.C.J.E., Delcour, J.A., (2006). Large-scale production and characterisation of wheat bran arabinoxylooligosaccharides. Journal of the Science of Food and Agriculture 86(11), 1722-1731.

Takahashi, T., Furuichi, Y., Mizuno, T., Kato, M., Tabara, A., Kawada, Y., Hirano, Y., Kubo, K.-y., Onozuka, M., Kurita, O., (2009). Water-holding capacity of insoluble fibre decreases free water and elevates digesta viscosity in the rat. Journal of the Science of Food and Agriculture 89(2), 245-250.

Tanoue, K.-i., Tanaka, H., Kitano, H., Masuda, H., (2001). Numerical simulation of tribo-electrification of particles in a gas–solids two-phase flow. Powder Technology 118(1–2), 121-129.

Tatsushi, M., Hideo, Y., (1997). Charge-relaxation process dominates contact charging of a particle in atmospheric condition: II. The general model. Journal of Physics D: Applied Physics 30(15), 2170.

Tilmatine, A., Dascalescu, L., (2010). Set-point identification of a free-fall triboelectrostatic separation process for plastic particles. International Journal of Environmental Studies 67(1), 27-40.

Tilmatine, A., Medles, K., Younes, M., Bendaoud, A., Dascalescu, L., (2009). Roll-type versus free-fall electrostatic separation of tribocharged plastic particles. Conf Presentation Particles and Instruments.

Trigwell, S., Tennal, K.B., Mazumder, M.K., Lindquist, D.A., (2003). Precombustion cleaning of coal by triboelectric separation of minerals. Particulate Science and Technology 21(4), 353-364.

Tsukada, M., Irie, R., Yonemochi, Y., Noda, R., Kamiya, H., Watanabe, W., Kauppinen, E.I., (2004). Adhesion force measurement of a DPI size pharmaceutical particle by colloid probe atomic force microscopy. Powder Technology 141(3), 262-269.

van der Goot, A.J., Pelgrom, P.J.M., Berghout, J.A.M., Geerts, M.E.J., Jankowiak, L., Hardt, N.A., Keijer, J., Schutyser, M.A.I., Nikiforidis, C.V., Boom, R.M., (2016). Concepts for further sustainable production of foods. Journal of Food Engineering 168, 42-51.

Vieweg, H.F., (1925). Frictional electricity. The Journal of Physical Chemistry 30(7), 865-889.

Viollaz, P.E., Rovedo, C.O., (1999). Equilibrium sorption isotherms and thermodynamic properties of starch and gluten. Journal of Food Engineering 40(4), 287-292.

Vitaglione, P., Napolitano, A., Fogliano, V., (2008). Cereal dietary fibre: a natural functional ingredient to deliver phenolic compounds into the gut. Trends in Food Science & Technology 19(9), 451-463.

Wang, J., de Wit, M., Boom, R.M., Schutyser, M.A.I., (2015a). Charging and separation behavior of gluten–starch mixtures assessed with a custom-built electrostatic separator. Separation and Purification Technology 152, 164-171.

Wang, J., de Wit, M., Schutyser, M.A.I., Boom, R.M., (2014). Analysis of electrostatic powder charging for fractionation of foods. Innovative Food Science & Emerging Technologies 26(0), 360-365.

Wang, J., Smits, E., Boom, R.M., Schutyser, M.A.I., (2015b). Arabinoxylans concentrates from wheat bran by electrostatic separation. Journal of Food Engineering 155(0), 29-36.

Wang, T., Sun, X., Raddatz, J., Chen, G., (2013). Effects of microfluidization on microstructure and physicochemical properties of corn bran. Journal of Cereal Science 58(2), 355-361.

Watano, S., (2006). Mechanism and control of electrification in pneumatic conveying of powders. Chemical Engineering Science 61(7), 2271-2278.
Wu, G., Li, J., Xu, Z., (2013). Triboelectrostatic separation for granular plastic waste recycling: A review. Waste Management 33(3), 585-597.

Wu, Y.V., Stringfellow, A., (1995). Enriched protein and β-glucan fractions from high-protein oats by air classification. Cereal Chem 72(1), 132-134.

Yamamoto, H., Scarlett, B., (1986). Triboelectric charging of polymer particles by impact. Particle & Particle Systems Characterization 3(3), 117-121.

Younes, A., Younes, M., Sayah, H., Samuila, A., Dascalescu, L., (2015). Experimental and numerical modeling of a new tribo-electrostatic separation process for granular plastics mixtures. Particulate Science and Technology 33(2), 189-196.

Young, P., (2009). Sodium starch glycolate, in: Raymond C Rowe, Sheskey, P.J., Quinn, M.E. (Eds.), *Handbook of pharmaceutical excipients*, Sixth ed. Pharmaceutical Press, pp. 663-666.

Zhou, S., Liu, X., Guo, Y., Wang, Q., Peng, D., Cao, L., (2010). Comparison of the immunological activities of arabinoxylans from wheat bran with alkali and xylanase-aided extraction. Carbohydrate Polymers 81(4), 784-789.

Summary

Dry fractionation is a promising alternative to wet extraction processes for production of food ingredients, since it uses hardly any water, consumes less energy and retains the native functionality of the ingredients. It combines milling and dry separation to enrich agro-materials in specific components such as protein. Electrostatic separation recently emerged as a novel dry separation process and it relies on electrostatic forces for separation. Though the potential of electrostatic separation to fractionate agro-materials has been demonstrated, the effectiveness in terms of purity and yield and the influence of process parameters on charging and separation of food ingredients have not yet been systematically studied. Therefore, the objective of this thesis was to gain better understanding of the charging and separation behaviour of model and agro-materials, provide insight in the critical factors for successful electrostatic separation and explore the potential of this separation method to different agro-materials.

The charging step is critical to the effectiveness of electrostatic separation and is influenced by many factors. **Chapter 2** presents characterization of the charging behaviour of single-component model particles in nitrogen gas flowing through aluminium tubes, using a lab-scale electrostatic separator. Polystyrene particles and wheat gluten were used as model particles. Higher gas velocities led to a higher specific charge by increasing the normal component of impact velocity. Smaller particles gained more specific charge than larger ones because of their higher surface to volume ratio and their sensitivity towards gas flow pattern changes. Longer charging tube lengths allowed more contact between the particles and the wall and therefore resulted in higher specific charge. The relative humidity of the nitrogen gas flow within the range 0 – 60% had no influence on the charging behaviour of both model particles.

Chapter 3 demonstrates the potential of applying electrostatic separation to enrich arabinoxylans from wheat bran with the same lab-scale electrostatic

separator. A combination of larger particle size, higher gas velocity and shorter charging tube was preferred for separation, because it sufficiently charged the particles while agglomeration was minimized. Electrostatic separation with the optimum setting achieved a similar enrichment in arabinoxylans (from 23% to 30% dry matter basis) as sieving does. However, the combination of electrostatic separation and sieving further improved the enrichment and resulted in a fraction with an arabinoxylans content of 43% dry matter basis, which is around the maximum achievable purity that can be reached by dry fractionation.

To allow better defined charging and separation experiments, a bench-scale electrostatic separator was designed and constructed. With this custom-built separator, the charging and separation of model mixtures prepared from wheat gluten and starch were studied in **chapter 4**. The net charge of gluten-starch mixtures was not simply the sum of the charge of the two individual components, indicating that particle-particle interactions play an important role. We hypothesized that the formation of agglomerates between oppositely charged particles negatively influenced separation, which was supported by the fact that the dispersibility for mixtures of the two components was lower compared to that of individual components. We found that during electrostatic separation of mixtures, it is important to find the optimal condition that provides sufficient charge to charges, but avoids agglomeration between oppositely charged particles. This could be achieved by the combination of lower dosing rate and higher gas flow rate.

Chapter 5 reports on dry fractionation by combining milling and electrostatic separation with the custom-built bench-scale separator, providing an alternative to wet extraction of protein from lupine seeds. Relatively coarse milling was preferred because it disclosed sufficient protein bodies from the matrix, while avoiding poor dispersibility of the powder due to its very fine particle size. With the optimal settings of single-step electrostatic separation, a fraction with 57.3 g/100 g dry solids could be obtained. The protein content was further improved to 65.0% dry matter basis after two more separation steps, which is 15% higher than obtained by air classification. The yield of the protein enriched fraction was further increased by recycling the fractions from the filter bags, but this was accompanied by a decrease in protein content and vice versa. A significant shift

towards better yield and purities was achieved by re-milling the flour that was not collected on the electrodes. A final fraction with a protein content of 65.1% dry matter basis and a yield of 6% was obtained, which recovered 10% of the protein in the original flour.

Chapter 6 explores the possibility of enriching dietary fibre from defatted rice bran by dry fractionation, where the custom-built bench-scale electrostatic separator was used. All three tested separation routes produced fibre-enriched fractions with similar yield (20 – 21 % of the milled flour) and fibre content (67 – 68 % dry matter basis), which recovered 42 – 48 % of the fibre from the original flour. The enriched fractions obtained by a two-step electrostatic separation process contained more small particles compared to the other two, which resulted in different functional properties. Compared to the total dietary fibre extracted by the enzymatic-gravimetric method, the enriched fractions by dry fractionation had a similar water retention capacity and oil binding capacity. This suggests that the fibre-enriched fractions by dry fractionation can be applied in foods and provide similar technological properties and physiological effects as the wet-extracted dietary fibre does.

Chapter 7 concludes the thesis with a general discussion on the main findings, based on which two schemes for protein enrichment and fibre enrichment were proposed. Subsequently the challenges to achieve a successful electrostatic separation for agro-material and up-scaling are discussed. Finally, the chapter ends with an outlook on future research.

This thesis provided insight in the key factors for successful electrostatic separation. It demonstrated the potential of applying this separation method for functional ingredient production from different agro-materials and also gave directions for further improvement and scaling-up.

Acknowledgements

The completion of this PhD thesis was an amazing journey, which would not have been possible without the support from many great people.

Firstly, I would like to express my sincere gratitude to Anja Janssen, who guided me step-by-step into the world of food technology. Thank you for all the valuable suggestions and support, as my study advisor, master thesis supervisor, colleague and friend.

Next to that I would like to extend my sincere thanks to Maarten, my daily supervisor. Thank you for the continuous support of my PhD study, for your patience and motivation, and for helping me to keep on track especially at the last stage of my PhD. Your guidance helped me in all the time of research and writing of this thesis. Many thanks also to Remko, my promoter. I appreciate all the stimulating discussions with you and the insightful comments from you. Martin de Wit, thank you for our pleasant collaboration. Could not imagine how much longer I will need to finish this journey without your help. I would also like to thank Martin Korevaar, Johan Padding, Remco Hamoen and all the user committee members, for our fruitful discussions and your valuable input.

Furthermore, I would like to thank all my colleagues at FPE, for the great time we had together. Special thanks to Maurice, Jos, Jarno and Marjan for your technical and administrative support. Big thanks to my former office mates, Rupali, Angelica, Jorien, Jacqueline and Birgit, thank you for the companionship. All the office chat made the PhD life more enjoyable. Also to the “Orion Lunch Squad”, yes I just named it :), Sami, Ekaraj, Qi, Ali and Filippos, for making the lunch more than just a sandwich. Laura, Jaap and Anton, big thanks to you for making the last week of my PhD unforgettable. I would also like to thank my students, Erik, Shan, Wentao, Marjolein, Jun, Geng and Fabienne for your hard work and dedication.

I cannot forget friends who went through tough times together and celebrated each accomplishment: Kun, Hequn, Si, Wen, Chao, Xu, Yinghua, Yin, Wen, Duanyang, Yanmin, Jessie, Tze-yi, Eunice, Yanjing, Xiang, Huiming, Xuezhen, Wenjuan, Chang, Yawei, Binxiu, Jinyu, Xinyi, Dongdong, Chaoran, Xiaojing and Changle.

Above all, I would like to thank my parents, for their love, trust and support throughout my life.

Finally, to my long-suffering other half Feifei, thank you for always being there for me. Without your love, patience and encouragement, I would have never reached this point of my life. Words cannot express my gratitude for everything you have done. Thank you for accompanying me on this adventure, I look forward to our next one!

About the author

Jue Wang was born on January 8, 1986 in Shanxi, China. After completing her secondary education in Shanxi in 2004, she started her BSc study in Landscape Architecture at Beijing Forestry University, China. In 2008, she moved to the Netherlands to continue her study in MSc Landscape Architecture at Wageningen University. After two months she decided to change her major to Food Technology and spent one year in pre-Master study. In 2009, she was admitted to the MSc Program Food Technology of Wageningen University, specialized in product design. Jue did her mater thesis at Food Process Engineering group of Wageningen University, working on understanding the effect of molecular crowding on β-galactosidase from Bacillus circulans and its galacto-oligosaccharides production. During her internship at Process Technology Department of FrieslandCampina Research, Deventer, the Netherlands, she worked on method development for measuring stickiness of dairy powders.

Jue completed her MSc program in 2011, and continued working as a PhD at the Food Process Engineering group of Wageningen University on the project *Electrostatic separation for functional food ingredient production*. Since February 2016, she works as a Product Technologist at Research & Development Centre of Danone Nutricia Early Life Nutrition, Utrecht, the Netherlands.

List of publications

Wang, J., Zhao, J., de Wit, M., Boom, R.M., Schutyser, M.A.I., (2015). Lupine protein enrichment by milling and electrostatic separation. Innovative Food Science & Emerging Technologies.

Wang, J., de Wit, M., Boom, R.M., Schutyser, M.A.I., (2015). Charging and separation behavior of gluten–starch mixtures assessed with a custom-built electrostatic separator. Separation and Purification Technology 152, 164-171.

Korevaar, M.W., Padding, J.T., Deen, N.G., **Wang, J.**, de Wit, M., Schutyser, M.A.I., Kuipers, J.A.M., (2015). Hybrid PIV/PTV measurements of velocity and position distributions of gas-conveyed particles in small, narrow channels. AIChE Journal, 61, 3616-3627.

Wang, J., Smits, E., Boom, R.M., Schutyser, M.A.I., (2015). Arabinoxylans concentrates from wheat bran by electrostatic separation. Journal of Food Engineering 155(0), 29-36.

Pelgrom, P.J.M., **Wang, J.**, Boom, R.M., Schutyser, M.A.I., (2015). Pre- and post-treatment enhance the protein enrichment from milling and air classification of legumes. Journal of Food Engineering, 155(0), 53-61.

Wang, J., de Wit, M., Schutyser, M.A.I., Boom, R.M., (2014). Analysis of electrostatic powder charging for fractionation of foods. Innovative Food Science & Emerging Technologies 26(0), 360-365.

Wang, J., Suo, G., de Wit, M., Boom, R.M., & Schutyser, M.A., (2016). Dietary fibre enrichment from defatted rice bran by dry fractionation. Submitted for publication

Warmerdam, A., **Wang, J.**, Boom, R.M., Janssen, A.E.M., (2013). Effects of carbohydrates on the oNPG converting activity of β-galactosidases. Journal of Agricultural and Food Chemistry, 61 (26), 6458-6464.

Overview of completed training activities

Discipline specific activities

Courses

Numerical Methods for Chemical Engineers in Eindhoven (NL)	2012
Food Structure and Rheology in Wageningen (NL)	2012
Advanced Food Analysis in Wageningen (NL)	2013
Industrial Food Proteins in Wageningen (NL)	2013
Dry Fractionation of cereals in Montpellier (FR)	2015

Conferences

NPS11 Symposium in Papendal (NL)	2011
POWTECH in Nuremberg (DE)	2011
Hosokawa AlpineExpo in Augsburg (DE)	2012
FoodBalt2012 in Kaunas (LT)	2012
EFFoST in Montpellier (FR)	2012
BFF in Wageningen (NL)	2013
ECCE9 in Den Haag (NL)	2013
ESA in Cocoa Beach (USA)	2013
AACC International Annual Meeting in Rhode Island (USA)	2014
EFFoST in Uppsala (SE)	2014
ECCE10-ECAB3-EPIC5 in Nice (FR)	2015

General courses

VLAG PhD Week in Baarlo (NL)	2012
Project and Time Management in Wageningen (NL)	2012
Scientific Writing in Wageningen (NL)	2012
Competence assessment in Wageningen (NL)	2012
Teaching and supervising thesis students in Wageningen (NL)	2013

Techniques for Writing and Presenting Scientific Papers in Wageningen (NL)	2013
Data Management in Wageningen (NL)	2013
Career Orientation in Wageningen (NL)	2015

Optional activities

Scientific PhD excursion to Finland and Baltics, Food Process Engineering	2012
Scientific PhD excursion to Chile and Brazil, Food Process Engineering	2014
Organizing scientific PhD excursion to Chile and Brazil	2014
Weekly group meetings Food Process Engineering	2011-2015

The work presented in this thesis has received funding from the Technology Foundation STW and the Institute for Sustainable Process Technology (ISPT) under the framework of the SMARTSEP program (grant number 11399).

Cover and layout were designed by Rookie Design
Pictures on cover were licensed by Fotolia
Printed by GVO drukkers & vormgevers B.V.